ADDIS ABABA UNIVERSITY

CENTER FOR ENVIRONMENT AND DEVELOPMENT

COLLEGE OF DEVELOPMENT STUDIES

RUNOFF AND SEDIMENT YIELD SIMULATION IN THE WEYIB WATERSHED, GENALE-DAWA BASIN, ETHIOPIA

A Thesis submitted to the School of Graduate Studies, Addis Ababa University in Partial Fulfillment of the Requirements for the Master of Science Degree in Water Resource Management.

By: Abraham Getinet

Advisor: Ermias Teferi (PhD)

March, 2021

Addis Ababa, Ethiopia

APPROVAL SHEET

ADDIS ABABA UNIVERSITY
CENTER FOR ENVIRONMENT AND DEVELOPMENT
COLLEGE OF DEVELOPMENT STUDIES

This is to certify that the thesis prepared by Abraham Getinet, entitled: **Runoff and Sediment Yield Simulation in the Weyib Watershed, Genale-Dawa Basin, Ethiopia** and submitted in partial fulfillment of the requirements for the degree of Master of Sciences in Water Resource Management complies with the regulations of the university and meets the accepted standards with respect to originality and quality.

Approval by Board of Examiners

Ermias Teferi (PhD)	______________	____________
Advisor	Signature	Date
Shimeles Damene (PhD)	______________	____________
Internal Examiner	Signature	Date
Sirak Tekleab (PhD)	______________	____________
External Examiner	Signature	Date
__________________________	______________	____________
Chairperson (Department of Graduate Committee)	Signature	Date

CERTIFICATION

As thesis research advisor, I certify that I have read and evaluated this thesis prepared, under my guidance, by Abraham Getinet, entitled: Runoff and Sediment Yield Simulation in the Weyib Watershed, Genale-Dawa Basin, Ethiopia and here by recommend for acceptance by the Addis Ababa University in partial fulfillment of the requirements for the degree of Master of Science.

____

Ermias Teferi (PhD)

____

Date

DECLARATION AND COPY RIGHT

In presenting this thesis in partial fulfillment of the requirements for a master's degree at Addis Ababa University, first of all, I declare that this thesis is my original work and does not infringe or violate any rights of others. I have properly acknowledged all sources and materials used during the write up.

____

Abraham Getinet
elshabraham21@gmail.com

ACKNOWLEDGMENT

First and foremost, I would like to thank the Almighty God for providing me his boundless care, love throughout my life, that enabled me to begin and finish this work successfully. My sincere gratitude goes to my advisor, Dr. Ermias Teferi, for providing me with his genuine guidance and provision of references and constructive comments and encouragements all the way from the beginning to the completion of the time taking research work. I would like to express my warm feeling of appreciation to all staffs in the Ministry of Water, Irrigation and Energy especially, to those staffs in the Hydrology and Water Quality Directorate and Information and Communication Directorate and to the National Metrological Agency for providing me all the input data and information required for the study. I would also like to express my heartfelt gratitude to my parents for their diligent guidance and encouragement. Finally, I would also like to express my deepest gratitude to my families and all my friends whose names are too many to list here, but, who in one way or another, contributed to the successful competition of the research work.

Table of Contents

List of Figures

List of Tables

List of Abbreviations and Acronyms

^0C	Degree Centigrade
A	Surface Area
ACRU	Agricultural Catchment Research Unit
AGNPS	Agricultural Non-Point Source Pollution Model
AnnAGNPS	Annualized Agricultural Non-Point Source Model
ANSWERS	Areal Non-Point Source Watershed Environment Response Simulation
C	USLE Crop management factor
CFRG	Coarse Fragment Factor
CN	Curve Number
DEM	Digital Elevation Model
DewPOINT	Dew Point Temperature Calculator
DEWPT	Average Daily Dew Point Temperature in the Month
DSMW	Digital Soil Map of the World
DSS	Decision Support System
ENS	Nash-Sutcliffe's Simulation Efficiency
EUROSEM	European Soil Erosion Model
FAO	Food and Agricultural Organization
GDMP	Genale Dawa Master Plan Study
GIS	Geographical Information System
GPS	Global Positioning System
HRU	Hydrological Response Units
HSPF	Hydrologic Simulation Program Fortran
Ia	Initial abstractions
IRBM	Integrated River Basin Management
K	USLE Soil Erodibility factor
LH-OAT	Latin Hypercube One-factor-At-a-Time
LS	USLE Slope Length and Steepness factors
LULC	Land Use and Land Cover
m3/s	Cubic Meters per second
Mm	Millimeter
MoA	Ministry of Agriculture
MAF	Mean annual flood peak discharge
MAP	Mean annual precipitation
MAR	Mean annual runoff
Masl	Meters above Sea Level
MoWIE	Ministry of Water, Irrigation and Energy
MUSLE	Modified Universal Soil Loss Equation
NSE	Nash and Sutcliffe's Simulation Efficiency
P	USLE Conservation Practice factor

P-bias	Percent bias
Q	Discharge (m3/s)
Q_{pwak}	Peak runoff rate
Q_{surf}	Daily accumulated surface runoff or rainfall excess
R	USLE Rainfall Erosivity factor
R^2	Coefficient of Determination
RMSE	Root Mean Square Error
RSR	Ratio of Root Mean Square Error and standard deviation of observation
RUSLE	Revised Universal Soil Loss Equation
S	Retention parameter
SCRP	Soil Conservation Research Project
SCS	Soil Conservation Service
SCS-CN	Soil Conservation Service Curve Number
Sed	Sediment yield on a given day
SLEMSA	Soil Loss Estimation Model for South Africa
SOLARAV	Average Solar radiation
STDEV	Standard Deviation
SW0	Initial soil water content
SWAT	Soil and Water Assessment Tool
SWt	Final soil water content
TMP_MAX	Average Daily Maximum Temperature in the month
TMP_MIN	Average Daily Minimum Temperature in the month
TMPSTDMN	Standard Deviation of Minimum Temperature in the Month
TMPSTDMX	Standard Deviation of Maximum Temperature in the Month
USDA-ARS	US Department of Agriculture – Agriculture Research Service
WNDAV	Average Wind Speed
USLE	Universal Soil Loss Equation
UTM	Universal Transverse Mercator
WGEN	Weather Generator
WEPP	Water Erosion Prediction Project

ABSTRACT

The SWAT model was applied to simulate the runoff and sediment yield from the Weyib watershed. This watershed has an area of 24369.6 km^2 and located in South-Eastern part of Ethiopia, sharing two regional states, Oromia and Somali. The objective of this study was to estimate soil loss rate in the study watershed and to identify appropriate intervention measures to control erosion. In spite of the serious erosion problems in the study watershed, so far only few studies related to erosion are available. Consequently, this study was conducted with the aim of contributing to the exiting insufficient quantitative information on soil erosion problems. Due to the absence of measurements for some of the stations, about 25 years meteorological data and 21 years flow and sediment data generated by regional equations were used for the analysis. On the other hand, the SUFI2 program in the SWAT-CUP was applied for model calibration and validation using time series data from 1992-2012. The model prediction efficiency was evaluated using statistical model performance indicators like, coefficient of determination (R^2) and Nash-Sutcliffe model Efficiency (ENS) and the result showed that both surface runoff and sediment yield were estimated satisfactorily, with an R^2 and NSE values of greater than 0.67 each, both for calibration (1994–2004) and validation (2005-2012) periods. The model prediction for the average annual precipitation and run-off was 1029.2mm and 311.30mm, respectively; whereas, the model prediction for the average annual total sediment load was 1.23t/ha. The annual soil loss estimated by the model for the Weyib watershed during the simulation period 1992-2012 ranges from 12.49 ha^{-1} $year^{-1}$ to 88.36 ha^{-1} $year^{-1}$, with an average value of 37.33 tons ha^{-1} $year^{-1}$. In this study, Sub-watershed 6, 7, 8, 10 and 12 were found to have the maximum annual sediment load, having an annual sediment load of greater than 20 tons/ha/yr, sub-watershed 8 being the most erodible area, and as these sub-watersheds were most sensitive to erosion, they were labeled as erosion hotspot areas. Different intervention scenarios were developed for erosion control and proper management of the watershed. Simulation results for these scenarios reflected that, 35-78% sediment yield reduction could be achieved by implementing filter strips, stone bunds, contour farming, fanya juu, bench terraces and from the combination of these. On the other hand, conversion of agricultural lands to forest areas reflected a 10-45% sediment yield reduction.

Keywords: SWAT Sediment yield, Runoff, Soil Erosion, Weyib watershed

1 INTRODUCTION

1.1 Background of the study

Soil erosion has become a major problem in many parts of the world (Brevik *et al.,* 2015). Soil erosion seriously affects soil fertility, land productivity and disturbs the soil, water resources and ecosystem services (Pimentel, 2006 and Bayramin *et al.,* 2002).

According to Hurni *et al.* (2010), soil erosion by water has been the most serious environmental problem in Ethiopia. A study conducted by Hurni *et al.* (2015), estimated the country's average annual soil loss rate before 30 years ago to be 1500 million tons per year. The same study also revealed the current annual soil loss rate as 940 million tons per year. Deforestation and expansion to marginal lands that are often fragile and susceptible to soil erosion, which substantially affects production and productivity of the land, hamper the future development of the country leaving many people food unsecured and vulnerable. This is the consequence of the growing human population (Hurni *et al.,* 2015). According to this research, about 60% of all cropland in Ethiopia is affected by net erosion, resulting about 380 million tons of sediments per year or 20 t/ha/yr. of cropland.

Quantitative information on soil erosion in Ethiopia are scarce (Nyssen *et al.,* 2004). Existing information on soil loss rates (e.g., Hurni, 1993) was mainly based on plot level and/or empirical models such as Universal Soil Loss Equation (USLE), the output from which are too few in number to represent the diverse environments of the country (Tibebe and Bewket, 2011). The USLE model offered a good understanding on the interactions between soil loss under different cover, soils and slopes. However, since there are restrictions in its representation, and dependability of its outputs, the results cannot be extrapolated for an entire catchment directly (Setegn, 2008). The unsuccessfulness of the soil and water conservation programs that have been practiced in Ethiopia in the past four decades could be due to the decisions made based on such results.

For the past 40 years, the USLE model was the most practical method for soil erosion prediction (Dennis and Rorke, 1999 and Kinnell, 2000). Other process-based erosion models were developed but, they exhibited limitation in applicability because they were data and computation intensive (Lim *et al*., 2005). To take advantage of its integration of GIS and locally accessible data and data from similar areas that can be used to calibrate and validate the model, the SWAT model has been employed for this study.

1.2 Statement of the Problem

Weyib river is one of the three sub-basins of Genale-Dawa river, viz: - Genale, Dawa and Weyb (GDMP, 2007). The upper part of the Weyib watershed, the Sannete area (with an altitude of 4389m above sea level), is one of Ethiopia highlands, which receives high amount of rainfall (Abdulkerim and Arup, 2016). Thus, soil degradation, due to erosion by water is very high. This problem was exacerbated by the improper land use system followed for years. The undulating and rugged topography of the area has aggravated the issue.

Once this area was characterized by deep and fertile soil, intact natural forest, different and large number of wild lives, large number of livestock per household, low population density, etc. However, now a day there is a huge destruction in these natural resources, which resulted in land degradation/soil erosion, which is manifested as the soil physical, chemical and biological degradation and hence ultimately resulted in reduction of soil fertility, production and productivity of the land.

Currently, agricultural land use covers about 79.37% of the total area of the study watershed (Sisay *et al.,* 2019). Extensive land utilization for crop production reduced the available pasture land in the study area, which was once an area where a large number of livestock were tended. This has brought a great impact on the forest and soil resources.

Despite the severity of soil erosion and its consequences in the study watershed, so far only few soil erosion susceptibility analysis and map were available for this watershed. Previous works mainly assessed the hydrology and the impact of climate change on the water availability of the study watershed. Abdulkerim and Arup (2016) studied the performance of SWAT model in simulating stream flow for the upper Weyib watershed. In 2017, they also studied the spatial and temporal variation of current and projected water demand and water availability under climate change scenarios using the SWAT model and found a decrease of water availability in all months on the dry season, which might cause water shortage in the lowland region, and greater increase of water availability in intermediate and rainy seasons causing flooding to some flood prone region of the basin.

A study conducted by Sisay *et al.* (2019) mainly focused on the bio-physical characteristics of Weyib watershed. The study reported the mean annual precipitation, actual evapotranspiration and mean temperature of the watershed to be 1015 mm, 970.1 mm and 14 0C respectively. The study results exhibited the suitability of the Weyib watershed for widespread agricultural production.

On the other hand, Shawul *et al.* (2013) examined the SWAT model performance and its applicability in analyzing hydrologic parameters influence on the stream flow variability and in estimation of monthly and seasonal water yield at the outlet of Shaya, which is found inside Weyib watershed. The simulation result of the study indicated the mean monthly and annual water yield of Shaya mountains to be 25.8 mm and 309.0 mm, respectively. The study also demonstrated the good performance of SWAT in capturing the patterns and trend of the observed flow series and confirmed the appropriateness of the model for future scenario simulation. These previous studies mainly focused on the hydrology of the watershed and on the applicability of SWAT model in the watershed. However, in their studies the issue of erosion problems was not well address. Moreover, so far in the study watershed, little has been explored and no study was undertaken with respect to land degradation, specifically soil erosion. Though no researches related to erosion are available for the study area, soil erosion has become the most significant challenge for the livelihood of the watershed residents and to the ecosystem in general. To address the issue, the extent and spatial pattern of soil erosion need to be assessed.

Furthermore, the underlying causes of land degradation particularly soil erosion has to be identified and site-specific remedial measures has to be recommended, as this will provide a watershed specific and timely information on soil erosion to decision makers and land managers. Thus, it was presumed that this research bridges existing research gaps related to erosion problems and assists in the identification of erosion prone areas for planning and implementation of watershed-based soil and water conservation activities.

Therefore, this study was designed to quantify the runoff and sediment yield, to identify, analyze and to map erosion hotspot areas in the watershed and to recommend proper erosion control measures using the SWAT model.

1.3 Significance of the Study

It was assumed that this study would be helpful to figure out the severity of soil erosion in the study area. Soil erosion is the main threat for sustained agriculture, as soil is the basis of agricultural production. Erosion quantification under various land use /land cover conditions will help to prioritize the watershed for soil conservation planning in order to encourage effective natural resource conservation and sustainable development. Soil erosion assessment and mapping of erosion prone area serve the knowledge for soil conservation and watershed management. The intention of this study was not merely quantifying the erosion rate; but also, to provide results that would be vital inputs for any decision making and supportive in policy formulation for sustaining the environment as a whole and for improving land productivity in the watershed. In practice, areas at high risk have to be prioritized first before undertaking any management and conservation activities of natural resources specially soil and water. Hence, it is essential to assess soil erosion risk for soil conservation program. Furthermore, prediction of soil erosion rates is needed for timely and effective actions.

So far only few soil erosion susceptibility analysis and map were available for the study watershed. Previous works focused mainly on the hydrology and on the impact of climate change on the water availability of the study watershed (Abdulkerim and Arup, 2016). However, currently soil erosion is becoming the most important challenge for the livelihood of the watershed residents in particular and the ecosystem in general. Due to the high amount of rainfall, the study area is highly prone to soil erosion and flooding which damaged large areas of cropland, forming new rills and gullies. Therefore, the extent and spatial pattern of the watershed’s soil erosion needed to be assessed. This will assist the identification of erosion prone areas for planning and implementation of a watershed-based soil and water conservation plan.

Therefore, this study was designed to identify, quantify, analyze and to map parts of the watershed under soil erosion risk within the Weyib watershed using the SWAT model. Appropriate erosion intervention measures were also identified, for future development plans. Eventually the findings of this study were documented as a source of information for further future studies in the area.

1.4 Objectives of the Study

1.4.1 General objective

The general objective of this study was to estimate the runoff and soil loss rate in the Weyib watershed, Genale Dawa basin, Ethiopia.

1.4.2 Specific objectives

The specific objectives of this study were:

1. To estimate the sediment yields from different sub-watersheds of Weyib,
2. To identify erosion hotspot areas and to prioritize them for intervention measures;
3. To identify appropriate intervention measures that can effectively reduce sediment yield/soil erosion.

1.5 Research Questions

This research was conducted with aim of answering the following questions;

1. What is the annual flow and soil loss rate in the study area?
2. What is the sediment yield from different sub-watersheds of Weyib?
3. Is there an interplay between rainfall, flow, slope, soil, land use and soil erosion/sediment yield?
4. Which part of the study area is at risk of erosion and hence needs immediate actions/ intervention?
5. Which intervention measures are appropriate for erosion control in the study area?

1.6 Scope of the Study

Whilst the bio-physical factors, the hydrology and the impact of climate change on the availability of water are well assessed for the Weyib watershed, less emphasis has been given to erosion problems in the area. There was no available station and recorded discharge and sediment data at the outlet of Weyib watershed near the Somali border, consequently these two data were derived using regional equations. The aim of this study was to identify, quantify, analyze and to map erosion hot spot areas in the Weyib watershed and to recommend appropriate intervention measures, thereby contributing to the existing erosion related research gaps in the watershed. Eventually the findings of this study were documented as a source of information for further future studies in the area.

2 LITERATURE REVIEW

2.1 Soil Erosion

Soil erosion is the removal of soil particles from the place where it belongs to elsewhere by water or wind (Taffa, 2002). Detachment, transport and deposition are the three main processes that are taking place in soil erosion the process. The soil will be detached by falling rain or wind, transported in the water or wind and then settle down when the velocity is lowered. Runoff occurs if the rain fall intensity exceeds the infiltration rate of the soil (Morgan, 1998). Long duration rainfall showers cause compaction of top soil and decreasing infiltration rate of the soil. As a result, surface runoff increases causing more erosion.

There are two major types of erosion; geological and accelerated erosion. Geological erosion takes place naturally and control measures cannot be taken (Morgan, 1998). It occurs without the influence of man and here, there is an equilibrium between soil formation and soil erosion. Whereas, accelerated erosion is a rapid removal of soil brought about by the intervention of man, disturbing balance of nature. Removal of the top fertile soil, loss of water, siltation and flooding are some of the damages resulting from accelerated erosion. (Hudson, 1996).

2.1.1 Soil Erosion by Water

Land degradation is principally caused by soil erosion by water and it is a major constraint to agricultural development. The key feature of soil erosion by water is the selective removal of the finer and more fertile fraction of the soil. Water erosions can be classified as Splash, Sheet, Rill, Gully and Stream bank erosion.

2.1.1.1 Splash Erosion

Splash erosion (also called raindrop erosion) is a type erosion that involves soil detachment and transport resulting from the impact of water drops directly on soil particles or on thin water surfaces (Taffa, 2002). During rainfall, tremendous quantities of soil particles are splashed into the air due to the kinetic energy of the raindrops directly striking the soil surface. Consequently because of repeated such impacts, large quantities of soil particles are detached and transported during a rainfall. The severity of raindrop erosion is very high on bare soils (Taffa, 2002).

2.1.1.2 Sheet erosion

Sheet (inter rill) erosion is the detachment and transport of soil by raindrop impact and shallow overland flow (Ringo, 1999). According to him, in this type of erosion, no noticeable channels are formed, rather it is a uniform thin layer removal of soil (soil surface layer), almost imperceptible layer. It is a process whereby there is a uniform removal of soil in thin layers from sloping land, resulting from sheet or overland flow. Sheet erosion can occur on any sloping land whose vegetative cover is low to reduce the velocity of direct runoff (Morgan, 1998).

2.1.1.3 Rill erosion

As rain falls on cultivated land, the water starts flowing downhill in concentration. This moving water creates shallow channels by washing away the surface soil. The channels so created are known as rills and the erosion process is called rill erosion (Taffa, 2002). According to his explanations, rills are small channels cut by concentrated runoff/flow, through which water flows during and immediately after rain. According to him, rill erosion is probably the most important form of soil loss in cultivated fields.

In rill erosion, soil detachment can be by splash or by the overland flow i.e., scouring. When the force of overland flow is high incision (deeper rills) will occur (Morgan, 1998). They are distinguished in size from gullies by the fact that they are largely obliterated by tillage operation. That is rills differ from gullies in that they are temporary features and can be easily destroyed during ploughing, whereas gullies are more permanent features in the landscape. These two types of erosion, account for the major impact of soil erosion on land productivity.

2.1.1.4 Gully erosion

Gully erosion is the severest type of erosion in which channels larger than rills are produced. These channels carry water during and immediately after rains; and as distinguished from rills, gullies cannot be obliterated by tillage ((Morgan, 1998 and Taffa, 2002).

2.1.1.5 Stream channel erosion

Stream channel erosion consists of soil removal from stream banks or soil movements in the channel. According Taffa (2002), stream channel erosion and gully erosion are distinguished primarily in that stream channel erosion applies to the lower end of headwater tributaries and to streams that have nearly continuous flow and relatively flat gradients, whereas gully erosion generally occurs in intermittent streams near the upper end of headwater tributaries.

Stream banks erode either by runoff flowing over the side of the stream bank or by scouring and undercutting below the water surface. Stream bank erosion, less serious than scour erosion, is often increased by the removal of vegetation, overgrazing, tilling too near the banks or straightening of the channel. Scour erosion is influenced by velocity and direction of flow, depth and width of the channel and soil texture (Morgan, 1998).

2.2 Factors affecting soil erosion

2.2.1 Size of a Watershed

The volume of water that can be generated from rainfall is influenced by the size of the watershed (Taffa, 2002). On large watersheds the total flood flow will take more time to pass the outlet, while on smaller watersheds the flood water collects quickly.

2.2.2 Shape of a Watershed

A long shape watershed generates, for the same rainfall, a lower outlet flow, as the concentration time is higher. A watershed having a fan-shape (more or less circular) presents a lower concentration time i.e., would result in runoff from various parts of the watershed reaching the outlet at the same time, and it generates higher (peak) flow. An elliptical watershed having the outlet at one end of the major axis and having the same area as the circular watershed would cause the runoff to be spread out over time, thus producing a smaller flood peak than that of the circular watershed (Taffa, 2002).

2.2.3 Soil

Soil factors affecting soil erosion are Physical factors such as; structure, texture, organic matter content, moisture content, density or compactness, the chemical and biological characteristics of the soil (Morgan, 1998). Physical properties of soil affect the infiltration capacity and the extent to which particles can be detached and transported. The corresponding soil characteristics that describe the ease with which soil particles may be eroded are soil detachability and soil transportability. In general, soil detachability increases as the size of the soil particles or aggregates increase; and soil transportability increases with a decrease in the particle or aggregate size. That is, clay particles are more difficult to detach than sand, but clay is more easily transported.

Wischemeier and Smith (1978) established a regression equation or nomograph for the parameters to estimate soil erodibility (K). according to them, soil erodibility increases with increase in silt plus very fine sand content of the soil, however, it decreases with increasing clay and organic matter content.

2.2.4 Vegetation cover

The major effects of vegetation in reducing erosion are (1) interception of rainfall by absorbing the energy of the raindrops and thus reducing the surface sealing and runoff, (2) retardation of erosion by decreased surface velocity, (3) physical restraint of soil movement, (4) improvement of aggregation and porosity of the soil by roots and plant residue, (5) increased biological activity in the soil and (6) transpiration which decreases soil water, resulting in increased storage capacity and less runoff (Taffa, 2002).

2.2.5 Topography

Topographic features that influence erosion are degree of slope, shape and length of slope and size and shape of the watershed (Morgan, 1998). According to him, there are three factors of a slope affecting erosion; namely steepness, length, and curvature of a slope. The steeper and/or the longer the slope the more will be the erosion. On steep slopes, runoff water is more erosive and can more easily transport detached sediment down-slope. On longer slopes, an increased accumulation of overland flow tends to increase rill erosion. There are two types of slope curvatures; namely convex and concave. Concave slopes, with lower slopes at the foot of the hill are less erosive than convex slopes (Morgan, 1998 and Taffa, 2002). Generally, soil erosion increases exponentially with increase in slope gradient (Bobe, 2004).

2.2.6 Characteristics of Precipitation

The basic energy input required to drive erosion processes is provided by rainfall and runoff (Taffa, 2002). Therefore, rainfall is identified as the main cause of water erosion. The ability of rain to cause erosion is defined as erosivity and it is a function of rainfall. According to Morgan (1998), soil loss is closely related to rainfall partly through the detaching power of raindrops striking the soil surface and partly through the contribution of rain to runoff. This applies particularly to erosion by overland flow and rills for which intensity is generally considered to be the most important rainfall characteristics.

The amount and peak intensity are two main important characteristics of a rainstorm that influence its potential ability of causing erosion. Volume and peak rate of runoff are measures of runoff erosivity (Morgan, 1998). That is soil movement by rainfall (raindrop splash) is usually greatest and most noticeable during short duration, high-intensity thunderstorms. Generally, the type of precipitation (either rain or snow), the intensity of rainfall, the duration of the rainfall, the distribution of the rainfall, the direction of the prevailing storm are major characteristics of the precipitation that affect soil erosion (Taffa, 2002). He further explains that, climatic conditions such as temperature, wind, humidity, etc. also affect the losses from the drainage basin and, therefore, affect the runoff and hence the soil erosion. If losses are more, runoff will be less and vice-versa.

2.2.7 Socio-economic Factors

Farm income, size of the farm, land tenure system, grazing by livestock and traditional customs are the main factors of socio-economic conditions that influence soil erosion (Morgan, 1998). According to him, if the farmer has no good income erosion control cannot be improved. Small farms are uneconomic for farmers to follow the soil conservation practice due to small income. Soil conservation should be a harmonic action in which everybody and organization must actively participate.

2.2.8 Impacts of Soil Erosion

Both agricultural activities and the physical environment are negatively affected by soil erosion (Pimentel, 2006). Soil erosion reduces crop productivity through decreasing the availability of nutrient, water, soil organic matter, and crop rooting depth. It is thus becoming an alarming ecosystem problem through deteriorating land productivity, reduction in agricultural production, poverty, food insecurity, which further caused loss of biodiversity, change in land use/cover, and water quality depletion.

2.3 Methods of Soil Erosion Assessment

Erosion occurs at varying rates over the landscapes, over a field, and even along a slope profile within a field (Morgan, 1995). Hence to understand soil erosion over an area, it is necessary to assess soil erosion at different landforms. Soil erosion can be predicted by certain method that is reflected by a magnitude of soil loss or relative erosion rates for a given area. Estimation of soil loss rate has to be done in order to assess whether a defined landform has soil loss rate above or below the tolerance level (Morgan, 1995).

2.3.1 Erosion Modeling

A model is a simplified representation of a complex system or models are of necessity simplifications of reality (Taffa, 2002). Mathematical description of soil particle detachment, transport, and deposition on the surfaces of the land is called Soil erosion modeling. Moreover; erosion models can be used as tools for understanding erosion processes and their impacts (Morgan, 1995).

Even though erosion prediction or modeling approaches are not new concepts, these technologies emerged after mainframe computers became readily available (Jain and Kothyari, 2009). Now a day's available model can be categorized in many ways. However, it is vitally important to understand the principles behind the development of erosion models and types of models in order to understand the model's applicability for different locations with variable parameters.

Based on the development principle, erosion models can be classified in to three broad categories, namely empirical or statistical, conceptual and physically based or analytical component models (Morgan, 1998).

2.3.1.1 Empirical Models

Empirical models are statistical in nature and they describe the erosion primarily based on observations (i.e., mathematical correlations are obtained based on observed data analysis). These models indicate the statistical relationships between assumed important variables where a reasonable database exists (Morgan, 1998). In these models, it is assumed that the underlying conditions remain unchanged for the duration of the study (Bobe, 2004). Furthermore, Inputs and out-puts are related through some transformation function. USLE (the Universal Soil Loss Equation), RUSLE (Revised Universal Soil Loss Equation) and SLEMSA (Soil Loss Estimation Model for South Africa) are some of the commonly used empirical erosion models.

2.3.1.2 Conceptual Models

These models are based on spatially lumped forms of water and sediment continuity equations and they describe processes in the watershed, but giving less emphasis to detailed processes and interactions, as this need detail watershed information (Merritt *et al.*, 2003). Conceptual models have an intermediate feature between empirical and physically based models. However, unlike the empirical models, conceptual models whilst they tend to be aggregated, they still reflect the hypothesis about the processes governing the system behavior (Merritt *et al.*, 2003). Among the conceptual models that are used in erosion and/or water quality studies are: The Agricultural Catchment Research Unit (ACRU), Agricultural Non-Point Source Pollution Model (AGNPS) and Hydrologic Simulation Program Fortran (HSPF).

2.3.1.3 Physically Based or Analytical Component Models

Physically based models are based on explaining fundamental physical equations describing stream flow and sediment and associated nutrient generations in a catchment (Merritt *et al.,* 2003). According to Morgan (1998), these models are developed to predict the spatial distribution of runoff and sediment over the land surface during the individual storms in addition to total runoff and soil loss. The European Soil Erosion Model (EUROSEM), the Areal Non-Point Source Water Shed Environment response simulation (ANSWERS) and Water Erosion Prediction Project (WEPP) and are some of the commonly used physically based models used in water erosion studies. Less input requirement, computational simplicity, wide applicability and relative validity are the main criteria that are considered for selection of soil erosion models (Morgan, 1998).

2.3.2 Based on the spatial representation

Based on spatial representation, erosion models can also be classified as lumped, semi-distributed and distributed.

2.3.2.1 Lumped Models

Lumped models provide non-spatially varying representation of hydrological processes, so they do not account for variations of climate in altitude, including temperature drift, and so on ((Ali *et al.*, 2019). The parameters often do not represent physical features of hydrologic processes and usually involve certain degree of empiricism. These models are not usually applicable to event-scale processes. If the interest is primarily in the discharge prediction only, then these models can provide just as good simulations as complex physically based models.

2.3.2.2 Distributed models

Here parameters of the model are entirely allowed to vary in space at a resolution usually chosen by the user. Distributed modelling approach attempts to incorporate data concerning the spatial distribution of parameter variations together with computational algorithms to evaluate the influence of this distribution on simulated precipitation-runoff behavior (Ali *et al.,* 2019). Distributed models generally require large amount of (often-unavailable) data. However, the governing physical processes are modelled in detail, and if properly applied, they can provide the highest degree of accuracy.

2.3.2.3 Semi-distributed models

In semi-distributed model parameters are partially allowed to vary in space by dividing the basin in to a number of smaller sub-basins. These models have an advantage in that their structure is more physically based than the structure of lumped models, requiring less input data than fully distributed models. SWAT (Arnold *et al.*, 1993). HEC-HMS (USACE, 2001), HBV (Bergström, 1995), are considered as semi-distributed models. These models allow for variability, but not for fully distributed values. However, these models are normally computationally fast and provide a good trade-off between representation of spatial variability and short computational time (Ali *et al.*, 2019).

2.3.3 SWAT (Soil and Water Assessment) Model

SWAT is a semi-distributed river basin model that works on a daily time series (Arnold *et al.*, 2012). It is a process-based model developed to assess the land use and management practices effects on water, sediment, and agricultural chemical yields in ungauged watersheds. This model is also physically based and computationally efficient and it has the capacity of an extended simulation for long periods of time. Among the major components of the model are hydrology, weather, soil temperature and properties, plant growth, nutrients, pesticides, bacteria and pathogens, and land management. For the purpose of providing outputs at sub-basin or sub watershed basis, the SWAT model needs information on soils, land use, topography, drainage and climate (Arnold *et al.,* 2012). The sub-watersheds contain hydrological response units (HRUs), i.e., portions of a land in the sub-watersheds that differ their land cover, soil and management combinations regardless of their spatial location from other land areas. The computation is made for each HRU separately and then it routes the water, sediment and nutrients from HRU outlets to the sub-basin outlets and then to the basin outlet to obtain total basin loadings (Neitsch *et al.*, 2005).

2.3.3.1 The Strength and Limitations of SWAT model

Its world-wide application makes the SWAT a multipurpose model making it applicable for coordinated numerous natural forms/processes (Neitsch *et al.*, 2005). The fundamental strength of the model is that, it combines the upland and channel processes by incorporating them in to one simulation package. It has also the capacity of simulation based on physical processes associated with soil-water interaction. The capacity of long-term simulation of watersheds varying in areas from few hectares to thousands of square kilometers is another strength of the model.

SWAT model is flexible in its input data requirement, to incorporate crop characteristics, crop stage and duration, etc. Moreover, it is freely available and hence can easily be downloaded from the official website http://swatmodel.tamu.edu. However, the SWAT model has also some limitations. For instance, the model output is affected by the number of observation points/stations distributed in the study watershed. Adequate number of observation points are required to reflect the presence of spatial variability in hydro-meteorological characteristics in the watershed. Moreover, the SWAT model still needs GIS software and other tools to pre-process the spatial and temporal input data required by the model and to run the model.

2.3.3.2 Hydrological Components of SWAT model

In the SWAT model, the driving force behind all the processes in a given watershed is the water balance. Thus, hydrological processes have to be well simulated in order to precisely predict pesticides, sediments and nutrients. In the SWAT model simulation of the hydrology of a watershed involves two steps (Neitsch *et al.*, 2005). The land phase and routing phase. While the land phase controls the amount of sediment, nutrient and pesticides loading to the main channel in each sub-basin, the routing phase determines the movement of water, sediments, and nutrients through the channel network of the catchment to the outlet. The SWAT model employs the Modified Soil Conservation Service curve number (SCS-CN) method for the estimation of surface runoff volume; whereas, the lateral flow and the return flow are estimated by employing kinematic storage model and by creating a shallow aquifer respectively (Arnold *et al.*, 1998). Channel flood routing is predicted by the Muskingum method. Factors like transmission losses, evaporation, return flow etc., are adjusted for estimation of outflow from a channel.

According to Neitsch *et al.* (2005), the land phase of the hydrologic processes is simulated based on the water balance equation given below

$$\mathbf{SWt = SW0 + \sum_{i=1}^{t}(Rday - Qsurf - Ea - Wseep - Qgw)}$$

Where: **SWt** = the final soil water content (mm);

SW_0 =the initial soil water content on day i(mm);

R_{day} =the amount of precipitation on day i (mm);

Q_{surf} =the amount of surface runoff on day i (mm);

Ea = the amount of evapotranspiration (ET) on day i (mm);

Wseep =the amount of water entering the vadose zone from the soil profile on day i (mm);

Qgw = the amount of return flow on day i (mm).

2.3.3.2.1 Surface Runoff Generation

SWAT provides two methods for surface runoff computation; viz. a modification of the Soil Conservation Service (SCS) Curve Number (CN) method (SCS, 1972) and the Green & Ampt infiltration method (Green and Ampt, 1911). The CN method was initially developed for small agricultural watersheds. The CN varies non-linearly with the moisture content of the soil. It drops to zero as the soil approaches the wilting point and increases to 100 as the soil approaches saturation, with higher CNs associated with higher runoff potential watershed (Arnold *et al.,* 1998). In this method, the ratio of actual retention to maximum retention is assumed to be equal to the ratio of direct runoff to rainfall minus initial abstraction. By using daily or sub-daily rainfall amounts, the surface runoff volumes and peak runoff rates for each HRU are simulated by the SWAT model. When compared with the Green-Ampt method, the SCS-CN method has less data requirement; because, the former needs sub-daily data. The Soil Conservation Service curve number (SCS-CN) surface runoff equation is given by (SCS, 1972):

$$\mathbf{Q_{surf}} = \frac{(\mathbf{P} - \mathbf{I_a})^2}{(\mathbf{P} - \mathbf{I_a} + \mathbf{S})}$$

Where:

$\mathbf{Q_{surf}}$ = Rainfall excess (mm),

P = Rainfall depth (mm),

Ia = Initial abstractions (mm) and

S= Retention parameter (mm).

The value of S varies with antecedent soil moisture and other variables, it can be estimated as. Given the Curve Number for the day (CN), S can be computed as

$$\mathbf{S = 25.4\left(\frac{1000}{CN} - 10\right)}$$

Usually, the initial abstractions (Ia) is approximated as **0.2S**, and thus, the above equation can be rewritten as (SCS, 1972):

$$Q_{surf} = \frac{(P - 0.2S)^2}{(P + 0.8S)}$$

- Runoff will only occur when P >Ia (=0.2S).

The SWAT model can also be employed to calculate the peak runoff rate using a modified rational method (Neitsch *et al.*, 2005). The maximum runoff rate that occurs for a given rainfall event is known as the peak runoff rate. It expresses the erosive power of a given storm. It is an important input for the prediction of sediment loss/soil erosion. According to Neitsch *et al.* (2005), the peak runoff rate in the SWAT model is computed by using the modified rational method. The equation is given by:

$$q = \frac{CIA}{3.6}$$

Where: **q =** peak runoff rate (m^3/s),

C = Runoff coefficient,

I = Rainfall intensity (mm/h),

A= sub-watershed area (km^2)

2.3.3.2.2 Lateral Sub-surface Flow

This is the streamflow contribution which originates below the surface but above the zone where rocks are saturated with water. Interflow in the soil profile is calculated simultaneously with redistribution. It can have an important influence on storm hydrographs particularly when vertical percolation is retarded by a shallow, less permeable soil layer (Neitsch *et al.*, 2005).

In order to compute subsurface flow as a function of the drainable volume of water, saturated hydraulic conductivity, soil slope, hill slope length, and drainable porosity, a kinematic storage model is incorporated in the SWAT model (Sloan and Moore, 1984). Along its downward movement, the sub-surface flow is predicted by the model in a two-dimensional cross-section. The kinematic wave approximation of saturated subsurface/lateral flow assumes that the lines of flow in the saturated zone are parallel to the impermeable boundary; whereas, the hydraulic gradient equals the slope of the bed.

In areas with soils having high hydraulic conductivities in surface layers and an impermeable or semi permeable layer at a shallow depth, lateral flow is significant (Sloan and Moore, 1984). Such systems are characterized by vertical percolation of a rainfall until it encounters the impermeable layer. The water then ponds above the impermeable layer forming a saturated zone of water, which ultimately becomes the source of water for lateral subsurface flow. The equation to compute lateral flow is given as:

$$\mathbf{Q_L = 0.024} * \left(\frac{\mathbf{2.\,DW\,.\,K_s.\;Sl}}{\mathbf{\emptyset_d\,.\,L_h}}\right)$$

Where:

$\mathbf{Q_L}$= lateral flow in mm day^{-1},

$\mathbf{DW}$ = drainable volume of soil water in mm,

Sl = slope in m/m,

$\emptyset_\mathbf{d}$**=** drainable porosity (mm/mm),

$\mathbf{K_s}$ = is saturated hydraulic conductivity (mm/ hr) and

$\mathbf{L_h}$ = is the hill slope length (m).

2.3.3.2.3 Return Flow

Return flow or base flow is the volume of stream flow originating from groundwater (Arnold *et al.,*1993). Groundwater is classified into two aquifer systems: a shallow, unconfined aquifer which contributes return flow to streams within the watershed and a deep, confined aquifer which contributes return flow to streams outside the watershed groundwater, which can be regarded as a loss from the watershed system (Arnold *et al.,*1993). Water percolating down below the root zone is divided into two fractions and each fraction becomes recharge for one of the aquifers. The water stored in the shallow aquifer may replenish moisture in the soil profile in very dry conditions or be directly removed by plant. Moreover, the water in the shallow or deep aquifer may be removed for different uses.

The contribution of ground water to stream flow is simulated by creating a shallow aquifer storage which is recharged by percolation from the unsaturated zone, and discharges to the reach of the watershed. Thus, the water balance for the shallow aquifer is (Neitsch *et al.*, 2005):

$$\mathbf{Aq_{sh,i} = Aq_{sh,i-1} + W_{rech} - Q_{gw} - W_{rev} - W_{d} - WU_{sa}}$$

Where:

$\mathbf{Aq_{sh,i}}$ = shallow aquifer storage in mm on day i,

$\mathbf{Aq_{sh,i-1}}$=shallow aquifer storage in mm on day i-1,

$\mathbf{W_{rech}}$ =the recharge entering the aquifer on day i in mm,

$\mathbf{Q_{gw}}$ = base flow into the main channel on day i in mm and it can be computed as:

$$\mathbf{Q_{gw,i} = Q_{gw,i} * e^{-\alpha\Delta t} + W_{rech}(1 - e^{-\alpha\Delta t})}$$

$\mathbf{W_{rev}}$, =is the amount of water moving into the soil zone in response to water deficiencies on day_{i} (mm),

$\mathbf{W_{d}}$ =the water entering down from the shallow to the deep aquifer on day i (mm),

$\mathbf{WU_{sa}}$ =the water uses from the shallow aquifer (mm),

$\boldsymbol{\alpha}$ =is the recession constant which describes the lag flow from the aquifer, (it can be best estimated by analyzing measured stream flow during periods of no recharge in the watershed) and

$\mathbf{\Delta t}$ =is the time step.

2.3.3.2.4 Flow Routing

The routing phase of the hydrologic cycle is the other component during the simulation of the hydrology of a watershed (Neitsch *et al.*, 2005). The rain that falls directly on the channel and/or addition of water from point source discharges can supplement a flow.

The rate and velocity of flow are defined in the SWAT model using the Manning's equation. Whereas, the digital elevation model (DEM) is used to compute the channel cross section and longitudinal slope. The Routing Outputs to Outlet (ROTO) model developed by Arnold *et al.*

(1996), which is latter on merged to SWAT2005, is used to route the flows through channels and reservoirs in order to support an assessment of the downstream impact of water management. The flow through a channel can also be routed by applying the variable storage coefficient method developed by Williams (1969) or the Muskingum routing method.

2.3.4 Soil Erosion/sediment yield Simulation

The surface erosion caused by rainfall and runoff within each HRU can be estimated by applying the SWAT model, which employs the Modified Universal Soil Loss Equation (MUSLE) developed by Williams and Brendt (Williams and Brendt, 1977).

MUSLE is a version of USLE that directly considers runoff to estimate sediment yield. The difference between the USLE and MUSLE is that, in USLE, the average annual gross erosion is predicted as a function of rainfall energy. However, in MUSLE, the rainfall energy factor is replaced by the runoff factor (Williams, 1975). This has an advantage in that it enhances the sediment yield prediction, avoiding the need for delivery ratios, and hence allows the equation to be applied to individual storm events. The improvement in sediment yield prediction is because of the fact that runoff is a function of antecedent moisture condition and rainfall energy. Since the rainfall factor represents energy used in detachment only, the USLE requires the delivery ratios (the sediment yield at any point along the channel divided by the source erosion above that point). However, delivery ratios are not necessary with MUSLE, because the runoff factor represents the energy used both in the detachment and transport process of the sediment. The modified universal soil loss equation (MUSLE) is given by (Williams, 1975):

$$\mathbf{Sed = 11.8Q_{surf}.\,q_{peak}.\,area_{hru})^{0.56}.\,K_{USLE.}\,C_{USLE}\,P_{USLE}\,LS_{USLE}\,CFRG}$$

Where: Sed = the sediment yield on a given day in metric tons,

Q_{surf} =the volume of surface runoff in mm ha^{-1},

q_{peak} =peak runoff rate in m^3s^{-1}

$Area_{hru}$= the area of the HRU (ha)

K_{USLE} = USLE soil erodibility factor

C_{USLE} =the USLE cover and management factor,

P_{USLE} =the USLE support practice factor,

LS_{USLE}= the USLE topographic factor and

CFRG =the coarse fragment factor.

The runoff erosive energy variable is calculated from the volume of surface runoff and peak runoff rate, which are in turn estimated from the hydrological model component.

2.3.4.1 Sediment Routing in Stream Channel

Peak flow rate and mean daily flow are the two most important variables for sediment routing. During discretization of watershed in to sub-watersheds, every single sub-watershed will have a minimum of one main routing reach. Thus, the sediment load at the downstream reaches will be the summation of the sediment loads routed from each upstream reach (Neitsch *et al.*, 2011).

$$\mathbf{Conc_{sed,max} = C_{SP} * V_{pk}{}^{sp\ exp}}$$

Where: --

$\mathbf{Conc_{sed,max}}$= maximum sediment concentration that the water can transport in ton m^{-3} or (kg/l)

$\mathbf{C_{SP}}$ = user defined coefficient

sp exp= user defined exponents

$\mathbf{V_{peak}}$ =is the peak channel velocity ms^{-1}

In the above equation the value of the exponent (sp exp) for SWAT2012 varies between 1.0 and 1.5 (Arnold *et al.*, 2012).

The value of the peak channel velocity (m/s) ($V_{ch,pk}$) is given by

$$\mathbf{V_{peak} = \frac{q_{peak}}{A_{channel}}}$$

Where: -

$\mathbf{q_{peak}}$=Peak flow rate (m3/s)

$\mathbf{A_{channel}}$ =cross sectional area of the channel(m2)

Moreover, the peak flow rate is determined from the average rate of flow using the following relation

$$\mathbf{q_{peak} = pradjf * q_{flow}}$$

Where: -

$\mathbf{pradjf}$ =is the peak rate adjustment factor

$\mathbf{q_{flow}}$= is the average rate of flow (m3/s)

The maximum concentration of sediment, $\mathbf{Conc_{sed,max}}$, and the concentration of sediment in the reach at the beginning of the time step, $\mathbf{Conc_{sed,ch,i}}$. are compared each other in order to start routing in every reach. Consequently, the sediment yield level at the outlet of a given watershed is affected by these two principal channel processes; sediment degradation and aggradation. Thus,

i. If $\mathbf{Conc_{sed,ch,i}}$ is greater than $\mathbf{Conc_{sed,ch,mx}}$, the main process in the reach segment will be deposition, and the net amount of sediment deposited is computed using the following equation.

$$\mathbf{Sed_{depos}} = \left(\mathbf{Conc_{sed,ch,i}} - \mathbf{Conc_{sed,ch,max}}\right) * \mathbf{V_{watr}}$$

Where: -

$\mathbf{Sed_{depos}}$=the quantity of sediment entering reach segment in metric ton,

$\mathbf{V_{wtr}}$=is the volume of water in the reach segment in m3/s

ii. On the other hand, if $\mathbf{Conc_{sed,ch,i}}$ is less than $\mathbf{Conc_{sed,ch,max}}$, the main process in the reach segment is degradation, and the net amount of sediment re-entrained is computed as;

$$\mathbf{Sed_{deg}} = \left(\mathbf{Conc_{sed,ch,mx}} - \mathbf{Conc_{sedd,ch,i}}\right) * \mathbf{V_{ch}} * \mathbf{K_{CH}} * \mathbf{C_{CH}}$$

Where: -

$\mathbf{Sed_{deg}}$=is the sediment entering the reach segment in metric-ton,

$\mathbf{K_{CH}}$= Erodibility factor of the channel in cm hr^{-1} pa^{-1}, which is conceptually similar to USLE's soil erodibility factor (Neitsch *et al.*, 2011). K_{CH}value< K values in USLE;

$\mathbf{C_{CH}}$= is the cover factor for a channel (i.e., channel degradation from a specified vegetation cover divided by channel degradation from an equivalent area with no vegetation cover (Neitsch *et al.*, 2011).

After computing the amount of deposition and degradation, the total sediment in the reach can be determined using the following formula (Neitsch *et al.*, 2011).

$$\mathbf{Sed_{ch} = Sed_{ch,i} - Sed_{dep} + Sed_{deg}}$$

Where: -

$\mathbf{Sed_{ch}}$ the suspended sediment in the reach (metric-ton)

$\mathbf{Sed_{ch,i}}$= is the initial quantity of suspended sediment in the reach in metric ton

$\mathbf{Sed_{dep}}$=is the sediment deposited in the reach in metric ton, and

$\mathbf{Sed_{deg}}$= is the sediment re-entrained in the reach in metric ton

On the other hand, the quantity of sediment that exits from the reach is computed as;

$$\mathbf{Sed_{out} = Sed_{ch} * \frac{V_{out}}{V_{ch}}}$$

Where: -

$\mathbf{Sed_{out}}$=the sediment that leaves the reach in metric ton,

$\mathbf{V_{out}}$=is the volume of outflow during the time step in m^3 and

$\mathbf{V_{ch}}$ = is the volume of water in the reach segment in m3

The channel peak velocity has a direct proportionality to that of the sediment transport capacity of a given channel, and according to Neitsch *et al.* (2011), this is expressed in the SWAT model:

$$\mathbf{Tch = \alpha v^{b}}$$

Where:

Tch (t/m^3) = is the channel transport capacity;

v (m/s) = is the peak velocity of the channel;

α and b =are coefficients.

The peak velocity of the channel turn is computed by applying the Manning's equation.

$$\mathbf{v = \frac{1}{n} R_{ch}{}^{2/3} S_{ch}{}^{1/2}}$$

Where:

n is Manning's roughness coefficient;

$\mathbf{R_{ch}}$ (m) is the hydraulic radius;

$\mathbf{S_{ch}}$ (m/ m) is the channel bed slope.

Flow velocity increases with slope length and steepness; this in turn intensifies the soil erosion in the watershed (Taffa, 2002).

2.4 Erosion Control Practices

Erosion control/conservation practices are classified broadly as Agronomic, Mechanical measures and Soil Management (Morgan, 1985). There are several agronomic principles and crop management techniques that can reduce soil erosion and maintain or improve fertility of the soil. The various agronomic techniques that can be applied under various farming conditions include: crop rotations, intercropping, strip cropping, ley cropping, alley cropping, cover/green manure crops, stubble mulching/crop residue management, contour cultivation and fertilization.

2.4.1 Filter strips

Filter strip are strips of dense vegetation designed to control or intercept transport of nutrients and pesticides-enriched sediments from upslope area (Gardiner and Miller, 2004). Generally, filter-strips are planted on the lower end of a field to prevent sediment from entering adjacent ditches or streams. These measures facilitate sediment deposition by reducing the velocity of overland flow. Filter-strip parameter are represented in the SWAT model by FILTERW, which is the width of filter strip and is applied to the land slope between 0 and 20% (Gardiner and Miller, 2004). The sediment trapping efficiency of filter strips ranges from 24% to 100% (White and Arnold, 2009). The values recommended by Arabi *et al.* (2007) can be used for parameter adjustment.

2.4.2 Contour Farming

It is a practice of ploughing the land and planting crops along a contour line as opposed to along the slope. Contour farming can effectively reduce sediment yield at watershed scale. It can reduce sediment loading by 49% (Gassman *et al.*, 2006) and Arabi *et al.*, 2008). Contour farming/ contour bunds reduce the volume and velocity of surface runoff and hence small amount of soil is eroded and even eroded particles are retained in the bund. In the SWAT model contour farming is represented by SCS curve number (CN) and USLE practice factor (USLE-P). The impact of contour farming is assessed by modifying these two parameters. The recommended values for curve number (CN) can be derived from the table given by (Neitsch *et al.*, 2005). In the recommendation table, beside to contour farming, the impacts of strip cropping, terracing and residual management on the curve number are also included. The following table presents the USLE erosion control practice factor (USLE-P) for fields under contouring, strip cropping and terraced conditions. These values can be used to simulate the erosion reduction that results from the implementation of the corresponding control practice.

Table 1 USLE-P factor value (adapted from Arabi *et al.,* 2008).

Land Slope	**USLE-P**			
	Contour Farming	Strip Cropping	Terracing	
			Type-1[a]	Type-2[b]
1-2	0.6	0.3	0.12	0.05
3-5	0.5	0.25	0.1	0.05
6-8	0.5	0.25	0.1	0.05
9-12	0.6	0.3	0.12	0.05
13-16	0.7	0.35	0.14	0.05
17-20	0.8	0.4	0.16	0.06
21-25	0.9	0.45	0.18	0.06

[a]Type-1: Graded channel sod outlet

[b]Type-2: Steep Backslope underground outlets

2.4.3 Terraces

Terraces are soil conservation structures consisting of a series of horizontal ridges constructed on hillsides (Neitsch *et al.,* 2005). Terraces are constructed to reshape the land in areas of high rainfall and hence to reduce erosion, to remove excess surface water and to retain maximum amount of moisture for crop production (Gardner and Miller, 2004). These structures divide a long slope in to a series of shorter and relatively to level steps, there by shortening the length of the slope. Applying physical structures such as terraces made from stone bunds reinforced by biological measures like filter strips in low slope areas of a given watershed could give potential effect (Betrie *et al.,* 2011). In SWAT model, terracing can be simulated by changing both erosion and runoff parameters (Arnold *et al.*, 2012).

There are different types of terraces. Some of them are Fanya juu, Stone/soil bund, bench terraces, etc. Fanya-juu terrace are usually applied on land slope ranging between 20 and 40%, the bench terraces are applied on land slope of greater than 40%. Whereas, the stone-bunds are applied on land slope of 0-20% (Neitsch *et al.*, 2005).

2.5 Effectiveness of SWC measures

several case studies in Ethiopia indicate the positive effects of SWC measures at various spatial scales (plot, hillslope, and small and medium watersheds). Studies conducted by Haregeweyn *et al.* (2015) revealed that major erosion control measures (such as: stone bunds, trenches with or without bunds, fanya juu terraces, ex-closures, and watershed management and conservation tillage) can reduce the runoff by about 4% in Andit Tid (North-west Ethiopia) and 62% in Gununo (Southern Ethiopia) with a mean seasonal runoff by 40%. Likewise, the range in soil loss was from 35-89%, with an average of 65%. Moreover, studies carried out at large basin scale level also revealed the effectiveness of conservation structures. A sediment management model of the Blue Nile Basin using the SWAT model by Betrie *et al.* (2011) presented the effectiveness of conservation structures in sediment yield reduction. The study revealed that implementation of grass strips reduced the SY at the outlet of the Upper Blue Nile Basin by 44% on the other hand, stone bunds application was also effective thereby reducing the sediment yield by 41% and reforestation measures reduced the sediment yield by 11%. Generally, soil and water conservation efforts in Ethiopia are more effective in semi-arid areas when compared with the effects in humid area (Hurni *et al.*, 2005). Taye *et al.* (2013) studied the gradual changes in the effectiveness of stone bunds and trenches for the reduction of runoff and soil loss in the semi-arid Ethiopian highlands and found that, stone bunds and trenches are only fully effective in the first year of their implementation. Other studies also ratify these findings. In the second year of their implementation, the effectiveness of unmaintained soil and water conservation structures decreases by 80% of their original value, in the third by 50% and in the fourth year its effect declines nearly to 0% (Haregeweyn *et al.*, 2015).

2.5.1 Effects of Soil and water control practices on runoff

Soil and water conservation structures strongly affect seasonal runoff coefficient (Taye *et al.*, 2013). When soil and water conservation structures are installed, the runoff coefficient decreases with increasing slope gradient. The structures hold water into small ditches; thus, allowing water to percolate down the soil profile more efficiently. Due to the reduction in slope length, this structures also reduce peak flow rates (Taffa, 2002). The considerable decrease in surface runoff also reflects the role of terraces in flood control since much of the flood water will be retained and permitted to percolate down the soil profile. Though soil and water conservation measures vary in their efficiency, all soil and water conservation measures reduce runoff (Taye *et al.,* 2013). Furthermore, the study findings demonstrated that the absolute effect of individual soil and water conservation measures on runoff coefficient is affected by slope gradient. In croplands, effects of individual soil and water conservation measures on runoff coefficient is affected by slope gradient, with a reduction of 20 to 45% for stone bunds and 56 to 76% for stone bunds with trenches. Likewise, Hurni *et al*. (2005) studied the effects of level stone terraces over 80% of a catchment in semi-arid Eretria and found a runoff coefficient reduction of 50% at catchment scale, with an area of 1.77 km2. However, the findings of Hurni *et al.,* (2005) and Herweg and Ludi (1999) for more humid highlands in Ethiopia at runoff plot scale exhibited a small (i.e., 10%) reduction in runoff coefficient for graded SWC structures (i.e., for 15% graded fanya juu and graded bunds).

2.5.2 Effects of Soil and water control practices on Soil loss

Studies indicate that, regardless of land use types and slope gradients, soil and water conservation measures significantly influence soil loss from plots. Though the effects of individual soil and water control measures on soil loss is a function of slope position, their effects relative to their respective control plots is not affected by slope gradient (Taye *et al.,* 2013). Implementation of stone bunds on cropland at farmer's field scale reduce soil loss by 68% (Gebremichael *et al.,* 2005). While their application in rangelands and croplands reduces soil loss on average by 63% and 47%, respectively (Taye *et al.,* 2013). soil and water control measures also significantly influence sediment transport processes, which is attributed to the small sediment retention basins created behind the structures. After implementation of physical soil and water conservation measures, Nyssen et al. (2009a) found that, the soil loss at catchment scale (i.e., 1.87km^2) reduced from 14.3-ton ha^{-1} yr^{-1} to 9 t ha^{-1} yr^{-1}. Generally, except for stone bunds with trenches which showed a soil loss of 1.5-ton ha^{-1} yr^{-1} for both range and croplands, for similar soil and water conservation measures, seasonal soil loss is less on cropland compared to rangeland (Taye *et al.,* 2013). Those plots treated with stone bunds exhibited a mean seasonal soil loss of 14.6-ton ha^{-1} in rangeland, while the soil loss from cropland was only 6-ton ha^{-1}. Moreover, the study findings endorsed that, areas having high rock fragment cover at the surface reflected less soil loss for higher slope gradient.

2.5.3 Effects of Land use practices on runoff and Soil loss

The major effects of land use and land cover in reducing erosion are (1) interception of rainfall by absorbing the energy of the raindrops and thus reducing the surface sealing and runoff, (2) retardation of erosion by decreased surface velocity, (3) physical restraint of soil movement, (4) improvement of aggregation and porosity of the soil by roots and plant residue, (5) increased biological activity in the soil and (6) transpiration which decreases soil water, resulting in increased storage capacity and less runoff (Morgan, 1998). Rangelands exhibit higher runoff response, which is attributed to intensive grazing and surface compaction (Taye *et al.*, 2013). A study on event bases at runoff plot scale on rangelands in the central highlands of Ethiopia showed a high runoff coefficient of 39-72%, which is a consequence of intensity in grazing (Mwendera and Mohamed, 1997). On the other hand, tillage operation creates a rough soil surface, which provides space for surface storage, thereby reducing the runoff and soil loss (Bewket and Sterk, 2003). Taye *et al.* (2013) observed that, the average soil loss from rangelands (i.e., 39 tons ha^{-1}) is higher than the average soil loss from resulting from croplands, which is 11 tons ha^{-1}. This is attributed to the higher runoff coefficient in rangelands resulting from intensive grazing and soil compaction during the rainy season. Whereas, soil tillage contributed to lower runoff coefficient and soil loss in croplands. The study conducted by Nyssen *et al.* (2009) at runoff plot scale in Tigrai revealed a higher soil loss from rangelands, 17.4 tons ha^{-1} yr^{-1}, while, the soil loss from cropland being 9.7 tons ha^{-1} yr^{-1}. Similarly, the study by Mwendera and Mohamed (1997) at Deberezeit, Ethiopia, demonstrated a higher soil erosion rate of 4.9 tons yr^{-1} from intensively grazed rangeland of 4-8% slope gradient. This attributed to the removal of vegetation cover and trampling by livestock.

3 MATERIALS AND METHODS

3.1 Study Area Description

3.1.1 Location

Weyib watershed is located in the south eastern part of Ethiopia, sharing the Oromia and Somali regional states, and is located between 6° 50′ 00″ – 7° 25′ 00″N latitudes and 39° 30′ 00″ – 40° 34′ 00″E longitudes (GDMP, 2007). Weyib river is one of the three sub-basins of Genale-Dawa river, viz. Genale, Dawa and Weyib (GDMP, 2007). According to Genale Dawa Master Plan study (GDMP) (2007), the Weyib main river, starting its course from the northern margins of Bale Mountains, flows to the Indian ocean through the Ethiopia-Somali lands. The study watershed has an area of 24369.6 km^2 and its altitude variation ranges from 4389 (m.a.s.l) at the highest point to 898 (m a.s.l) at its outlet (Abdulkerim and Arup, 2016). The upstream part of the Weyib watershed, the 'Sannete' area (with an altitude of 4389 m above sea level), is one of Ethiopia highlands, which receives high amount of rainfall. The northern flank of the Bale Mountain is the source of the Weyib river. It then flows north – eastwards before changing its direction to the east and south-eastwards for the rest of its course. Before leaving Ethiopia, it finally joins the Genale and Dawa Rivers near Ethiopia-Somalia border and makes its journey to Somali lowlands (Abdulkerim and Arup, 2016). Its major tributaries are Shaya, Tegona and Tebel. The Tebel River originates close to the northern Wabi-Shebelle divide near Ginir.

3.1.2 Climate

The study area receives a mean annual rainfall of about 1015 mm and reaches 1688 mm at the highlands of Dinsho, western part of the study watershed (Sisay *et al.*, 2019). The maximum rainfall, which covers 33% of the annual rainfall occurs during February – April. Whereas, the next rainfall period covers the period from June to September (Sisay *et al.*, 2019). The rainfall of the study area has got a bimodal shape with double peaks in the month of April and August (Abdulkerim and Arup, 2016). The annual air temperature of the watershed ranges between 3.0 ^{0}C and 25 ^{0}C and the mean annual temperature is 14 ^{0}C. The climate of the watershed varies from humid subtropical to arid (Sisay *et al.*, 2019). According to them, the mean annual reference evapotranspiration of the study area is 842.7 mm whereas, the actual evapotranspiration is 970.1 mm. The mean daily evapotranspiration ranges from 3.1 to 3.9 mm/day, with an average of 3.4 mm/day.

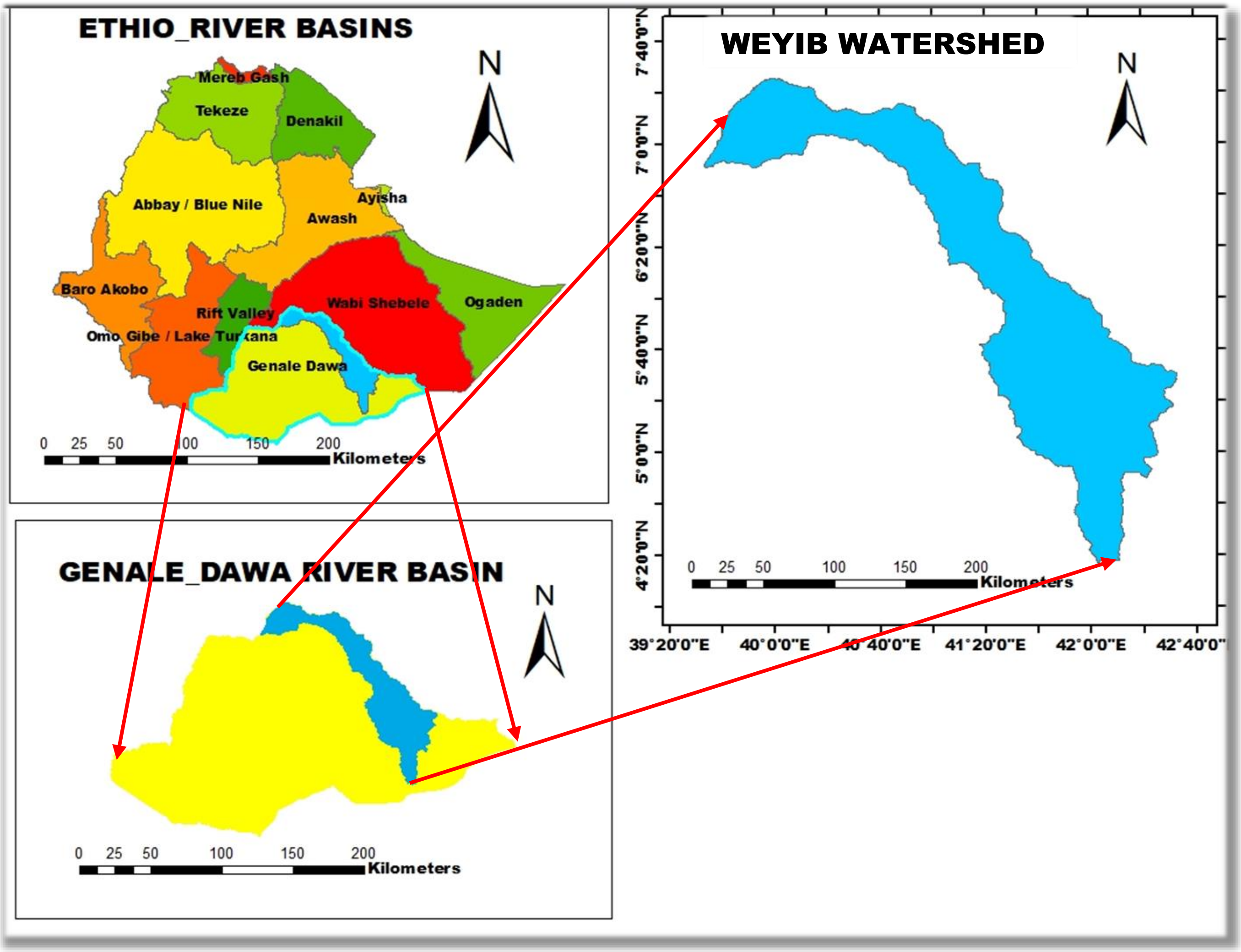

Figure 1: Location map of Weyib watershed (Source: adapted from GDMP, 2007)

3.1.3 Topography

A great variation in elevation characterizes the upstream and downstream portions of the study watershed. Since the upstream portion of the watershed is the steepest part, it requires serious consideration. Moreover, Bale Mountains National Park is found in this part of the watershed; which is hydrologically the most sensitive part (Sisay *et al.*, 2019). The slope class of the study area is characterized by gentle (0-7%), moderate (7-25%) and steep slope of (25-56%), with an area coverage of 2.65% steep hills and mountains, 23.70% flat to undulating, and 73.65% gentle slope (Sisay *et al.*, 2019). Gentle slopes are found in the middle part of the watershed including, Agarfa, Sinana, Gasera, lower parts of Goba and Dinsho districts.

3.1.4 Soil

The major soil types of the study area are Cambisol, Luvisol, Vertisol, Regosol and Leptosol (GDMP, 2007). Among these, the dominant soil types are Cambisol, Luvisol, Leptosol and Calcisol, which have an area coverage of 30.94, 19.11% 15.12% and 12.26% respectively.

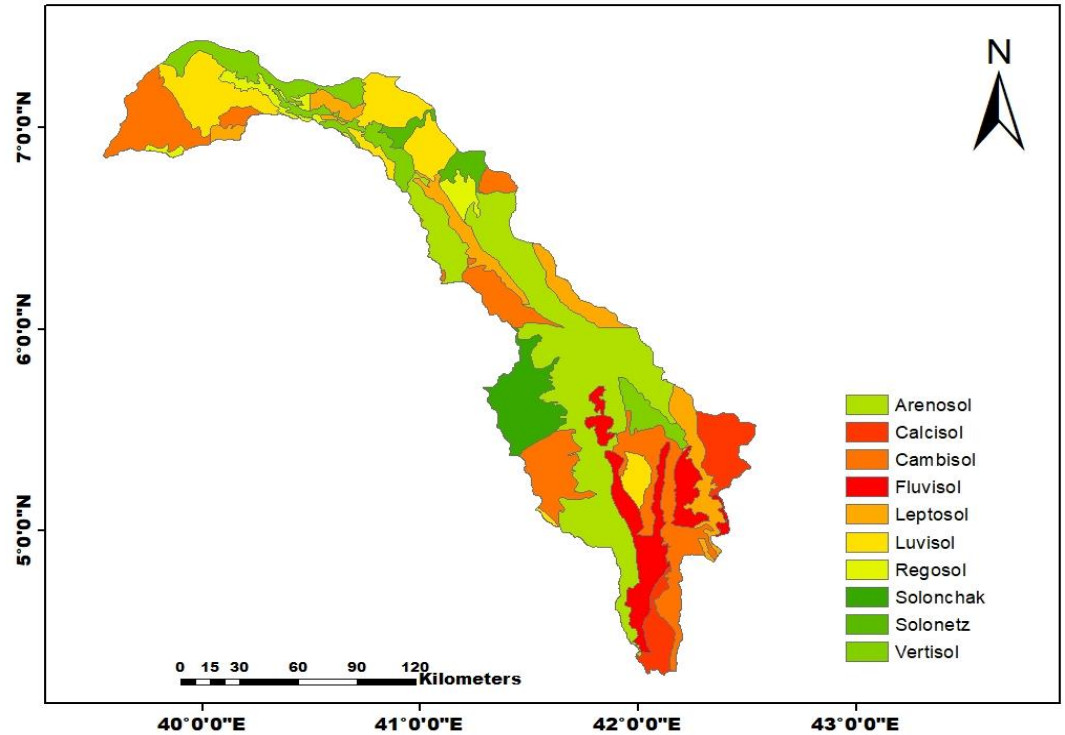

Figure 2: Soil map Weyib watershed (Source: adapted from GDMP, 2007)

Table 2 Major soil types of Weyib watershed (adapted from Sisay *et al.*, 2019 and GDMP, 2007)

SOIL TYPE	AREA (km^2)	AREA (%)
Cambisol	7541.14	30.94
Leptosol	3685.3	15.12
Arenosol	2064.09	8.47
Regosol	742.31	3.05
Luvisol	4656.91	19.11
Fluvisol	948.38	3.89
Solonchak	450.11	1.85
Calcisol	2987.36	12.26
Vertisol	1274.71	5.23
Solontez	19.29	0.08
Total	**24369.6**	**100**

3.1.5 Population size

The Weyb watershed is shared between Oromia and Somali reginal state. It includes Bale west Arsi (some part), Afder and Liben zones. Among the woredas which are found in the study watershed are: Agarfa, Afder, Chereti, Dolo Bay, Dolo Odo, Elkere, Dinsho, Sinana, Goba, Goro, Gasera, Gura Damole, Rayitu, Seweyna and Ginir (GDMP, 2007). According to the Central statistical Agency, the total population living in the Weyb watershed in 2007 was 534,348 and its annual growth rate is assumed similar to the national population growth rate of 2.6% (Sisay *et al.*, 2019).

3.1.6 Land Use/Land Cover (LULC)

According to GDMP (2007), there are three major types of land use types in the watershed, viz. agricultural land use covering 79.37%, pasture land covering 15.5 % and forests covering 2.18%. The afro-alpine ecosystem that is known to be the largest area in Ethiopia is found in the upper most part of the watershed. Whereas, a dense forest is commonly found in the upper part of the watershed in Dinsho and Sannete highlands, and also in the lower part of the watershed near Sof-umer (GDMP, 2007).

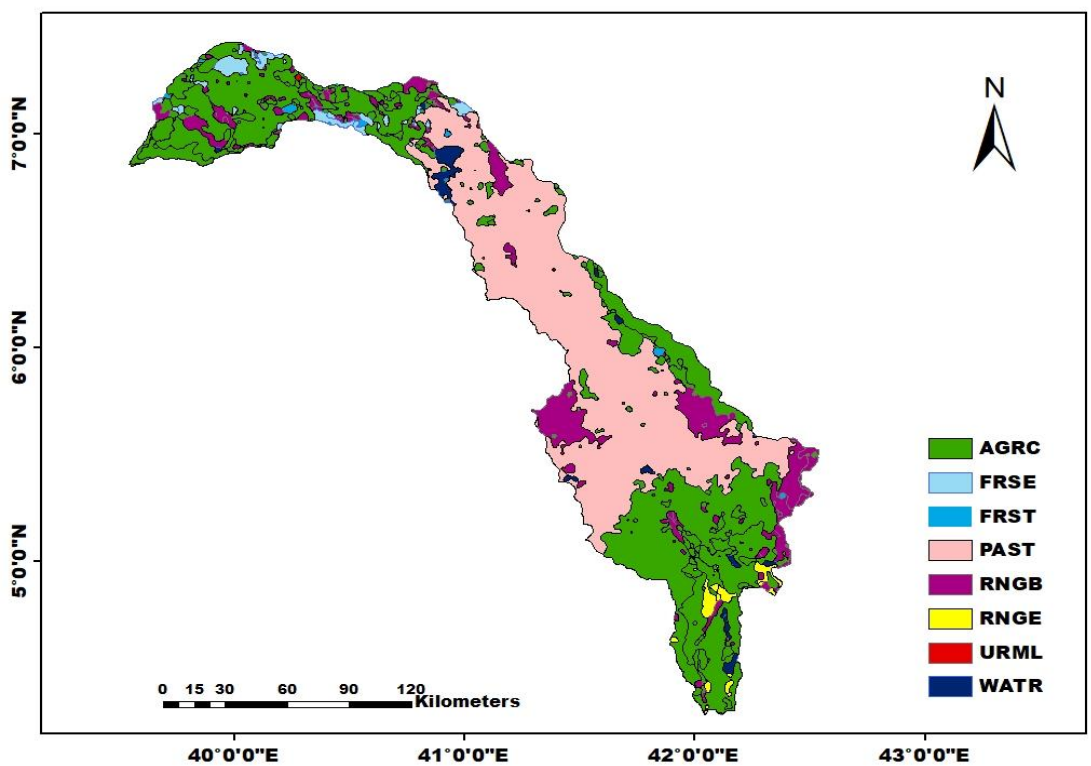

Figure 3 land use map of the Weyib watershed (Source: adapted from GDMP, 2007)

3.2 Materials and Tools Used

A variety of materials and equipment were used to collect the necessary input data for this study analysis. For this study, the Digital Elevation Model**,** DEM with a resolution of (30 mx30m) obtained from the Information and Communication Directorate of the Ministry of Water, Irrigation and Electricity was used. Other materials which were used in this study include: GPS for collection of geographic coordinate points, Land use/Land cover map of the study area, Computer, Microsoft Excel, Microsoft Word and Access and other miscellaneous stationeries were used. ArcGIS 10.2 software was used to generate DEM (Digital Elevation Model), Slope and Aspect, for delineation of watershed boundary and to develop the Land use/ Land cover of the study area. On the other hand, ArcSWAT (arcswat_201210_219) was used to preprocess GIS data. Arc SWAT provides a graphical user-interface that allows for GIS data to be easily formatted for use in SWAT model simulations.

3.3 Justification for Selection of the model

A number of criteria are there to choose the right model for a given study. Those criteria are often project specific, as projects have their own specific requirements and needs. Criteria can also be user dependent (i.e., related to personal preferences). According to Cunderlic (2003), there are four main common considered criteria; viz,

- The model outputs required for the intended purpose and therefore to be estimated by the model
- The hydrologic processes that need to be modeled to estimate the desired outputs adequately
- Availability of input data required by the model
- Price

Moreover, the major problem that is going to be addressed has to be the main driver for model selection. One of the most commonly and widely applied conceptual Daily rainfall-runoff model when there is adequate rainfall and runoff data for calibration and validation is using Arc-SWAT model. Arc-SWAT has got wider acceptance in many parts of Ethiopia, including the study area. Consequently, SWAT model was selected for this study.

3.4 Data used for the study

3.4.1 Model Inputs/data

Identifying the spatial inputs/ parameters of static variables such as; topography, soil layer and land use data and temporal inputs like rainfall, minimum and maximum temperature, relative humidity, solar radiation, and wind speed, is a necessary pre-simulation task to get a satisfactory output. The following were some of the data used for the study.

3.4.1.1 Digital elevation model

The SWAT model employs the Digital Elevation Model (DEM), which is a digital representation of topographic surfaces at certain spatial resolution, to delineate a watershed and sub-watersheds and to define drainage networks. Furthermore, it was also employed to derive sub-watershed parameters like the slope, slope length, and to determine stream networks in the watershed. These data were processed in ArcGIS software. A Digital Elevation Model, DEM, with a resolution of 30 m obtained from the Information and Communication Directorate of the MoWIE was used for this study.

3.4.1.2 Stream flow and Sediment data

The Study watershed has one main river which is called Weyib River. The daily hydrological data consisting of stream flow and suspended sediment load for the period 1992-2012, at Shaya, Sofumer, Tegona, Denbel, Alemkerem and Tebel gauging stations was acquired from the Hydrology and water Quality Directorate of the Ministry of Water, Irrigation and Energy. This data was checked for its reliability. Among the stations mentioned, the flow data of the Sofumer gauging station was selected and transferred to the location of interest (i.e., Weyib outlet) using regional equation as it has been described in section 3.7.2.1., because the location selected as an outlet for this study lacks recorded flow and sediment data. Consequently, this flow data which was obtained by the regional equation was used for the purpose of sensitivity analysis, calibration and validation of SWAT model. Similarly, the sediment data for the location under consideration was derived using regional equations developed by McMahon *et al.* (2002) and WWDSE (2011) as described in section 3.7.2.2. Then, the flow and sediment load data were reprocessed in excel spread sheet and organized as pe the inputs needs of the Arc SWAT model. Then, the dataset for the period 1992-2004 was applied for model calibration, and the remaining stream discharge data (i.e., from 2005-2012) was applied for model validation.

3.4.1.3 Meteorological/climatic data

The SWAT model needs daily records of meteorological data. These data can either be obtained by direct measurement or they can be prepared by using the weather generator (XWGEN). The key essential meteorological data needed by the model include Precipitation, maximum and minimum air temperature, relative humidity, wind speed and solar radiation. Daily meteorological data of the Dinsho, Homa. Goro, Adaba, Dodola, Agarfa, Sinana, Meliyu, Gassera, Ginnir woredas' and Robe town weather stations, which are inside the watershed, were used to calculate the average areal rainfall using the Thiessen polygon extension in ArcGIS. These meteorological data were collected from National Meteorological Agency. Once collected, the daily recorded data were rearranged using excel spreadsheet, and converted and saved in text format, (to the format that the SWAT model requires).

The meteorological stations at Robe and Ginir (Robe22 and Ginir31) contain all the meteorological data required by the SWAT model, i.e., precipitation, maximum and minimum temperature, relative humidity and sunshine hours. Whereas, Adaba43, Dinsho13, Gassera23, Goro13, Meliyu33 and Sinana43 stations contain records of rainfall data and maximum and minimum air temperature. On the other hand, Dodola24, Homa14, Meliyu24, Gassera14, Agrafa14 and Goro31 contain records of the precipitation data only. The table below shows those stations which have good data quality (with fair missing data) and hence selected for input data (XWGEN) preparation.

Table 3 Meteorological station location and duration of records

ID	Name of station	Lat	Long	Elevation	Data series
1	Robe22	795077.99	4453559.00	2480.00	1988-2012
2	Agarfa14	808048.74	4427597.07	2550.00	1988-2012
3	Agarfa21	778400.00	4436862.93	2550.00	1988-2012
4	Dinsho13	789518.00	4422038.07	3072.00	1988-2012
5	Dodola24	777639.60	4358295.60	3000.00	1988-2012
6	Gassera14	795077.26	4442421.26	1680.00	1988-2012
7	Ginnir31	795077.93	4525826.00	1750.00	1988-2012
8	Homa14	795077.96	4442414.59	1680.00	1988-2012
9	Adaba43	780253.07	4381272.00	2420.00	1988-2012
10	Sinana43	786553.40	4472830.40	2500.00	1988-2012
11	Meliyu24	761703.96	4503590.00	1580.00	1988-2012
12	Goro13	778400.00	4499891.41		1988-2012
13	Goro31	778400.00	4499891.41		1988-2012

3.4.1.3.1 Precipitation/rainfall data

All selected stations have the same precipitation data period, from 1988-2012, though with different degrees of missing records. The meteorological stations at Robe and Ginir (Robe22 and Ginir31) have relatively small missing precipitation data values. Consequently, these two meteorological stations were used for weather generator data preparation, this weather generator in turn was used to generate data for those stations with missing records.

3.4.1.3.2 Temperature

The annual air temperature of the watershed ranges between 3.0 ^{0}C and 25 ^{0}C and the mean annual temperature is 14 ^{0}C. The climate of the watershed varies from humid subtropical to arid (Sisay *et al.,* 2019). With regard to temperature, only Robe22 and Ginir31 meteorological stations have a daily maximum and minimum air temperature of full records for the time period selected, with a relatively small missing temperature record. Consequently, these two meteorological stations were used for weather generator data preparation.

3.4.1.3.3 Other climatic data

Other climatic data needed to prepare the weather generator include Relative humidity, solar radiation and wind speed. For this purpose, Robe22 and Ginir21 were selected, because these stations contain all the meteorological input data required by the SWAT model (including, daily relative humidity, daily solar radiation and daily wind speed). The corresponding location tables were prepared in text format to make it compatible for the SWAT model. Eventually, these data were integrated into the model using the weather data input wizard. Dew point temperature calculator (DEW02) was used to calculate the monthly average dew point temperatures. On the other hand, the main input parameters required by the Weather Generator, including the average monthly precipitation, the standard deviation, the skew coefficient, etc., were estimated using PcpSTA software. Moreover, in order to convert sunshine hour to Solar Radiation an empirical equation developed by Angstrom was applied.

3.5 Data Quality analysis

Precipitation data needs to be tested for its accuracy/consistency before it is used for further analysis. Data quality control was carried out by visual inspection, filling of missing data, and by applying and plotting cumulative/ accumulated plot and double mass curve. Since incorrect input data to the model yields an incorrect output, the precipitation data was first tested for missing records or gaps in the data series and for outliers. In the same way, the Stream flow data of the

Weyib watershed at Sofumer gauging station was checked for data quality by visual inspection, filling of missing data and by applying and plotting cumulative/ accumulated plot and double mass curve. At the same time, the data was also checked for unrealistic data record or for outliers. These outliers are observations that appears to deviate distinctly from other observations in the sample.

Generally, for further application of the stream flow and rainfall data, their consistency was checked using double mass curve analysis. This plot of accumulated discharge/rainfall data at base station against the accumulated average at the surrounding stations was generally used to check consistency of stream flow /rainfall data. Beside to the double mass curve, the values of coefficient of correlation provided by Nemec, (1973) were used to check the degree of consistency, which states that a value of coefficient of correlation, r=1 implies direct linear correlation, an r value between o.6 and 1 implies good direct correlation, a value between -0.6 and 0 shows insufficient – reciprocal correlation, a value between -1 and 0.6 is a good reciprocal correlation and an r value r=-1 expresses a reciprocal linear correlation. For this study, the value of correlation coefficient for the stations selected was found to be mor than 0.85 consequently, it can be inferred that the data records of these stations was consistent.

3.5.1 Visual Inspection

The priority task for inspecting data quality was visual inspection. This was done by inspecting the existence of complete records of date and time and the existence of patterns of physical variation (gauging instrument malfunctioning). For this purpose, the time series data was plotted against time. Moreover, tabular and graphical comparison was made for daily and monthly data. Then suspicious data detection was performed by comparing the monthly totals, maxima and minima of the data of selected stations. The percentage of missing precipitation data points for the period 1988-2012 is shown in the following table. From the table it can be seen that, Goro31 station has 3545 missing data values, which accounts about 38% of the total data available. Meliyu24 station has the next higher missing data values with missing data of 3344, which is 33% of the total data pints.

Table 4 the total number of precipitation data points and missing values

Station Name	Data points	No. of missing data	Points with data	% of missing data
Adaba43	9133	2557	6576	28.00
Agarfa14	9133	1827	7306	20.00
Dinsho13	9133	835	8298	9.14
Gassera14	9133	950	8183	10.40
Ginir31	9133	992	8141	10.86
Goro31	9133	3545	5588	38.82
Homa14	9133	1625	7508	17.79
Meliyu24	9133	3044	6089	33.33
Robe22	9133	134	8999	1.47

3.5.1.1 Missing Rainfall data

Gaps in the record of rainfall at the monitoring station can arise from instrumental failure or malfunction or damage in the recording devices or absence of station operator (observer) from a station or due to any other reason. Before using this rainfall data for further analysis, the gaps in the records should be filled by using different methods of estimating missing rainfall data. The techniques for these estimates are based on simultaneous records for the surrounding stations nearest to and fairly distributed about the station with missing records. By assuming hydro meteorological similarity between group stations, the missing data was filled by using the values of surrounding stations located within the basin. To fill these missing data, various methods are available. Some of them are arithmetic mean, Normal ratio, Regression equation and inverse distance weighing method (Richard, 1998). According to him, if the normal annual precipitation doesn't exceed ten percent of the gauge/station data, the missing data are filled by using the Arithmetic mean method. Whereas, if the normal annual precipitation at the index stations exceeds the precipitation station by ten percent, the normal ratio method is applied. On the other hand, if the normal annual rainfall for the stations is lacking, the inverse distance weighing method can be applied to fill the missing data. Accordingly, for this study, both arithmetic mean and normal ratio method were applied.

I. Arithmetic Mean Method

Simple Arithmetic Mean method is often employed to estimate missing values when the normal annual precipitation at each of the neighboring stations is within ten percent of that of the station with missing records (Richard, 1998).

$$\mathbf{P_{a}} = \sum_{i=1}^{n} \frac{(\mathbf{P_1} + \mathbf{P_2} + \mathbf{P_3} + \cdots + \mathbf{P_n})}{\mathbf{n}}$$

Where: - $\mathbf{P_a}$ **is** the value of the missing rainfall

$\mathbf{P_1}$, $\mathbf{P_2}$, $\mathbf{P_3}$ **and** $\mathbf{P_n}$ are individual value of each precipitation stations

n is the number of precipitation stations in the watershed.

II. Normal Ratio Method

This method is actually applied on the occasion that the normal annual precipitation of the surrounding station differs by more than ten percent 10% of the missing stations (Richard, 1998).

$$\frac{P_x}{N_x} = \frac{1}{N}\left(\sum_{i=1}^{n} \frac{P_i}{N_i}\right)$$

Where: -

Px= missing precipitation at station x

Nx= normal long term, usually annual precipitation at station X

Pi= precipitation value at neighboring station i

N= normal long-term precipitation for neighboring station i

n= number of neighboring stations

3.5.2 Consistency and homogeneity of rainfall data

Time series data such as rainfall are often subject to changes due to measurement techniques, observational procedures, environmental characteristics, structures and location of stations. Thus, before using these time series data for analysis, the variation of the statistical properties has to be examined. For the purpose of selecting typical meteorological station, the homogeneity of neighboring stations has to be examined. The homogeneity of the representative meteorological stations was computed as the ratio of the long term averaged monthly precipitation for a given station to that of the average yearly precipitation of the stations, called non-dimensional parametrization method. The homogeneity of the rainfall data was computed by using the following equation.

$$\mathbf{Pi} = \frac{\mathbf{P_{i,avr}}}{\mathbf{P_{avr}}} * \mathbf{100}$$

Where:

$\mathbf{P_i}$ is the value of the precipitation for the month I and station i

$\mathbf{P_{i,avr}}$ is the long term averaged monthly precipitation for the station i

$\mathbf{P_{avr}}$ is the average yearly precipitation of the stations

For comparison purpose, records of selected precipitation station were plotted against each other (Fig 9 below). The figure/graph indicated the same trend for the stations; hence, these representative stations were found to be homogeneous.

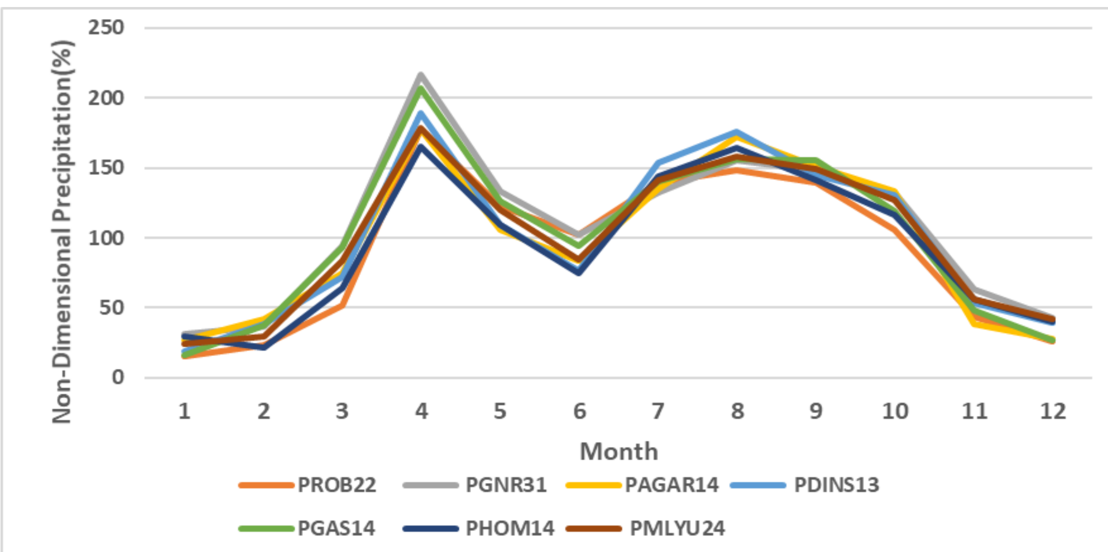

Figure 4 Homogeneity test for selected meteorological stations at Weyib watershed

There can often be a substantial shift in and around a specific rain gauge station. These modifications begin to impact the recorded data. It may be realized late after years that the information recorded/read from these gauging stations is inconsistent. Thus, this inconsistency has to be adjusted. For this study, Double Mass Curve analysis method was applied to detect such inconsistency, and hence to correct and adjust the reported rainfall values.

The double-mass curve theory is based on the fact that during the same period, a graph of the cumulation of one quantity against the cumulation of another quantity will plot as a straight line as long as the data is proportional; the line slope will represent the proportionality constant between the quantities (Subramanya, 2008). A break in the slope of the double-mass curve means that a change in the constant of proportionality between the two variables has occurred or perhaps that the proportionality is not constant at all rates of cumulation. If the possibility of a variable ratio between the two quantities can be ignored, a break in the slope indicates the time at which a change occurs in the relation between the two quantities.

Furthermore, in double mass curve analysis if recorded data are from the same source, they are said to be consistent (Subramanya, 2008). On the other hand, if there is a gradient difference in the plot of the double mass curve, there is inconsistency and it must be adjusted by applying the following formula:

$$\mathbf{P_{CS} = P_S(\frac{M_c}{M_a})}$$

Where: -

PCS = Adjusted precipitation for station **S** for any time

PS = Precipitation for station **S** and for any time t before adjustment

Mc = Slope of the double mass curve after the break

Ma = Slope of the double mass curve before the break

In this study, groups of neighboring stations nearby the doubtful station were chosen. The average annual rainfall values of certain representative stations were organized in decreasing order of their corresponding years. Finally, to check for inconsistency of the recorded precipitation data, the average annual cumulative values of PADAB43, PAGAR14, PDINS13, PGOR13, PGAS14, PHOM14 AND PMLYU 24 was plotted against the average annual cumulative of the PROB22 and PGNR31 (which were selected as base stations), as these two stations hold all meteorological data with small missing data points. The results of the Double Mass Curve displayed the same gradient for all the stations; hence, there was no inconsistency in the precipitation data.

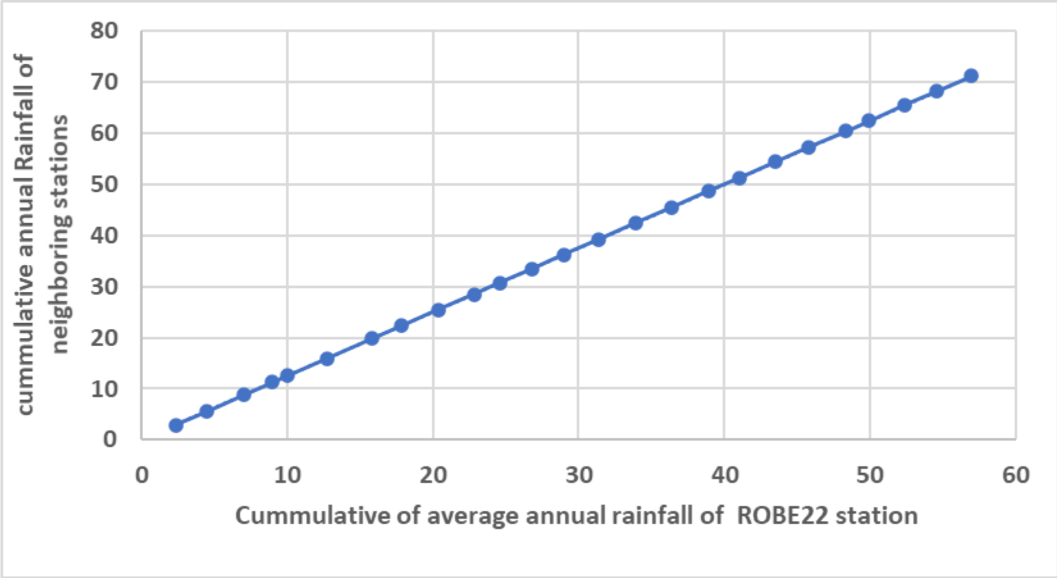

Figure 5 Double mass curve of ROBE22 station after adjustment

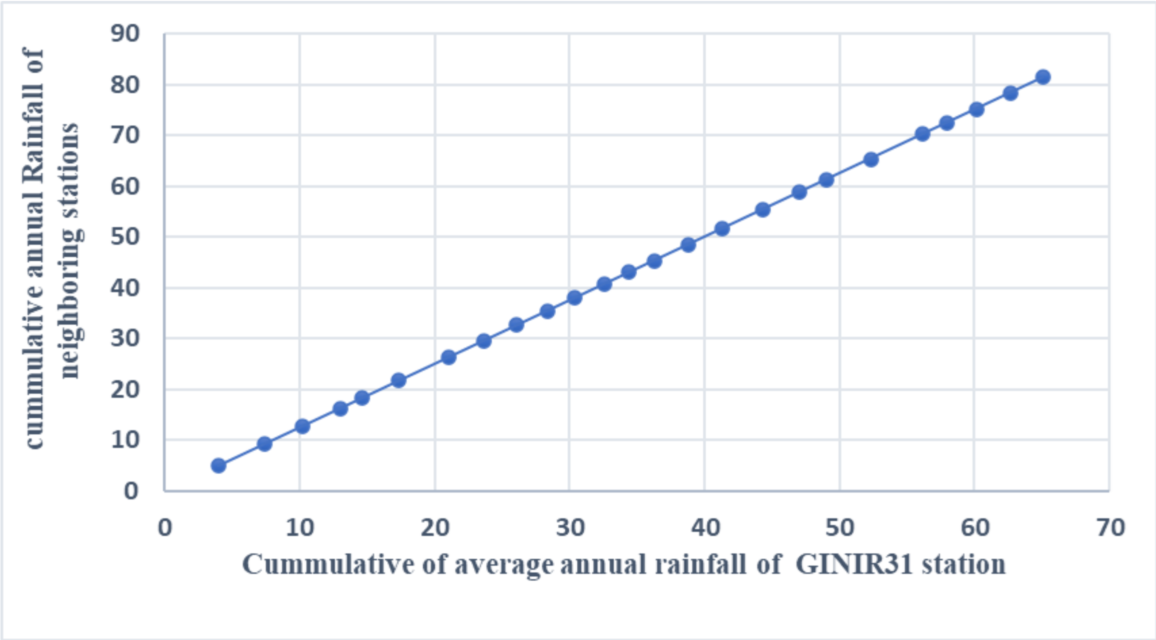

Figure 6 Double mass curve of GINIR31 station after adjustment

3.5.3 Outlier test for Precipitation data

Data points that significantly deviate from the trend of the remaining data are called outliers. There are different types of outlier detection techniques (Mirzaei *et al.*, 2014).

3.4.1.1 Grubbs' test

This method is based on the comparison the statistics generated for each data by Grubb's formula with standard amount of each data. If it exceeds the standard, it is considered as an outlier.

The statistics of this test (G) is derived as follows.

$$\mathbf{G} = \frac{\mathbf{max}|\mathbf{x_1} - \bar{\mathbf{x}}|}{\mathbf{S}}$$

Where: - $x_{1,}$ $\bar{x}$ and S are the biggest or smallest data, data mean and Standard deviation, respectively

3.4.1.2 The American Water Resource Association

This a method which was proposed by American Water Resource Association and used for elimination of outliers (Mirzaei *et al.*, 2014). During outliers testing, if the kurtosis at a given station is greater than +0.4, tests for high outliers are considered first; whereas, if the skewness is less than -0.4, tests for low outliers are considered first; on the other hand, if the skewness is between -0.4 and +0.4, tests for both high and low outliers should be applied before rejecting any outliers from the dataset (Mirzaei *et al.*, 2014).

The following equations were applied to detect for higher (XH) and lower (XL) outliers.

$$\mathbf{XH} = \mathbf{X_{av}} + \mathbf{K_N} * \mathbf{S}$$

$$\mathbf{XL} = \mathbf{X_{av}} - \mathbf{K_N} * \mathbf{S}$$

Where:

XH=Logarithmic High-outlier threshold

XL=Logarithmic Low-outlier threshold

X_{av}=the Logarithm value of the average yearly rainfall

K_N= is critical value for outlier test statistics at10-percent significance level for sample size of N from Normal Distribution and could be derived from a table or using the following equation at 10% significance level and sample size ranging between 10-150 (Mirzaei et al., 2014):

$$\mathbf{K_N = 3.62201 + 6.23446N^{0.25} - 2.47832N^{0.5} + 0.491436N^{0.75} - 0.037911N}$$

S=Standard Deviation

If the Logarithms of values in the sample are greater than the computed XH value using the above equation, then they are considered as High-outliers; whereas, if they are less than XL, they are considered as Low-outliers.

3.4.1.3 Mahala Nobis Distance

In this method the distance is a criterion for the distance between each observation in multi-dimensional space and mean center of all observations. For a P-dimensional multivariate sample, Mahala Nobis Distance for i^{th} observation is derived as follows (Mirzaei *et al.*, 2014).

$$\mathbf{MD_i = (x_i \;\; \bar{x})^T c^1 (x_i \;\; \bar{x})^{1/2}}$$

Where: -

x_i $\bar{x}$ and c stand for variables' vector for i^{th} observation, mean variables' vector (centroid of observations) and sample covariance matrix, respectively.

In this study, The American Water Resource Association Method was applied for outlier testing (Mirzaei *et al.*, 2014).

The following equations were applied to detect for higher (XH) and lower (XL) outliers.

$$\mathbf{XH = X_{av} + K_N * S}$$

$$\mathbf{XL = X_{av} - K_N * S}$$

Where:

XH=Logarithmic High-outlier threshold

XL=Logarithmic Low-outlier threshold

X_{av}=the Logarithm value of the average yearly rainfall

K_N= is critical value for outlier test statistics at10-percent significance level for sample size of N from Normal Distribution and could be derived from a table or using the following equation at 10% significance level and sample size ranging between 10-150 (Mirzaei *et al.*, 2014):

$$\mathbf{K_N = 3.62201 + 6.23446N^{0.25} - 2.47832N^{0.5} + 0.491436N^{0.75} - 0.037911N}$$

S=Standard Deviation

If the Logarithms of values in the sample are greater than the computed XH value using the above equation, then they are considered as High-outliers; whereas, if they are less than XL, they are considered as Low-outliers. For this study, outlier test was carried out for some basic stations as shown in the following table, whereby test for both high and low outliers was applied. The results of the outlier test are provided in the following table.

Table 5 Outliers Test Results for Average yearly Precipitation

Year	ROBE22		PGNR31		PAGAR14		PDINS13		PGAS14		PHOM14		PMLYU24	
	Ave pcp	Log value	Ave pcp	Log value	Ave pcp	Log value	Ave pcp	Log value	Ave pcp	Log value	Ave pcp	Log value	Ave pcp	Log value
1988	65.15	1.81	29.88	1.48	33.80	1.53	65.15	1.81	30.18	1.48	18.66	1.27	33.19	1.52
1989	78.55	1.90	30.04	1.48	25.67	1.41	67.85	1.83	29.59	1.47	23.12	1.36	49.38	1.69
1990	61.12	1.79	25.41	1.41	35.85	1.55	61.12	1.79	24.42	1.39	17.78	1.25	48.95	1.69
1991	47.41	1.68	46.33	1.67	24.23	1.38	47.41	1.68	32.06	1.51	32.01	1.51	42.37	1.63
1992	76.35	1.88	46.67	1.67	33.88	1.53	66.35	1.82	43.52	1.64	23.28	1.37	44.57	1.65
1993	72.43	1.86	39.46	1.60	31.78	1.50	62.43	1.80	38.49	1.59	27.84	1.44	47.80	1.68
1994	61.98	1.79	22.34	1.35	33.61	1.53	61.98	1.79	36.98	1.57	36.00	1.56	31.49	1.50
1995	44.59	1.65	32.71	1.51	27.62	1.44	44.59	1.65	32.32	1.51	49.15	1.69	37.36	1.57
1996	38.50	1.59	35.63	1.55	42.34	1.63	38.50	1.59	32.02	1.51	30.90	1.49	46.15	1.66
1997	47.88	1.68	29.97	1.48	54.19	1.73	47.88	1.68	34.31	1.54	35.71	1.55	52.31	1.72
1998	47.50	1.68	23.87	1.38	51.00	1.71	47.50	1.68	31.94	1.50	47.67	1.68	45.03	1.65
1999	40.62	1.61	22.50	1.35	46.04	1.66	40.62	1.61	32.32	1.51	27.99	1.45	43.07	1.63
2000	35.61	1.55	21.66	1.34	44.70	1.65	35.61	1.55	29.62	1.47	27.31	1.44	32.39	1.51
2001	37.61	1.58	26.65	1.43	47.28	1.67	37.61	1.58	33.25	1.52	30.53	1.48	46.76	1.67
2002	30.19	1.48	23.60	1.37	40.13	1.60	30.19	1.48	26.69	1.43	25.10	1.40	39.26	1.59
2003	28.78	1.46	27.64	1.44	26.51	1.42	28.78	1.46	34.36	1.54	33.14	1.52	34.20	1.53
2004	29.45	1.47	30.00	1.48	32.93	1.52	29.45	1.47	25.54	1.41	25.83	1.41	43.05	1.63
2005	32.27	1.51	46.60	1.67	34.32	1.54	32.27	1.51	34.51	1.54	34.96	1.54	49.75	1.70
2006	36.23	1.56	34.10	1.53	24.73	1.39	36.23	1.56	36.37	1.56	44.58	1.65	45.00	1.65
2007	42.43	1.63	33.13	1.52	39.81	1.60	42.43	1.63	34.74	1.54	27.19	1.43	42.60	1.63
2008	37.44	1.57	31.30	1.50	36.00	1.56	31.56	1.50	28.20	1.45	30.36	1.48	37.44	1.57
2009	27.89	1.45	55.91	1.75	33.60	1.53	27.89	1.45	38.25	1.58	32.66	1.51	33.72	1.53
2010	45.33	1.66	33.49	1.52	32.40	1.51	45.33	1.66	44.98	1.65	50.62	1.70	32.40	1.51

Year	ROBE22		PGNR31		PAGAR14		PDINS13		PGAS14		PHOM14		PMLYU24	
	Ave pcp	Log value	Ave pcp	Log value	Ave pcp	Log value	Ave pcp	Ave pcp	Log value	Ave pcp	Log value	Ave pcp	Log value	Ave pcp
2011	22.77	1.36	40.88	1.61	36.00	1.56	22.77	1.36	36.19	1.56	22.69	1.36	31.44	1.50
2012	39.53	1.60	47.54	1.68	33.72	1.53	39.53	1.60	27.22	1.43	30.61	1.49	31.56	1.50
Xave		1.63		1.51		1.55		1.62		1.52		1.48		1.61
Skew		0.28		0.33		0.12		0.06		0.07		0.15		-0.23
Stdv		0.14		0.12		0.09		0.13		0.07		0.12		0.07
Kn	2.47		2.47		2.47		2.47		2.47		2.47		2.47	
XH	1.99		1.80		1.78		1.95		1.68		1.77		1.79	
Log.v	1.90		1.75		1.73		1.83		1.65		1.70		1.72	
Pcp	78.55		55.91		54.19		67.85		44.98		50.62		52.31	
XL	1.27		1.22		1.31		1.29		1.35		1.19		1.42	
Log.v	1.36		1.34		1.38		1.36		1.39		1.25		1.50	
Pcp	22.77		21.66		24.23		22.77		24.42		17.78		31.44	

The outlier test results revealed that, the highest recorded average yearly rain fall value (78.55 mm with log value of 1.90) didn't exceed the high outlier test threshold value (i.e., 1.99); at the same time, the lowest recorded average yearly rainfall value (17.88mm with a log value of 1.25) was not below the low-outlier test threshold value (i.e., 1.19). Thus, in this study both high and low outliers were not detected.

3.5.4 Filling Missing Stream Flow Data

Daily records of flow data for the duration and stations under consideration are required for the analysis of hydrological data and simulation purpose. Often, it may so happen that some flow-gauge/stations are not functional for a part of a month or year. Thus, it becomes mandatory to fill the missing values. In this study, arithmetic mean method was employed to fill the missing values, because the gauging station selected was a station with a missing value of less than 10 percent. The Denbel, Alemkerem, Tegona and Shaya gauging station were used to calculate the missing values of Sofumer gauging station, which was selected and transferred to the Weyib outlet location using the regional equation as explained in section 3.7.2.1.

3.5.5 Outlier Test for Flow Data

The same procedure that was applied for the precipitation data was also applied for the average yearly flow data at Sofumer gauging station. The following table 6 presents the outlier test results for the flow data at sofumer Gauging station.

Table 6 Test results for outliers for yearly average flow data

Year	Average Yearly flow (m3/s)	Log values	Year	Average Yearly flow (m3/s)	Log values
1992	15.21	1.18	2003	15.93	1.20
1993	12.33	1.09	2004	6.99	0.84
1994	13.26	1.12	2005	12.28	1.09
1995	18.35	1.26	2006	15.61	1.19
1996	17.90	1.25	2007	15.81	1.2
1997	14.5	1.16	2008	6.77	0.83
1998	23.04	1.36	2009	3.01	0.5
1999	46.57	1.67	2010	8.91	0.95
2000	62.66	1.8	2011	3.87	0.59
2001	65.61	1.82	2012	3.10	0.49
2002	5.28	0.72	-	-	-
Xave					1.11
Skew					0.15
Stdev					0.4
K_N					2.4

From the table: -

- The Maximum flow recorded was 65.60 m^3/s with a log value of 1.82
- The Minimum flow recorded was 3.01 m^3/s with a log value of=0.48
- High outlier test $XH=X_{av}+K_N*S=1.11+2.4*0.37= 2.01$
- This implies that the corresponding flow data is $Q=10^{2.01}=101.87m^3/s$
- Low outlier test $XL= X_{av}-K_N*S=1.11-2.4*0.37= 0.21$
- The corresponding flow data for this value is $Q=10^{0.21}=1.63\ m^3/s$

The outlier test results revealed that, the highest recorded average yearly flow (65.60 m^3/s with log value of 1.82) didn't exceed the high outlier test threshold value (i.e., 2.01); at the same time, the lowest recorded average yearly flow (3.01 m^3/s with a log value of 0.48) was not below the low-outlier test threshold value (i.e., 0.21). Thus, in this study both high and low outliers were not detected and hence this flow data was transferred to the area of interest.

3.6 Methodology

3.6.1 General on the methodology

Since SWAT is a physically semi-distributed model that uninterruptedly predicts the effect of land management practices on water, sediment and agricultural chemical yields from a watershed, the SWAT (Soil and Water Assessment) model was used for this study. Here, all the necessary data required to run the model was collected and prepared. The geospatial data including the digital elevation map, land use/land cover map, soil map and the time series data such as hydro-meteorological data including the daily stream flow data and sediment load/concentration data (1992-2012), daily rainfall data (1988-2012), maximum and minimum daily air temperature data, relative humidity, sunshine hour and wind speed data (1988-2012) were all collected and processed and prepared as per the input requirement format of the SWAT model.

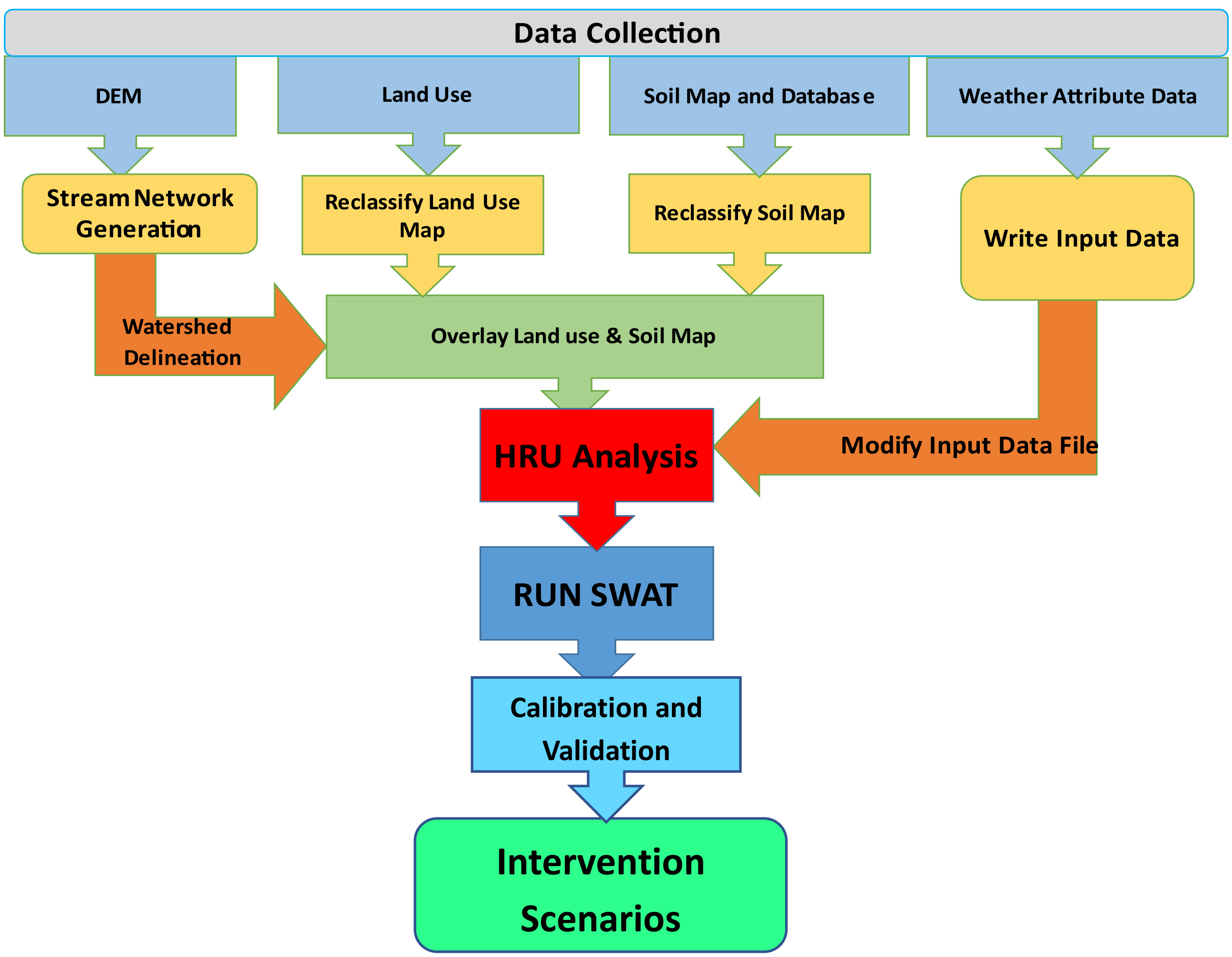

Figure 7 General Flowchart of the methodology

3.6.2 Arc SWAT Model Setup

The SWAT (Soil and Water Assessment Tool) model is an ArcGIS extension with its own user interface, including the configuration of the SWAT project, delineation of watershed, Analysis of HRU, writing input tables, editing the inputs and finally simulation (SWAT run) (Arnold *et al.*, 1998).

While employing the SWAT mode for this study, first a directory was opened in the SWAT project setup section, where all the SWAT model outputs were saved; then the study watershed was delineated using the imported DEM data, in which the model uses it for the whole process to create sub-watersheds and HRUs. The automatic watershed delineator option was used for the delineation. Here a mask was manually delineated over the DEM in order to extract the area of interest. By using a minimum threshold area of 8200 ha the watershed was discretized in to sub-watershed. The land use and land cover data and the soil maps of the watershed under consideration were then categorized/reclassified and superimposed (overlaid). These were combined together to makeup HRUs (distinct grouping of certain land use types, soil types and slope classes). For this study, multiple HRU with 10% land use, 10% soil and 20% slope were adopted. These threshold levels have been set to ignore minor land uses, soils and slope categories in each sub-watershed (Neitsch, *et al.,* 2002). After HRU analysis was successfully completed, all the SWAT input data were written to the SWAT data base for model processing in the Write input tables section. Then soil and land use/land cover data properties were put in to the SWAT data base in the form that the model understands the codes through the Edit SWAT input. After successfully completing these stages the model was run for simulation.

3.6.3 Watershed Delineation

The process of watershed delineation involves five major steps, DEM setup, stream definition, outlet and inlet definition, watershed outlets selection and definition and calculation of sub-basin parameters. Delineation of the watershed from a DEM was the first step in creating SWAT model input. The inputs to be fed into the SWAT model were organized to have spatial characteristics. The watershed, the sub-watersheds, and the hydrologic response units (HRUs) are the three spatial levels that are provided by the SWAT model. Each level was characterized by a parameter set and input data. The largest spatial level, the watershed, refers to the entire area being represented by the model. Then, the study watershed was partitioned into sub watersheds by assigning a threshold area value.

In order to delineate the study watershed, the automated watershed delineation embedded in ArcSWAT interface was applied. The watershed and sub-watershed were delineated by using DEM data. DEM was imported into the SWAT model and then projected to WGS_1984_ UTM_ zone 37N, projection area of Ethiopia. In order to remove the specific part, to delineate the border of the watershed and digitize the stream networks in the study watershed, a mask was manually delineated over the DEM. This has an advantage in that it reduces the time of processing.

3.6.4 Hydrological Response Units

Hydrologic response units (HRUs) are lumped land areas within the sub -watersheds that contains unique land cover, soil and management combinations (Luzio *et al.*, 2002). HRUs enable the model to reflect differences in evapotranspiration and other hydrologic conditions for different land covers and soil.

The next step after watershed delineation was sub-division of sub-watersheds into small hydrologic response units (HRUs) that had unique land use, soil and slope combination. These datasets (the land use, soil and slope datasets) were projected into the same projection with that of the DEM. The land use and the soil data in a projected shape file format were loaded into the SWAT interface to determine the area and hydrologic parameters of each land-soil category simulated within each sub-watershed. The land cover classes were defined using the look up table. A look-up table that identifies the 4-letter SWAT code for the different categories of land cover/land use was prepared so as to relate the grid values to SWAT land cover/land use classes.

After projection was completed, these datasets were reclassified, overlapped and connected with the SWAT catalogues and hence prepared for HRU definition. For this purpose, multiple HRU description option was selected because, it better refers to the heterogeneity inside the watershed and as it precisely replicates the hydrologic executions (Arnold *et al.,* 2012). To define the number of HRUs within the sub-watershed in particular and within the watershed in general, a threshold level that was set for land use, soil and slope was used. Multiple slope classification option was chosen for this classification purpose, and it was executed based on the prescribed minimum, maximum, mean and median watershed slope statistics. Accordingly, for land use, soil class and slope, the smallest threshold area of 10%, 10% and 20% respectively was used. Those percentage areas covering less than the average of the threshold area of land use, soil and slopes have been overlooked and then the remaining areas were reclassified; so that hundred percent of the land area in the sub-watershed could be used in the simulation execution.

3.6.5 Weather generator data preparation

Another major part of ArcSWAT is Weather Data. The weather generator model included in SWAT was used to fill in gaps in measured records. This weather generator was developed for U.S. and since Weyib watershed is located outside U.S., weather generator has to be developed for the study watershed by providing it with all the necessary statistical information from the meteorological records of the watershed.

If there are no daily values for weather, the SWAT model can generate these from average monthly values. The model generates a set of weather data for each sub basin. SWAT usually requires daily precipitation (mm), maximum/minimum air temperature (°C), solar radiation (MJ/m²/day), wind speed (m/s) and relative humidity (percentage), (Arnold *et al.*, 2012).

In this study, statistical weather parameter calculators (pcpSTAT.exe and Dew02) obtained from the official SWAT website (http://www.brc.tamus.edu/swat/soft_links.html) were applied to generate the required input data. From pcpSTAT.exe., the statistical parameters of daily precipitation data that are used by the weather generator were computed (Liersch, 2003). The result is shown in Table-3 below. On the other hand, the statistical calculator Dew02 software was applied to perform the statistical parameters calculation for temperature data. This software calculates the temperature data to be used in the weather generator by taking the average of daily maximum and minimum air temperature. The results of the Dew02 calculator for the weather generator station Robe22 is shown below in table-4. For this study weather generator parameters were calculated for Robe22 and Ginir31 stations. The reason they were selected as weather generator stations is because they hold relatively all the meteorological data required by the SWAT model (i.e., they hold daily records of precipitation data, maximum and minimum temperature, relative humidity, wind speed and sunshine hours) with different degree of missing data.

3.6.6 Precipitation Data

For this study, the precipitation data of Robe22 and Ginir31 stations were used for statistical weather generator parameters calculation and the results of the daily precipitation data statistics for Robe22 station are presented below in table-7. The PCPSTAT calculates such statistical parameters like (Average monthly precipitation (mm) (PCP_MM), standard deviation (PCPSTD), Coefficient of Skewness (CPSKW), Probability of wet day following a dry day (PR_W), Probability of wet day following a wet day (PR_W2) and average number of precipitation days in a month (PCPD).

Statistical Analysis of Daily Precipitation Data (1988-2012)

Input Filename=roberainfall.txt

Number of Years = 25

Number of Leap Years = 7

Number of Records = 9132

Number of No Data values =   0

Table 7 PcpSTAT output of weather generator station (Robe meteorological station)

Month	PCP_MM	PCPSTD	PCPSKW	PR_W1	PR_W2	PCPD	RAINHHM
Jan.	18.07	2.7248	7.1441	0.064	0.4773	3.52	9.035
Feb.	25.19	3.8422	7.6458	0.0795	0.5146	4.12	12.595
Mar.	59.62	5.0345	4.2702	0.1931	0.5873	10.08	29.81
Apr.	120.13	7.0928	2.8542	0.4204	0.6403	16.68	60.065
May.	75.48	4.6242	3.2887	0.3734	0.6071	15.68	37.74
Jun.	54.32	3.6822	3.3169	0.342	0.535	13.16	27.16
Jul.	105.41	7.4669	4.4719	0.4553	0.5899	16.68	52.705
Aug.	143.97	9.1084	5.3733	0.5179	0.7233	20.96	71.985
Sep.	117.05	5.4219	2.5016	0.5273	0.7528	21.2	58.525
Oct.	81.63	4.9152	3.2794	0.2541	0.7337	16.52	40.815
Nov.	35.07	3.7279	4.9714	0.1088	0.5679	6.48	17.535
Dec.	18.93	2.734	7.5148	0.0743	0.4804	4.08	9.465

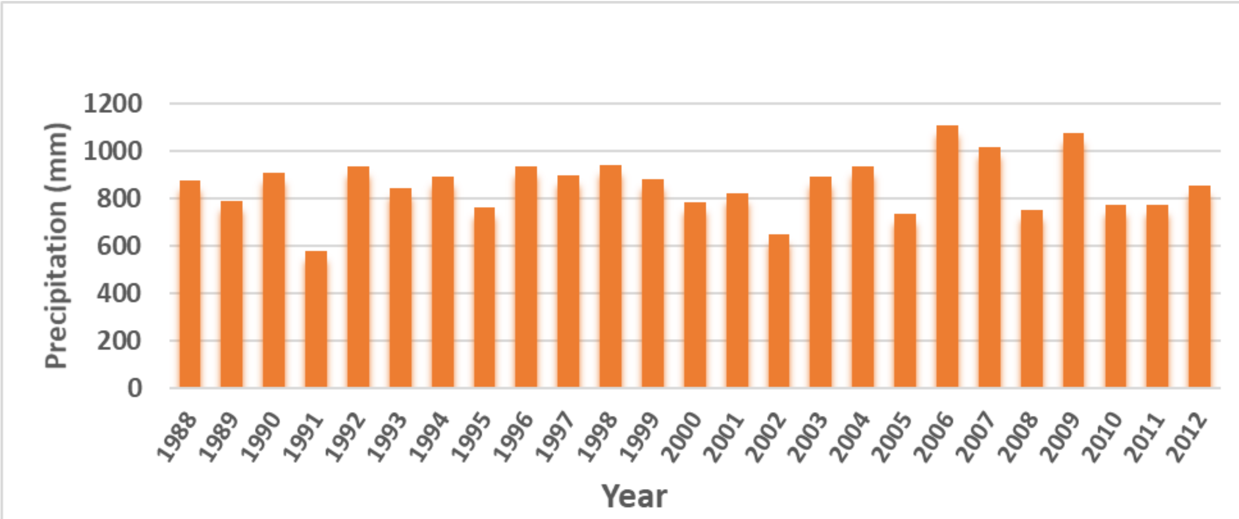

Figure 8 Total Annual Precipitation at Robe22 Station (1988-2012)

From figure 8 above, it can be seen that the periods 2006 and 2009 were the wettest years whereas, 1991 and 2002 were relatively drier years.

3.6.7 Temperature Data

The time span for the Robe and Ginir temperature data (i.e., Robe22 and Ginir21) is the same as that for the recording of precipitation data. This has a benefit in that it simplifies the preparation of input data because the SWAT model needs precipitation and temperature data that have the same length of time.

The results of the Dew02 software for Robe22 meteorological station are given below in table-8. The outputs from the Dew02 include average daily value of maximum temperature in month (max T) (°C), average daily minimum temperature in month (Min T) (°C)), average daily humidity in month (Humidity) (percent) and the average daily dew point temperature in month (DEWPT) (°C)

Table 8 Average Daily Dew Point Temperature outputs for Period (1988 - 2012)

Month	Max T	Min T	Humidity	DEWPT
Jan	22.76	6.18	56.97	7.51
Feb	23.72	7.08	53.08	7.24
Mar	23.38	8.33	60.15	9.24
Apr	22.03	9.68	70.73	11.36
May	22.31	9.58	69.02	11.17

Month	Max T	Min T	Humidity	DEWPT
Jun	22.88	9.21	67.75	11.17
Jul	21.95	9.25	74.03	11.97
Aug	21.29	9.19	76.71	12.09
Sep	20.9	9.07	75.54	11.55
Oct	19.78	8.64	74.9	10.52
Nov	20.58	6.71	68.44	9.03
Dec	21.54	6.03	61.96	7.9

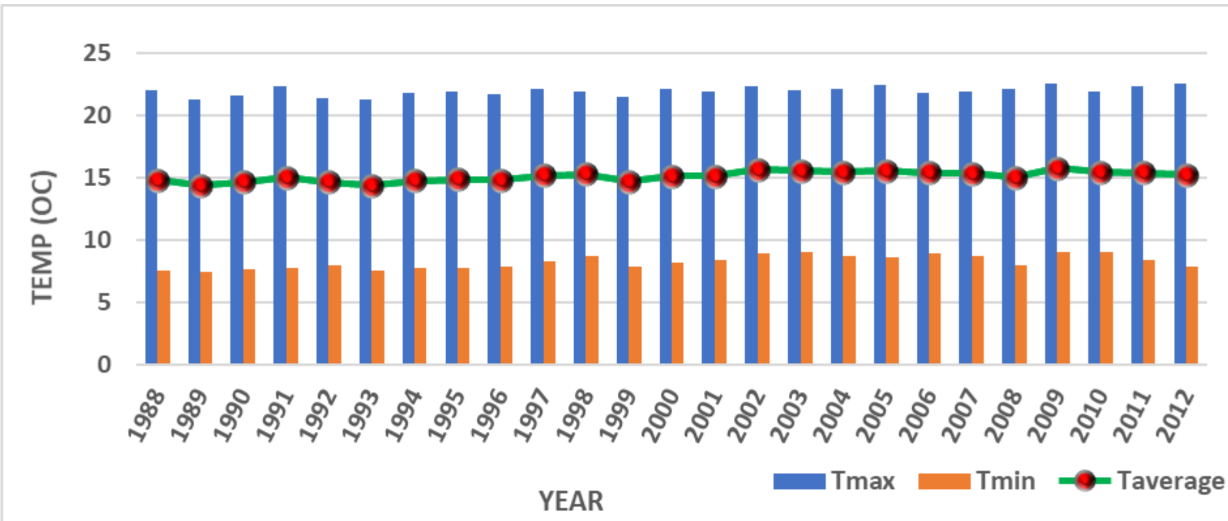

Figure 9 Daily Maximum and minimum temperature of Robe22 meteorological station

3.6.8 Solar Radiation

In the land phase of the hydrologic cycle, the movement of water is often highly controlled by the available energy (i.e., solar radiation). The input data required by the SWAT model is daily solar radiation; however, the data acquired from the National Meteorological Agency (NMA) is sunshine hour. Thus, this variable was converted in to the required input data format using the empirical equation given below (Richard *et al.*, 2006).

$$\mathbf{Rs} = \left(\mathbf{As} + \mathbf{Bs} * \frac{\mathbf{n}}{\mathbf{N}}\right)\mathbf{Ra}$$

Where: -

Rs is the solar or shortwave radiation [MJ m-2 day-1],

n is the actual duration of sunshine [hour],

N is the potential sunshine or daylight hours duration (hour),

n/N is the relative sunshine duration [-],

Ra is the extraterrestrial radiation [MJ m-2 day-1],

As+Bs is the portion of extraterrestrial radiation that, on clear days, enters the ground (n=N)

As is constant of regression (The component of extraterrestrial radiation that enters the planet on cloudy days (n is equal to 0),

3.6.9 Soil data

Soil is one of the most important spatial data required by SWAT model. For this study, the **s**oil map developed by the Food and Agriculture Organization of the United Nations (FAO-UNESCO) at a scale of 1:5,000,000 downloaded from the official website (http://www.fao.org/soils-portal/soil-survey/soil-maps-and-databases/FAO-UNESCO soil-map of the world/en/ was used in the SWAT model. Furthermore, the soil data with a resolution of one kilometer (1km) that mainly incudes soil texture, soil depth and soil drainage attributes required by the SWAT model were derived from the Harmonized World Soil Database V1.2, (which is a database that combines existing Regional and National soil information). It was downloaded from (http://www.fao.org/soils-portal/soil-survey/soil-maps-and-databases/harmonized world soil database-v.1,2/en/). Thus, major soil physico-chemical properties for the study watershed were acquired by integrating this with the Integrated resource Development Master Plan review of the Genale-Dawa River Basin (GDMP, 2007). All the soil data with their detail properties in the study watershed required by the model were imported to the SWAT data base in the HRU's analysis portion of the SWAT interface. To classify the soils in the study watershed, the FAO/world soil (FAO/UNESCO) classification scheme was applied. According to FAO classification system and the GDMP (Integrated resource Development Master plan review of the Genale-Dawa River Basin) (2007), ten major soils types were identified for the study area as shown in the table below. Among these, the dominant soil types are Cambisol, Luvisol, Leptosol and Calcisol, which have an area coverage of 30.94, 19.11% 15.12% and 12.26% respectively. The MWswat-database was used as a database for user-soil. Eventually, the soil data was pre-processed and the look-up table was prepared in text format so that it could be compatible with the input needs of the model.

Table 9 Soil types of the Weyib watershed

SOIL TYPE	AREA (km^2)	AREA (%)
Cambisol	7541.14	30.94
Leptosol	3685.3	15.12
Arenosol	2064.09	8.47
Regosol	742.31	3.05
Luvisol	4656.91	19.11
Fluvisol	948.38	3.89
Solonchak	450.11	1.85
Calcisol	2987.36	12.26
Vertisol	1274.71	5.23
Solontez	19.29	0.08
Total	24369.6	100

3.6.10 Land use land cover data

The other key spatial input data required by SWAT model is land use and land cover. It principally affects surface runoff, evapo-transpiration, erosion processes and other watershed hydrological process (Neistch *et al.*, 2005). The Genale Dawa river master plan study (2007), acquired from the Ministry of Water, Irrigation and Energy, was used as a source for the land use and land cover map and datasets preparation for the study area. The primary form of land use in the study area, which covers about 79 percent, is agriculture. Pasture, Forest, Range grass and Forest evergreen cover the remaining major land use types with a percent coverage of 15.5 %, 2.18%, 1.13% and 0.96%% respectively. The land use and Land cover look-up table was prepared in such a way that they were compatible with the input needs of the model.

According to Singh *et al.* (2014), in order to use the SWAT model, the different input data required by the model, such as land use types, maps and look-up tables, were prepared in agreement with the SWAT model's input specifications. The different SWAT codes for the dominant land use types in the study watershed are provided in table 10 below.

Table 10 SWAT codes for Land Use (adapted from SWAT user manual, 2002 and GDMP,2007)

ID	SWAT CODE	LAND USE	AREA (Km^2)	AREA (%)
1	AGRC	Agricultural Land-Close-grown	21779.12	79.37
2	PAST	Pasture	1339.57	15.50
3	FRST	Forest-Mixed	532.12	2.18
4	FRSE	Forest-Evergreen	233.08	0.96
5	RNGB	Range-Brush	205.89	0.84
6	RNGE	Range-Grasses	276.12	1.13
7	URML	Residential-Med/Low Density	3.25	0.01
8	WATR	Water	0.44	0.01
#	Total		24369.60	100

3.6.11 Slope

Beside to the land use and soil input data, the slope of the study watershed is another important input data required by the model, which was derived by using the DEM data. By using the slope data, the SWAT determines the Hydrological Response Unit (HRU). During definition of HRUs, the SWAT model permits the combination of land slopes up to five classes. In this study, five slope classes were considered for the study watershed by selecting the multiple slope classes option. Table 11 below shows the different slope distribution of Weyib watershed.

Table 11 Slope distribution of Weyib watershed (adapted from GDMP, 2007)

No	Slope (%)	Area [km^2]	% Area of coverage
1	0-5	3631.36	14.90
2	5-10	7814.75	32.07
3	10-15	3853.79	15.81
4	15-20	86.71	0.36
5	>20	8982.98	36.86
#	Total	24369.6	100

3.7 Uncertainty analysis

The most important issue with calibration of watershed models is its uncertainty in the predictions. Watershed models can be highly influenced by model uncertainties. According to Abbaspour *et al.* (2014), these uncertainties can be divided into: -

a) Conceptual model uncertainty (or structural uncertainty)
b) Input uncertainty, (uncertainties caused by errors in input data such as rainfall, and more importantly, extension of point data to large areas in distributed models).
c) Parameter uncertainty

It is very important to separate quantitatively the effect of different uncertainties on model outputs, even though this is very difficult to do. Model uncertainties can be decreased by removing some probable sources of modeling and calibration errors by applying such packages like SWAT-CUP.

3.8 Parameterization of Weyib watershed for SWAT

In this study ArcSWAT2012 model was set up to suit the Weyib watershed and was used to simulate the baseline hydrological and sediment processes. The hydrological model was done first then followed by a sediment model. The climate input data was obtained from National Meteorological Agency (NMA). About 13 meteorological stations were selected. Among these, Robe and Ginir (Robe22 and Ginir31) stations have relatively all climatic input data required by SWAT model with small missing precipitation data values. Consequently, these two meteorological stations were used for weather generator data preparation, this weather generator in turn was used to generate data for those stations with missing records. Under this process, the watershed was divided into 31 sub watersheds, which were further subdivided into smaller units called hydrological response units (HRUs). Each HRU has a unique combination of land-use, soil and slope characteristics. SWAT computes all simulations at HRU scale and prints output at HRU, sub-watershed and watershed scales. For land use, soil class and slope, the smallest threshold area of 10%, 10% and 20% respectively was used. A total of 80 HRUs were created for the study watershed. The **s**oil map developed by the Food and Agriculture Organization of the United Nations (FAO-UNESCO) downloaded from the official its website was used in the SWAT model. Furthermore, the soil data with a resolution of one kilometer (1km) that mainly incudes soil texture, soil depth and soil drainage attributes required by the SWAT model were derived from the Harmonized World Soil Database V1.2, (which is a database that combines existing Regional and National soil information). The soil type used to generate the HRUs in this study has four layers with saturated hydraulic conductivity of 1180 mm/hr for the first layer and 324.43 mm/hr for the second, 14.31mm/hr for third and 4.1mm/hr for the fourth layers. To properly regionalize soil parameters into SWAT for the study watershed, the soil data was overlaid with land-use data and thus reclassified based on land-use type and slope classes. The Genale Dawa river master plan study (2007), acquired from the Ministry of Water, Irrigation and Energy, was used as a source for the land use and land cover map and datasets preparation and for model setup and this was considered a baseline during scenario analysis. The SCS Runoff Curve Number method for estimating surface runoff from precipitation was applied while the Hargreaves method for estimating potential evapotranspiration was chosen. For channel water routing, the variable-storage method was used. The model was run for the period 1992 - 2012 with a 2-year warm up period. Thus, the model produced output for 20 years at daily time step.

3.9 Sensitivity Analysis

After loading all the temporal and spatial input data required for the SWAT model, flow was simulated for twenty-five years starting from 1988 through 2002. Then, the model simulation result was applied for flow parameters sensitivity analysis and for calibration of the model using SWAT-CUP program. In addition to hydrologic parameters, observed and simulated daily streamflow values of Weyib watershed were used as an input. After running a sensitivity analysis, the sensitivity parameters were ranked and hence effective hydrologic parameters for the simulation of streamflow in the watershed were identified. Consequently, these parameters were used for streamflow calibration.

In this study around twenty-six (26) flow parameters were used to evaluate their effect on the model simulation. List of flow parameters with their allowable range are provide in table 12.

Table 12 list of sensitive flow parameters and their initial permissible ranges

No	Parameter Name	Description	Range	
			Min	Max
1	R__CN2.mgt	SCS runoff curve number (dimensionless)	-0.25	0.25
2	V__ALPHA_BF.gw	Base-flow alpha factor (days)	0	1
3	A__ESCO.hru	Soil evaporation compensation factor (dimensionless)	0	1
4	R__SOL_AWC(..).sol	Available water capacity of the soil layer (mm H2O/mm soil)	-0.25	0.25
5	R__RCHRG_DP.gw	Deep aquifer percolation fraction (dimensionless)	0	1
6	SLSOIL	Slope length for lateral sub-surface flow	0	150
7	R__SOL_Z(..).sol	Depth from soil surface to bottom of layer	-0.25	0.25
8	R__CANMX.hru	Maximum canopy storage (mm)	0	10

No	Parameter Name	Description	Range	
			Min	Max
9	V__REVAPMN.gw	Threshold depth of water in the shallow aquifer for "revap" to occur (mm)	-100	100
10	R__SOL_K(..).sol	Saturated hydraulic conductivity	-0.25	0.25
11	V__GW_REVAP.gw	Groundwater "revap" coefficient (dimensionless)	-0.036	0.036
12	V__GWQMN.gw	Threshold depth of water in the shallow aquifer required for return flow to occur (mm)	-1000	1000
13	R__BLAI{..}.plant.dat	Maximum potential leaf area index	0	1
14	V__CH_K2.rte	Effective hydraulic conductivity in main channel alluvium (mm/h)	0	150
15	R__SURLAG.bsn	Surface runoff lag time [days]	0	10
16	V__GW_DELAY.gw	Groundwater delay (days)	-10	10
17	R__CH_N1.sub	Manning value for the tributary channels	0	1
18	R__EPCO.bsn	Plant uptake compensation factor	0	1
19	R__SOL_BD(..).so	Moist bulk density	-0.5	0.6
20	R__OV_N.hru	Manning's n value for overland flow	-0.2	0
21	R__HRU_SLP.hru	Average slope steepness	0	0.2
22	R__SLSUBBSN.hru	Average slope length (m)	0	0.2
23	V__CH_N2.rte	Manning's n value for the main channel	0	0.3
24	V__ALPHA_BNK.rte	Base-flow alpha factor for bank storage	0	1
25	R__SOL_ALB(..).sol	Moist Soil Albedo	-0.25	0.25
26	R__BIOMIX.mgt	Maximum potential leaf area index	0	10

In order to determine the parameter that significantly influences the flow, the Global Sensitivity analysis technique was applied. To separate the most sensitive parameters, the P-value and t-stat values from Global sensitivity output were evaluated and 12 flow parameters, which have a P-value of less than 0.5 were considered as most sensitive and hence selected for model calibration and validation for flow.

Around sixteen model parameters that are considered to be highly influencing the sediment yield were evaluated, and based on the global sensitivity analysis outcome, 8 (eight) of them were found to be highly sensitive and therefore chosen for model calibration and validation. List of sensitive sediment parameters and their permissible ranges are provided in table 13 below.

Table 13 List of Sensitive sediment parameters and their initial ranges

No.	Parameter Name	File ext	method	Min_value	Max_value
1	CN2	.mgt	R relative	0.338	0.412
2	SPEXP	.bsn	V replace	1	1.5
3	SPCON	.bsn	V replace	0.0001	0.01
4	LAT_SED	.hru	R relative	0	5000
5	HRU_SLP	Hru	R relative	0	1
6	CH_COV1	.rte	V replace	-0.05	0.6
7	CH_COV2	.rte	V replace	-0.001	1
8	CH_BED_BD	.rte	V replace	1.1	1.8
9	CH_N2.rte	.rte	V replace	0	0.3
10	CH_ERODMO	.rte	V replace	0	1
11	USLE_K	.sol	V replace	0	0.65
12	SOL_AWC	.sol	R relative	0.067	0.172
13	BIOMIX	.mgt	V replace	0	1
14	RSDIN	.hru	R relative	0	10000
15	USLE_P	.mgt	V replace	0	1
16	SLSUBBSN	Hru	R relative	10	100

3.10 Model Calibration and Validation

An iterative process that repeatedly compares the output from the model to the observed data, adjusts the numeric values of the parameters and then reruns the model is called Model calibration (Arnold *et al.*, 2012).

After selecting the most sensitive parameters that can highly influence the model prediction, calibration process continued by comparing the flow data simulated by the model for the period 1992-2012 against the observed streamflow data derived by the regional equation until the average simulated value for flow and sediment yield data came closer to the measured values. Here, the time period 1992 and 1993 was used as warm up periods and the time period from 1994-2004 was used for model calibration. The calibration process continued until the satisfactory testing model performance statics $R^2 > 0.6$, $E > 0.5$, $RSR \leq 0.70$ and PBIAS within the ±25 was achieved. Moreover, once the simulation results for the calibration period had fulfilled the above statistical criteria, then model Validation was made for an independent period of records from 01 January, 2005 to 31 December, 2012. Hence, the results were compared against an independently measured discharge data of the study watershed.

In the same way to that of model calibration for flow, the calibration for sediment was carried out for thirteen years. However, the output of regional equation is in yearly time step thus, both the calibration and validation processes for sediment yield was carried out in yearly time step. Model calibration was performed using yearly measured sediment data for the period of 1992 to 2004. Here, the first year was used for model stabilization/warm up. The dataset for remaining time periods i.e., from 2005 to 2012 was assigned for model validation. The calibration for sediment was performed after the flow calibration was completed. After calibrating for flow, flow parameter ranges were kept unchanged and then sediment parameters were added. Initially, those parameters that are sensitive to sediment only were added, then other parameters that affect both the sediment and flow were added step by step.

SWAT model simulates the total sediment load including the bed load. Hence, this bed load has to be added to the suspended load to get the total sediment load for model calibration. The bed load to suspended load, in most rivers, ranges from 10 to 30% (Church, 2006). Weyib river flows on a moderate to gentle slope throughout its course. Hence, the bedload was assumed to be 10% of the suspended sediment load derived by regional equation. This value was added to the suspended load during the model calibration and validation.

3.10.1 Calibration and validation for Hydrological (Flow Data)

For calibration and validation purpose the SWAT model requires observed flow data. The daily observed stream flow data of the Weyib river, at Sofumer, Denbel, Tegona and Tebel gauging station for the duration of 1992-2012 were taken from the Hydrology and Water Quality Directorate of the Ministry of water, Irrigation and energy. However, the outlet of the Weyib watershed which was selected for this study had no gauging station and available data for the time period of interest. Therefore, in order to derive flow data for the satiation under consideration, a relationship was developed between the nearby stations and the location under consideration. In areas where watersheds with flow records are near ungauged watersheds, which are of interest, information can be transferred from gauged watersheds to the ungauged watersheds (Admasu, 1989).

These daily time series data were transferred to the area of interest, i.e., to the outlet of Weyib watershed, which has no flow gauging station at its outlet point near Ethio-Somali border. Among the stream flow gaging stations located at (6^{0} 54'N, and 40^{0} 40' 50'E for Sofumer), (7^{0} 2'N and 40^{0} 48'E Denbel), (7^{0} 0' N and 39^{0} 59' E for Tegona) and (7^{0} 11' N and 40^{0} 44' E for Tebel) with a sub-watershed area of 3792.7 Km^2, 1215 km^2, 83 km^2 and 79 km^2, respectively, the information from Sofumer gauging station, which has the highest proportional area coverage, was transferred to the ungauged location in order to drive flow data for the location under consideration, i.e., the outlet.

The ratio of the discharges at the gauged and ungauged stations is assumed to be equal to the ratio of their corresponding watershed areas to some power, b, which varies from 0.5 to 0.85 and a value of 0.6 is usually recommended unless local evidence suggests otherwise (McMahon *et al.,* 2002).

Comparison of higher discharges at several gauge sites within the watershed may provide some guidance for selecting this exponent. The exponent depends mainly on the combined effects of the reduction in average rainfall intensity with increasing watershed area and the effect of natural storage in the watershed (McMahon *et al.,* 2002). The following equation was used to calculate the relationship at the higher discharges:

$$\mathbf{Q_U} = \left[\frac{\mathbf{A_U}}{\mathbf{A_G}}\right]^{\mathbf{b}} \mathbf{Q_G}$$

Where: - $\mathbf{Q_U}$= flow at ungauged site (m^3 /sec),

$\mathbf{A_U}$= ungauged site catchment area (km^2),

$\mathbf{A_G}$= gauged site catchment area (km^2),

$\mathbf{Q_G}$= flow at nearby gaged site (m3 /sec)

b= an exponent

Samples of Weyib discharge at its outlet computed by regional equation are provided in the Appendix section, Table 49. The monthly flow data of Weyib river are depicted in figure 10 below.

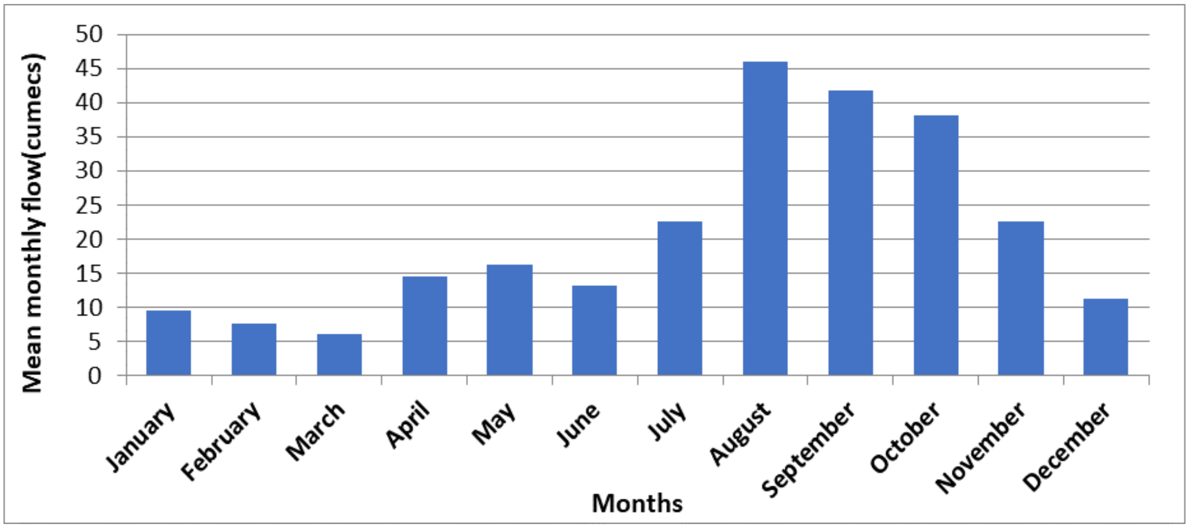

Figure 10 Mean monthly flow of Weyib at its outlet

As it can be seen in the figure 10 above, there was high flow during August, September and October. Whereas, there was relatively minimal flow during January, February and March.

Then, the flow data was prepared as per the input requirement of the SWAT-CUP Program in excel spread sheet and then used for model calibration and validation. The daily stream flow data from 1992-2004 was used for model calibration, while the remaining data i.e., from 2005-2012 was used for model validation.

3.10.1.1 Base flow Separation

The observed flow data is a combination of the surface runoff and base flow. Prior to any calibration and validation task these two components should be separated (Abbaspour *et al.,* 2014). Accordingly, in this study, an automated base flow separation and recession analysis technique was applied in order to divide the total daily stream flow in to the base flow and surface runoff.

3.10.2 Sediment Data

There was no reliable and adequate observed data to perform calibration of sediment parameters. To address this challenge and considering the modelling objective, the sediment model was simplified by applying a regional equation was applied to derive the suspended sediment load for time period of interest (1992-2012). According to WWDSE (2011), regional equations developed for larger Ethiopian dams can be applied to compute suspended sediment loads for locations that have no measured sediment data.

The outputs from the regional equation were finally compared with the sediment yield simulation results of SWAT model during calibration and validation of sediment yield. The equation was derived from main hydropower stations in Ethiopia, table 14 below.

The following equation was used to calculate Suspended sediment flux for the study watershed (McMahon *et al.*, 2002 and WWDSE, 2011).

$$\mathbf{S_S} = \frac{\mathbf{44085 * R_O^{0.4674}}}{\mathbf{A^{0.57083}}}$$

Where: -

$\mathbf{S_S}$ = Suspended sediment Inflow (t/ km^2 /yr.),

A=the area of the watershed (km^2),

$\mathbf{R_O}$=Annual Runoff (mm/yr.)

Table 14 Data for regional sediment equation derivation (adapted from WWDSE, 2011),

Hydropower reservoirs	Tons/Km2/year	Watershed area (Km2)	Annual runoff (mm/yr)
Gibe III	1900	34400	450
Tekeze Dam	1283	30390	123
Karadobi Dam	1150	82230	350
Wabi Shebele at Hamaro	296	63455	49

Since SWAT model simulates the total sediment load including the bed load, it is necessary to include this bed load on the suspended load to have total sediment load for the model calibration and validation. Studies indicate that, the bed-load for African rivers usually ranges from 5%-10% of the suspended sediment load (Walling and Webb, 1987). According to Alemu *et al.* (2018), in most rivers, the value of bed load to suspended load ranges from 10 to 30%.

Weyib river flows on a moderate to gentle slope throughout its course. Thus, the bed load was assumed to be 10% of the suspended sediment load derived by the regional equation. Finally, the total sediment load for the model calibration was derived by adding this amount on the suspended sediment load. Samples of the suspended sediment load and total yearly sediment load for Weyib watershed at its outlet with their computation procedure are presented in table 15 below.

Table 15 Sample from the sediment load computed using Regional Equation

Year	Month	Col_1	Col_2	Col_3 =1*2	Col_4	Col_5	Col_6=3*5	Col_7=6/4
		Days of month	Monthly mean flow (m3/s)	Monthly Flow (m3/s)	Area (million M2)	Time (sec)	Volume (m3)	Ro (mm)
1992	1	31	0.86	26.76	24369.6	86400	2312409.60	0.09
1992	2	28	2.32	64.82	24369.6	86400	5600865.10	0.23
1992	3	31	0.75	23.15	24369.6	86400	2000419.20	0.08
1992	4	30	1.25	37.56	24369.6	86400	3245097.60	0.13
1992	5	31	4.92	152.43	24369.6	86400	13170124.80	0.54
1992	6	30	3.01	90.16	24369.6	86400	7789737.60	0.32
1992	7	31	7.20	223.19	24369.6	86400	19283270.40	0.79
1992	8	31	57.35	1777.77	24369.6	86400	153599414.40	6.30
1992	9	30	20.39	611.58	24369.6	86400	52840339.20	2.17
1992	10	31	46.85	1452.43	24369.6	86400	125489606.40	5.15
1992	11	30	23.29	698.76	24369.6	86400	60373209.60	2.48
1992	12	31	13.07	405.10	24369.6	86400	35000380.80	1.44
1993	1	31	8.99	278.78	24369.6	86400	24086160.00	0.99
1993	2	28	18.56	519.79	24369.6	86400	44909683.20	1.84
1993	3	31	3.25	100.87	24369.6	86400	8715254.40	0.36
1993	4	30	6.08	182.25	24369.6	86400	15746572.80	0.65
1993	5	31	18.87	584.83	24369.6	86400	50528966.40	2.07
1993	6	30	10.73	321.91	24369.6	86400	27812764.80	1.14
1993	7	31	12.61	390.95	24369.6	86400	33778425.60	1.39
1993	8	31	19.04	590.09	24369.6	86400	50983430.40	2.09
1993	9	30	13.94	418.23	24369.6	86400	36134899.20	1.48
1993	10	31	19.29	597.88	24369.6	86400	51656486.40	2.12
1993	11	30	15.34	460.24	24369.6	86400	39764563.20	1.63
1993	12	31	1.82	56.31	24369.6	86400	4864924.80	0.20
1994	1	31	1.09	33.89	24369.6	86400	2928268.80	0.12
1994	2	28	0.81	22.80	24369.6	86400	1969574.40	0.08
1994	3	31	0.83	25.68	24369.6	86400	2218320.00	0.09
1994	4	30	2.63	79.01	24369.6	86400	6826118.40	0.28
1994	5	31	3.76	116.51	24369.6	86400	10066809.60	0.41
1994	6	30	2.60	78.13	24369.6	86400	6750518.40	0.28
1994	7	31	16.90	523.87	24369.6	86400	45262540.80	1.86
1994	8	31	59.05	1830.64	24369.6	86400	158167641.60	6.49

Year	Col_8	Col_9 =Regional Equation	Col_10 =0.1*9	Col_11 =9+10
	Average Ro (mm/yr)	Sus Sed Inflow (t/km2/yr)	Bed load (t/km2/yr)	total load (t/km2/yr)
1992	1.64	174.19	17.42	191.61
1993	1.33	157.78	15.78	173.56
1994	1.43	163.24	16.32	179.56

3.11 Calibration and uncertainty analysis procedure of SUFI-2

For this study, the SWAT-CUP program (SUFI-2) was applied for sensitivity analysis, calibration and validation. The auto-calibration procedure by the program was assisted by manual calibration in order to modify the default parameter values of the SWAT model.

The SUFI-2 in SWAT-CUP program can be used for calibration and uncertainty analysis. In this program, uncertainties in driving variables (e.g., rainfall), conceptual model, parameters, and measured data are included in parameter uncertainty analysis (Arnold *et al.,* 2012).

For bracketing the percentage of measured data, a method of 95% prediction uncertainty (95PPU) is used. The cumulative distribution of an output variable derived by Latin hypercube sampling is used to determine the 2.5% and 97.5% levels of the (95PPU) (Abbaspour *et al.,* 2014). All uncertainties are accounted for by the parameter uncertainties that produce the 95PPU, since the measurements represent all types of uncertainties. Even though it is quite difficult to do, breaking down the total uncertainty into its various components is very important. The P-factor (i.e., the percentage of measured data bracketed by the 95PPU) is used to measure and quantify the degree to which all uncertainties are accounted for. Moreover, the intensity of an analysis of calibration/uncertainty is measured/quantified by the R factor. It is determined as the 95PPU band average thickness divided by the measured data standard deviation. SUFI-2, hence seeks to bracket most of the measured data (large P-factor, maximum 100%). According to Abbaspour *et al.* (2014), the value of the P and R-factors ranges between 0 and 100% and 0 and infinity respectively. A simulation that exactly corresponds to the measured data will have a P-factor of 1 and an R-factor of zero. The calibrated parameter ranges can be generated with an acceptable value of the R-factor and P-factor.

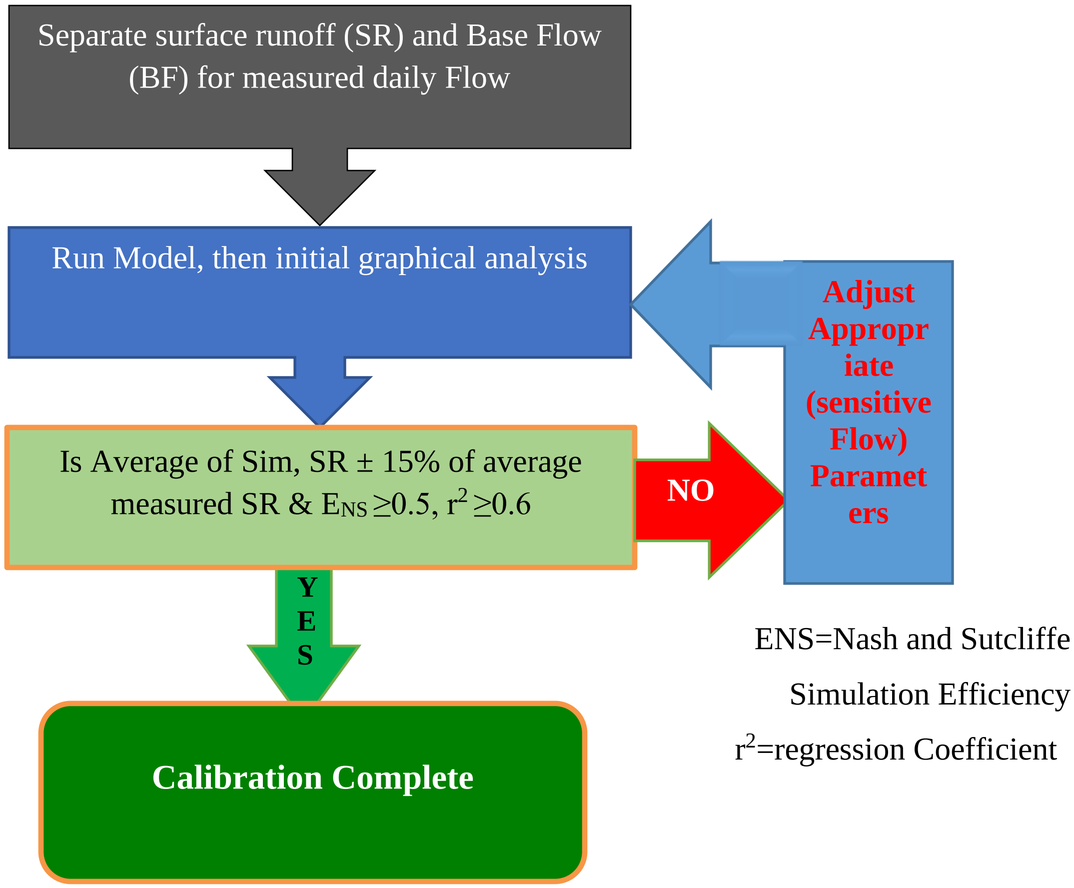

Figure 11 SWAT manual calibration flowchart (adapted from Santhi *et al.*, 2001)

3.12 Model performance evaluation

Once a model is calibrated and validated, it has to be tested for its reliability. There are different ways of evaluating the reliability or for best fit between the simulated and observed values during both calibration and validation process (Arnold *et al.*, 1998). For this purpose, the following four statistical model performance evaluation measures were used throughout the calibration and validation periods of both for flow and sediment, viz: - coefficient of determination (R2), Nash and Sutcliffe simulation efficiency (NSE), RSR (ratio of RMSE and standard deviation of observation) and Percent bias (P-bias). Table 16 below describes statistical model performance indicators and their performance ratings.

Table 16 Statistical model performance evaluation measures (Arnold *et al.*, 1998)

Statistics	Statistics equation	Performance ratings			
		Unsatis factory	Satisfactory	Good	Very Good
Coefficient of determination (R2)	$R^2 = \left(\frac{\sum[X_{obs} - X_{av}][Y_{obs} - Y_{avr}]^2}{\sum(X_{obs} - X_{av})^2 \sum(Y_{obs} - Y_{avr})^2}\right)$	<0.5	0.5-0.6	0.6-0.7	0.7-1
Nash Sutcliffe coefficient (NSE)	$NSE = 1 - \frac{\sum_{i=1}^{N}\left((X)_{obs,i} - X_{model}\right)^2}{\sum_{i=1}^{N}\left(X_{obs,i} - \overline{X}_{obs}\right)^2}$	< ±0.5	0.5-0.65	0.65-0.75	0.75-1
Ratio of Root Mean Square Error (RMSE) to the standard deviation of measured data	$RSR=\frac{RMSE}{STDEV_{obs}}$ Where: $RMSE=\sqrt{\frac{\sum_{i=1}^{N}(X_{obs}-X_{model}{}^2)}{N}}$	>0.7	0.6-0.7	0.5-0.6	0-0.5
Percent Bias	$PBIAS=\sum_{i=1}^{N}\frac{(Obs-Sim)^2*100}{\sum_{i=1}^{N}(obs)}$	≥ ±25%	±15-±25%	±10-±15	< ±10

Where:

Xav = mean of measured value,
Y = simulated value,
Yav = mean of simulated value.
X =observed vale
Sim = simulated value
Obs= observed,
Xmode =predicted outputs
N is the number of values

3.13 Methods of Data Analysis

In the SWAT model, MUSLE and SCS-CN methods are often employed for the predictions of erosion/sediment loss and runoff volume from a given watershed (Arnold *et al.*, 2012). The SWAT model needs information on soils, land use, topography, drainage and climate for a selected watershed and predicts outputs on sub watershed basis. The soil loss and runoff in the study watershed were simulated for 21 years (1992-2012). Surface runoff volume and discharge are the basic parameters for MUSLE's prediction of soil loss from a given watershed. The discharge was simulated in daily basis using SWAT. Then surface runoff (flow) was calibrated and validated to have a better estimation of the soil loss/ sediment yield.

The statistical correlation between the annual soil loss and particular land use types, soil types and slope classes were analyzed. From this, the important factor that contributes and aggravates the soil loss were determined.

3.13.1 Soil Loss Estimation

The surface erosion caused by rainfall and runoff within each HRU was estimated by applying the SWAT model, which employs the Modified Universal Soil Loss Equation (MUSLE) developed by Williams and Brendt (Williams and Brendt ,1977). Unlike USLE, MUSLE estimates the average sediment yield as a direct function of runoff.

The sediment yield for the study watersheds was simulated on daily basis from 1992 to 2012. The different levels of soil erosion in the study watershed (highest, medium, lowest average soil losses) were evaluated. Then, the correlation between the soil loss and the soil type, land use and slope gradient were examined. This statistical correlation between the sediment yield and the amount of rainfall, soil type and slope gradient was analyzed by using correlation coefficient.

3.13.2 Prioritization of hot spot areas

Hot spot areas in the study watershed were prioritized by comparison of estimated mean annual soil loss with the recommended threshold values for tolerable soil loss limits. Based on the amount of mean sediment yield, a rank was given whereby rank number one was assigned to the maximum locations or sub-watersheds of sediment yield. The last level/rank was given to those sub-watersheds with the least sediment production. A priority map was then prepared on the basis of the magnitude of the erosion. Sub-watershed prioritization was based on the threshold values of soil loss rates, in which sub-watersheds with a soil loss rate of >11 t/ha/yr were categorized under high priority area, 5-11 t/ha/yr under moderate priority and those sub-watersheds with a soil loss rate of <5 t/ha/yr regarded as low priority areas. This categorization was based on the recommended threshold values of the tolerable soil loss limit for tropical areas, which is equal to 11 t/ha/yr (Rose, 1994). Similar annual soil loss rates based sub-watershed classification was done by Tibebe and Bewket (2011) for Keleta watershed, in which sub-watershed with annual soil loss rate of <4 t $ha^{-1}yr^{-1}$ were categorized under low, 4-8 t $ha^{-1}yr^{-1}$ under moderate, 8-11 t $ha^{-1}yr^{-1}$ under high and sub-watersheds with >11 t $ha^{-1}yr^{-1}$ were put under very high severity classes. Moreover, the acceptable soil loss that can maintain an economic and a high level of production ranges from 5 to 11 t ha^{-1} $year^{-1}$ (Wischmeier and Smith 1978 and FAO, 1986 and Renard *et al.,* 1996). Therefore, this threshold was taken as benchmark for the categorization of the study watersheds.

3.14 Scenario Development for Erosion problems intervention

The main objective of this study was to identify erosion hotspot areas and to recommend different and appropriate intervention measures. For this purpose, different scenarios that reflect the effect of changes due to the intervention were developed. The main advantage of scenario development and analysis at this stage was that, it guides improved future management practices and decision making. Here possible future events were evaluated through consideration of possible alternative outcomes. Scenarios were developed by modification of interventions like physical structures such as terraces through modification of the models' USLE soil and water conservation practice factor (P-factor), the Curve Number (CN) and average slope length (SLSUBBSN). Other scenarios were developed by changing specific land use types by a certain percentage; so that the changes to the sediment yield due to this land use conversion could be quantified.

3.14.1 Scenarios Developed Based on Land Use Land Cover factor

To evaluate the changes in sediment yield due to land use changes, about five scenarios were considered. These scenarios were developed by changing the agricultural land use type (land use type from which the highest sediment load in the watershed was generated) to forest cover by 10% ,20%, 30%, 40%, and 50%, as agricultural land use type is the main contributor of soil erosion. These scenarios were the following.

Scenario	**Description**
Scenario-0	Original condition (without any intervention)
Scenario -1	Changing AGRC to FRST by 10%
Scenario -2	Changing AGRC to FRST by 20%
Scenario -3	Changing AGRC to FRST by 30%
Scenario -4	Changing AGRC to FRST by 40%
Scenario -5	Changing AGRC to FRST by 50%

Here, to appraise the impacts of changes in land use and covers on the sediment yield, the SWAT model that was calibrated and validated for sediment yield was applied to simulate the aforementioned land use and cover scenarios on the sediment yield.

3.14.2 Scenarios developed Based on land management/ support practices

Applying physical structures such as terraces made from stone bunds reinforced by biological measures like filter strips in low slope areas of a given watershed could give potential effect (Betrie *et al.,* 2011). In this study, different sediment reduction intervention measures (scenarios) were applied; including, filter strips, contour farming and terracing (fanya-juu, bench and stone bunds).

Terrace i**s** an earth embankment with a channel constructed across the slope at a fixed vertical interval and at an acceptable horizontal slope (Taffa, 2002). Terraces are constructed to reshape the land in areas of high rainfall and hence reduce erosion, to remove excess surface water and to retain maximum amount of moisture for crop production (Gardner and Miller, 2004). In SWAT model, terracing can be simulated by changing both erosion and runoff parameters (Arnold *et al.*, 2012). In this study, three types of terraces were applied; stone bund, fanya-juu terrace and Bench Terrace. While the fanya-juu terrace was applied on land slope ranging between 20 and 40%, the bench terrace was applied on land slope of greater than 40%. Whereas, the stone-bund was applied on land slope of 0-20%. Stone-bund, Fanya-juu terrace and Bench-terraces were simulated by adjusting the USLE practice factor (TERR_P), the slope length factor (TERR_SL) and the curve number factor (TERR_CN).

A filter strip, is a strip of dense vegetation designed to control or intercept transport of nutrients and pesticides-enriched sediments from upslope area (Gardiner and Miller, 2004). Usually filter-strips are planted on the lower end of a field to prevent sediment from entering adjacent ditches or streams. Filter strips decrease the velocity of the surface runoff due to increased roughness provided by the vegetation and in effect allow the sediments to settle due to the reduced sediment transport capacity of the runoff. They also enhance infiltration thereby reducing the amount of runoff and sediment transported thus aiding in sediment deposition (Yuan *et al.,* 2009 and Borin *et al.*, 2005).

Filter-strip parameter were represented in the SWAT model by FILTERW, which is the width of filter strip and was applied to the land slope between 0 and 20%.

SWAT uses the trapping efficiency equation provided below to model filter strips and according to the equation a filter width of 30 m would have a trapping efficiency of 1 (Parajuli *et al.,* 2008). Thus, increasing the filter strip width beyond 30 m would not be effective in reducing sediments loading in the channels.

$$\mathbf{Trap_{eff\_sed} = 0.367FILTERW^{0.2967}}$$

Where: - $\mathbf{Trap_{eff\_sed}}$= Trapping efficiency of the sediments and

FILTERW = the width of the filter strip (m).

Different scholars recommend different width of filter strips. For instance, Wolde and Thomas (1989) recommend installation of grass strips of 1.0 m to 1.5 m wide, where land is not scarce and 0.5 m where land is scarce in Kenya. This suggests that even smaller widths of grass strips would still be beneficial in reducing soil loss. Yuan *et al*. (2009) found that a 5 m buffer can trap up to 80% of the sediments. Whereas, Borin *et al.* (2005) found a 78% total suspended sediment load reduction from a 6 m buffer strip established from trees and grass. On the other hand, Robinson *et al.* (1996) revealed that the initial 3 m of vegetative filter strips trapped more than 70% of the sediment when simulated using SWAT.

In this study, taking the scarcity of land in to consideration and the efficiency of filter-strips reported by different researchers, a filter width of 1m was applied on land slope ranging from 0-20%.

In Scenario 2, stone bund was applied on all HRUs, on all soil types and on all slope classes (table-17 below). The Curve Number (CN2), average slope length (SLSUBBSN) and the USLE support practice factor (USLE P) were considered to be appropriate parameters to represent the effect of stone bunds. To evaluate the effect of stone bunds, SWAT model was simulated by decreasing the value of the Curve Number (CN_2), as CN is the ratio of surface runoff to that of the rainfall, and hence the value of CN decreases because of the reduction in the overland flow. Similarly, the value of the support practice factor (P-factor) was adjusted/reduced from the default value to account for the amount of sediment deposited due to stone bunds. Moreover, the value of average slope length (SLSUBBSN) factor was reduced from the default value, as stone-bunds reduce the slope length.

Generally, the effect of stone bunds is to reduce overland flow, sheet erosion and to reduce slope length to (Bracmort *et al.*, 2006). In the SWAT model, the HRU (.hru) input table were edited in order to adjust the value of the SLSSUBSN; the USLE P and CN2 values were adjusted by editing Management (.mgt) input table.

Table 17 Parameters used to represent management practices

Scenario	Description	SWAT Parameters			
		Parameters Name (input file)	Slope (%)	Calibrated Value	Modified Value
Scenari-0	Baseline	-	-	Default value	Default value
Scenario-1	Filter-strips	FILTERW (.hru)	0-20% slope	0	1m
Scenario-2	Stone-bund	SLSUBBSN (.hru)	0-10% slope	61m	10m
			10-20% slope	24m	10m
			>20% slope	9.1m	7.3m
		CN2 (.mgt)	0-20% slope	84m	77m
		USLE_P (.mgt)		0.95	0.32
Scenario-3	Contour Farming	CN2 (.mgt)	0-20% slope	84m	77m
		USLE_P (.mgt)		0.95	0.6
Scenario-4	Fanya juu terrace	CN2 (.mgt)	20-40%slope	84m	77m
		SLSUBBSN (.hru)		9.1m	7.3m
		USLE_P (.mgt)		0.95	0.25
Scenario-5	Bench Terrace	CN2 (.mgt)	>40% slope	84m	71m
		SLSUBBSN (.hru)		9.1m	7.3m
		USLE_P (.mgt)		0.95	0.2
Scenario-6	S1+S2+S3+S4+S5	FILTERW (.hru)	All	0	1m
		SLSUBBSN (.hru)	All	61m	7.3m
		CN2 (.mgt)	All	84m	71m
		USLE_P (.mgt)	All	0.95	0.2

Parameter values for SLSUBBSN were assigned based on the slope classes. The parameter values for the initial calibrated SWAT model with slope classes of 0–10%, 10–20% and greater than 20% were 61m, 24m and 9.1m respectively. The corresponding adjusted SLSUBBSN parameter value were 10 m for 0–10% and 10–20% slope classes, and 7.3 for slope of a land greater than 20%.

Whereas, the modified value for USLE P and CN2 were 0.32, and 77 respectively (Table 17 above). The SLSUBBSN is used in the SWAT model to represent the spacing of successive stone bunds in field conditions. In this study, the contoured and terraced condition values recommended by SWAT user manual version 2005 were used for assigning CN2 values (Neitsch *et al.*, 2005). The SLSUBBSN parameter value adjustment was based on a study paper for the Ethiopian highlands by Hurni (1985) and Herweg and Ludi (1999). Moreover, the values of USLE-P parameters were adjusted using the documented field experience by (Gebremichael *et al.*, 2005). The recommended values of P factor are given in table 50 in the appendix section. Furthermore, in table 50, a P- value of 0.8 and 0.5 was suggested for stone covers of 40% and 80%, respectively (Hurni, 1985). On the other hand, Gebremichael *et al.* (2005), provides the following equation for linear extrapolation of the rock fragment factor (PR) for other percentage covers.

$$\mathbf{P_R = -0.0063R_C + 1.0167} \qquad (\mathbf{R_C < 80}\%)$$

Where: - P_R=Rock fragment Factor

R_C=Stone Cover

The third scenario, Scenario-3 (Contour farming) was implemented in all HRUs with their slope ranging from 0-20%. To evaluate the effect of this scenario, SWAT model was simulated by adjusting the value of the Curve Number (CN_2) and USLE_P factors/parameters. In this study, while the value of CN was reduced by 5 from the calibrated value of 84, the value of the USLE_P was altered from 0.95 to 0.6. The values recommended by Arabi et al. (2007) and Neitsch *et al.* (2011) were referred for USLE_P parameter adjustment. Likewise, the values of the CN parameter were adjusted using the values recommended for CN for different practices given in (Neitsch *et al.*, 2011).

The next scenario, Fanya juu terracing was applied to HRUs with their slope ranging between 20 and 40%. The SWAT simulation for Fanya juu terracing was performed by adjusting the CN, USLE-P and SLSUBBN. The value of the CN parameter was reduced from the calibrated value of 84 to 77 and USLE_P was reduced from 0.95 to 0.25. The USLE P values suggested by Arabi et al. (2007) and Neitsch *et al.* (2005) for contoured and terraced farmlands were referred to modify the USLE P values. Here, to obtain slope length for Fanya juu terraces, the calibrated SWAT average slope length (SLSUBBSN) value was reduced by 20 percent, decreasing it from 9.1 m to 7.3 m. For bench terraces, a similar technique was applied, but it was applied to HRUs with a slope of > 40 percent. For bench terraces the value of CN was reduced from the calibrated value of 84 to 71, while its USLE_P value was reduced from 0.95 to 0.2. As bench terrace is more effective than fanya juu terraces, the reduction of CN for it was 2 units higher than that of the fanya juu terracs. This demonstrates the difference between the two. Moreover, Fanya juu terraces are implemented on 48.7% sloping land; while in those areas with a slope up to 55 percent the recommended structure is Bench Terrace (Hurni, 1985).

The final Combined Scenario was applied to all HRUs and to all slope classes. The Swat simulation for the combined scenario was performed by adjusting the CN, USLE-P and SLSUBBN simultaneously. Here, to account for the maximum reduction in sediment yield by the combined scenario, the value of CN was decreased by 13 units from the calibrated value of 84 to 71 and USLE_P was reduced from 0.95 to 0.2 and the SLSUBBN from the calibrated value of 61m to 7.3m.

Finally, to see the effect of individual scenarios, each scenario was simulated separately throughout the simulation period and compared with the base scenario.

4 RESULTS AND DISCUSSION

4.1 parameters' Sensitivity

During sensitivity analysis, some parameters were found to be highly influential to both the flow and sediment, while others being sensitive to either of the two. Consequently, sensitivity analysis was performed for each flow and sediment separately. The results of sensitivity analysis for both flow and sediment are discussed below.

4.1.1 Parameters sensitive to flow

Among the twenty-six (26) flow parameters that were considered to significantly influence the model simulation or model predictions, 12 of them were found to be highly sensitive to flow. Consequently, these parameters were used for streamflow calibration. Sensitive flow parameters, fitted values with their corresponding p-values, t-stat results and ranks are presented in table 18 below.

Table 18 List of flow parameters and their ranges a used for Sensitive analysis

No	Parameter Name	Description	Fitted Value	Range		P-Value	t-stat	Rank
				Min	Mxn			
1	R__CN2.mgt	SCS runoff curve number (dimensionless)	-0.12	-0.25	0.25	0	8.65	1
2	V__Alpha_B.gw	Base-flow alpha factor (days)	0.853	0	1	0.01	3.14	2
3	A__ESCO.hru	Soil evaporation compensation factor (dimensionless)	0.632	0	1	0.02	2.4	3
4	R__SOL_AWC(..).sol	Available water capacity of the soil layer (mm H2O/mm soil)	0.227	-0.25	0.25	0.06	-1.9	4
5	R__RCHRG_DP.gw	Deep aquifer percolation fraction (dimensionless)	0.781	0	1	0.21	1.26	5
6	SLSOIL	Slope length for lateral sub-surface flow	22.34	0	150	0.3	-1.1	6
7	R__SOL_Z(..).sol	Depth from soil surface to bottom of layer	0.214	-0.25	0.25	0.33	0.99	7
8	R__CANMX.hru	Maximum canopy storage (mm)	6.164	0	10	0.34	-1	8
9	V__REVAPMN.gw	Threshold depth of water in the shallow aquifer for "revap" to occur (mm)	91.84	-100	100	0.38	0.89	9

No	Parameter Name	Description	Fitted-value	Range		P-Value	t-stat	Rank
				Min	Max			
10	V__GW_REVAP.gw	Groundwater “revap” coefficient (dimensionless)	0.031	-0.04	0.04	0.4	0.85	10
11	R__SOL_K(..).sol	Saturated hydraulic conductivity	0.193	-0.25	0.25	0.49	-0.7	11
12	V__GWQMN.gw	Threshold depth of water in the shallow aquifer required for return flow to occur (mm)	867	0	5000	0.49	0.69	12
13	R__BLAI{..}.plant.dat	Maximum potential leaf area index	0.45	0	1	0.54	0.61	13
14	V__CH_K2.rte	Effective hydraulic conductivity in main channel alluvium (mm/h)	106	0	150	0.56	-0.6	14
15	R__SURLAG.bsn	Surface runoff lag time [days]	5.37	0	10	0.57	-0.6	15
16	V__GW_DELAY.gw	Groundwater delay (days)	0.084	-10	10	0.65	-0.5	16
17	R__CH_N1.sub	Manning value for the tributary channels	0.283	0	1	0.67	-0.4	17
18	R__EPCO.bsn	Plant uptake compensation factor	0.142	0	1	0.71	-0.3	18
19	R__SOL_BD(..).so	Moist bulk density	0.138	-0.5	0.6	0.76	0.25	19
20	R__OV_N.hru	Manning’s n value for overland flow	-0.13	-0.2	0	0.79	-0.2	20
21	R__HRU_SLP.hru	Average slope steepness	0.241	0	0.2	0.82	-0.1	21
22	R__SLSUBBSN.hru	Average slope length (m)	0.173	0	0.2	0.84	-0.1	22
23	V__CH_N2.rte	Manning’s n value for the main channel	0.162	0	0.3	0.87	0.09	23
24	V__ALPHA_BNK.rte	Base-flow alpha factor for bank storage	0.386	0	1	0.91	0.05	24
25	R__SOL_ALB(..).sol	Moist Soil Albedo	0.113	-0.25	0.25	0.92	0.05	25
26	R__BIOMIX.mgt	Maximum potential leaf area index	0.003	0	10	0.94	-0	26

Note: “A__” indicates that the value given is added to the existing value of the parameter, "V__" indicates that the value of the existing parameter is to be replaced by the value given, and "R__" indicates that the value of the existing parameter is multiplied by (1+ a given value).

The P-value and t-stat results were evaluated to distinguish sensitive parameters and those flow parameters, which have a P- value of less than 0.5 were considered as more sensitive model parameters for flow.

For flow calibration, the runoff curve numbers (CN2) were adjusted within 25% percent from the tabulated curve numbers. The SCS runoff curve number (CN2) followed by Base-flow alpha factor (ALPHA_BF), Soil evaporation compensation factor (ESCO), Available water capacity of the soil layer (SOL_AWC) and Deep aquifer percolation fraction (Rchrg_DP) were the highest in their sensitivity to flow. SLSOIL, SOL_Z, CANMX, REVAPMN, GW_REVAP, SOL_K and GWQMN (see table 18 above) were found to be the most effective hydrologic parameters for the simulation of streamflow in the study watershed and were adjusted from SWAT initial estimates to match the simulated and observed flows.

A decrease in Esco showed a decrease in water yield, surface runoff and base flow and an increase in evapotranspiration. The value of Esco varies between 0 and 1. As Esco is reduced the model is able to extract more of the evaporative demand from the lower layers. This has also been shown by other studies (Kannan *et al.*, 2007; Sang, 2005). On the other hand, GWQMN was found to have very slight (insignificant) effect on surface runoff. This is because it only deals with the water that have already infiltrated and percolated into the aquifer. Shallow aquifer contributes flow to the main channel as base flow. SWAT will only allow the base flow to enter the stream if the depth of water in the shallow aquifer exceeds GWQMN.

The soil type used to generate the HRUs in this study has four layers with saturated hydraulic conductivity of 1180 mm/hr for the first layer and 324.43 mm/hr for the second, 14.31mm/hr for third and 4.1mm/hr for the fourth layers. Due to low hydraulic conductivity of the lower layers compared to the top layer, the lateral flow was high. For a soil with multi-layers, if the hydraulic conductivity of the soil layer at the surface is high and the hydraulic conductivity of the soil layers at shallow depth is impermeable or semipermeable, then the rainfall will percolate vertically until it encounters the impermeable layer. This saturated zone of water is the source of lateral sub-surface flow (Sloan and Moore, 1984). This effect was manifested in this study with a very high lateral flow

4.1.2 Parameters sensitive to sediment

The SCS runoff curve number (CN2), Parameter of the exponent for sediment measurement entering the channel during sediment routing (SPEXP), a linear parameter to determine the overall sediment quantity that can enter during the routing of the channel sediment (SPCON), Average slope steepness (HRU_SLP), Average slope length (SLSUBBSN), Initial residue cover (RSDIN), Channel cover factor (CH_COV2), USLE equation soil erodibility (K) factor (USLE_K) (see table 19) were those parameters that were considered to highly influence the sediment simulation. The following table 19 presents the parameters that were used to evaluate sensitivity to sediment yield

Table 19 Parameters used for sediment yield sensitivity analysis

No.	Parameter Name	File ext.	Method	Min_value	Max_value	Fitted-Value
1	CN2	.mgt	R relative	0.338625	0.411677	0.361
2	SPEXP	.bsn	V replace	1	2	1.21
3	SPCON	.bsn	V replace	0.0001	0.01	0.001
4	LAT_SED	.hru	R relative	0	5000	334.21
5	HRU_SLP	Hru	R relative	0	1	0.322
6	CH_COV1	.rte	V replace	-0.05	0.6	0.55
7	CH_COV2	.rte	V replace	-0.001	1	0.56
8	CH_BED_BD	.rte	V replace	1.1	1.8	1.64
9	CH_N2.rte	.rte	V replace	0	0.3	0.16
10	CH_ERODMO	.rte	V replace	0	1	0.81
11	USLE_K	.sol	V replace	0	0.65	0.04
12	SOL_AWC	.sol	R relative	0.0677	0.1717	0.072
13	BIOMIX	.mgt	V replace	0	1	0.05
14	RSDIN	.hru	R relative	0	10000	356.2
15	USLE_P	.mgt	V replace	0	1	0.01
16	SLSUBBSN	Hru	R relative	0	150	17.81

Among the 16 sediment parameters that were considered to significantly influence the sediment yield and transport in the watershed, 8 (eight) of them were found most sensitive to sediment simulation. Sensitive Sediment yield parameters, the P-values and t-stat results with their corresponding ranks are provided in the table 20 below.

Table 20 Sensitive Sediment yield parameters and their respective Ranks

Parameter Name	t-Stat	P-Value	Rank
CN2	12.01	0.00	1
SOL_AWC	9.37	0.02	2
SPEX	6.14	0.05	3
HRU_SLP	4.16	0.08	4
USLE_K	3.72	0.13	5
USLE_P	1.67	0.15	6
CH_COV2	-1.58	0.16	7
CH_BED_BD.	-1.19	0.19	8

CN2 followed by SOL_AWC, SPEX, HRU_SLP, USLE_K, USLE_P, CH_COV2 and CH_BED_BD were those sediment parameters that were found to highly influence the sediment prediction of the model. The movement of sediments in the watershed is influenced by multiple variables because different components of the landscape and channel are involved. Upland and channel variables can be grouped into the parameters used in the sensitivity analysis. While the upland factors affect the sediment transport landscape portion, the channel factors affect the sediment transport channel component (Santhi *et al.*, 2001). Parameters such as USLE K, HRU SLP and SLSUBBSN are classified as Upland variables, while SPCON, SPEXP and CH COV 2 are classified as channel variables. In this study, both the upland and channel variables were found to be responsible for the transport of sediment. Parameters sensitivity decreases with increasing rank numbers and vice-versa. Thus, parameters that have low p-value and higher absolute t-value in the global sensitivity were regarded as highly sensitive (both for flow and sediment).

4.2 Model calibration and validation

4.2.1 Model calibration for flow

The results of an automated baseflow separation showed that about 28-54 percent of the total discharge was contributed by the surface water supply from the daily flow data derived by the regional equation.

Table 21 and figures 12 and 13 present the values and plots of observed and simulated monthly discharge at Weyib outlet for simple visual comparison. In order to determine the goodness of fit between them, the observed and simulated discharge were plotted against each other. The value of the coefficient of determination (R^2) and Nash-Sutcliffe coefficient of efficiency (NSE) for monthly stream flow for the calibration period was 0.74 and 0.67, respectively, which is good (Arnold *et al.*, 1998 and Morais *et al.*, 2007). The calibrated P-factor and R-factor of SUFI-2 for daily calibration was 0.87 and 0.92 respectively. From this it can be inferred that, based on the parameter ranges selected for calibration, the model could bracket 87% of the measured data by 95PPU. This result indicates that the model was capable of accounting for most of uncertainty sources during calibration

Table 21 Average Monthly observed and simulated value for flow during calibration

Period	Mean value of observed and simulated Flow during calibration (m3/s)		Efficiency of the Model		
	Observed value	Simulated value	R2	NSE	RSR
1994-2004	21.10	22.26	0.74	0.67	0.54

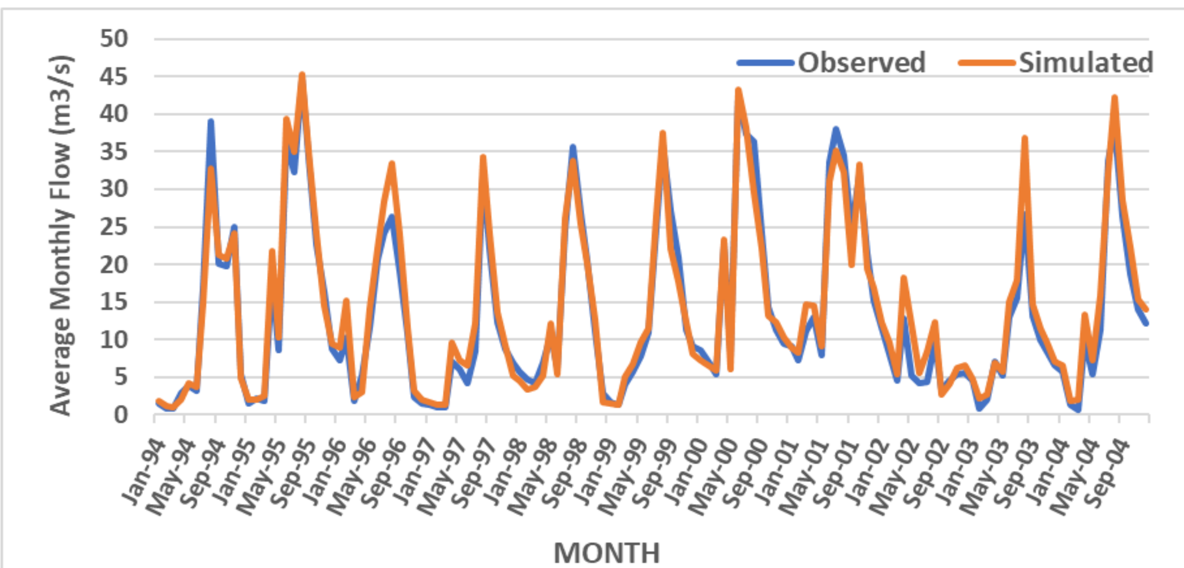

Figure 12 Average Monthly Observed and simulated flow during calibration

Thus, bracketing most of measured data enables the model to capture all the uncertainties. The R-factor of 0.92 implies that the ratio of width of the 95PPU band to standard deviation of measured data is within the acceptable threshold of <1.5. The R factor accounts for measurement errors, conceptual model uncertainty and parameter non-uniqueness problem (Schuol and Abbaspour, 2006). The model calibration result indicated a PBIAS value of -21. 2%, which is within the ± 25% range recommended by Moriasi *et al.* (2007). The slight overestimation bias of -21.2% can be attributed to higher simulated peak flows such as during 1995 and 1996 and due to uncertainties in measured data. The calibration result is highly influenced by parameter ranges, number of simulations and number of iterations (Kilemo, 2017).

The calibration results show a good agreement between the simulated and measured monthly flows. The statistical model performance indicators are all within the acceptable range, indicating a good agreement between the observed and simulated results.

Even though the model slightly over estimated the flow during the calibration period, the overall trend shows a good pattern. Figure 13 also shows the scatter plots between monthly observed and simulated flows and there was a positive relation between observed and simulated flows.

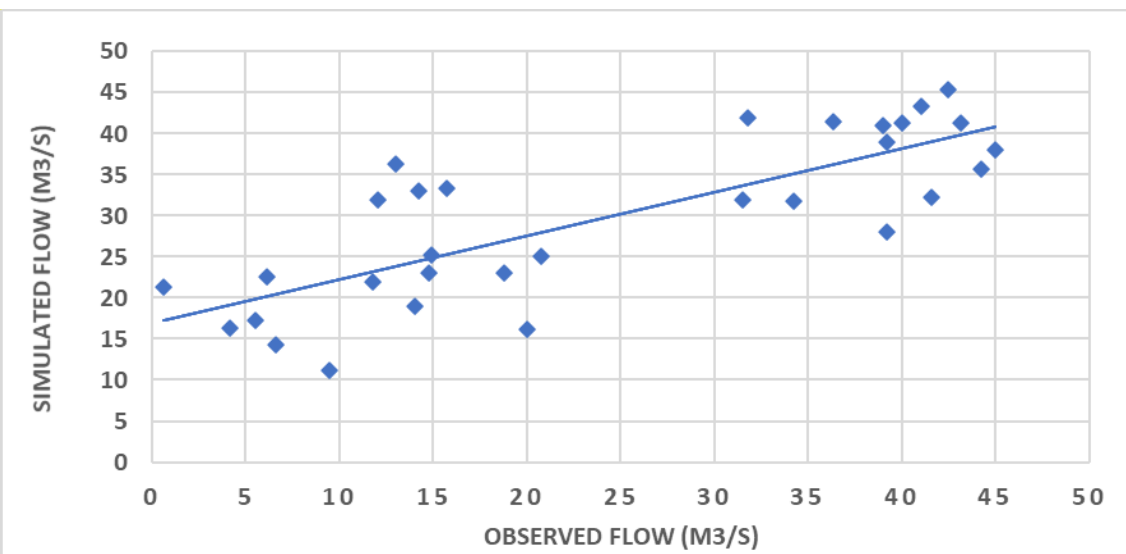

Figure 13 Fit line for Monthly Observed and simulated flow during calibration period

4.2.2 Model validation for flow

While in calibration the parameter values are modified until the predictions best fit with the observed data, validation parameters are dependent on calibrated parameter ranges; as a result, the validation performance metrics were a bit weaker than calibration performance values (Abbaspour *et al.*, 2014). The coefficient of determination (R^2) and the Nash-Sutcliffe efficiency (NS) for daily streamflow during 2005-2012 (validation period) were 0.82 and 0.79 respectively. Table 22 below shows the monthly observed and simulated daily stream flow for validation period. Measured water flow data greatly influence the performance of calibrated model and its associated uncertainties (Abbaspour *et al.*, 2014).

Table 22 Average monthly Observed and simulated Flow during Validation

Year	Average monthly observed and simulated Flow for Validation (m^3/s)		Model efficiency		
	Observed	Simulated	R2	NS	RSR
2005-2012	14.67	15.84	0.82	0.79	0.46

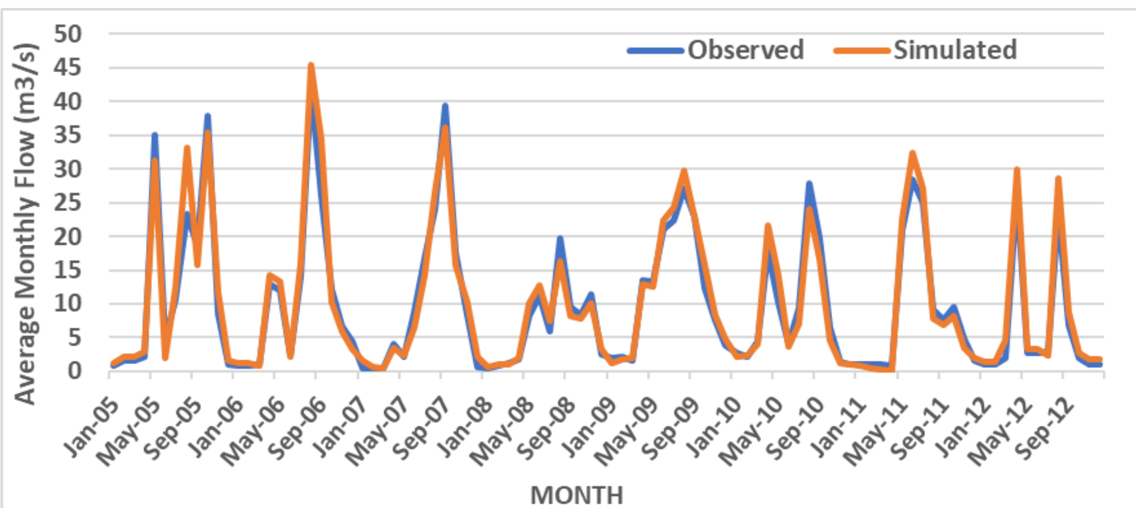

Figure 14 Average monthly Observed and simulated flow for Validation

Figure 15 below depicts the scatter plots between monthly observed and simulated flows. There is a positive relation between observed and simulated flows.

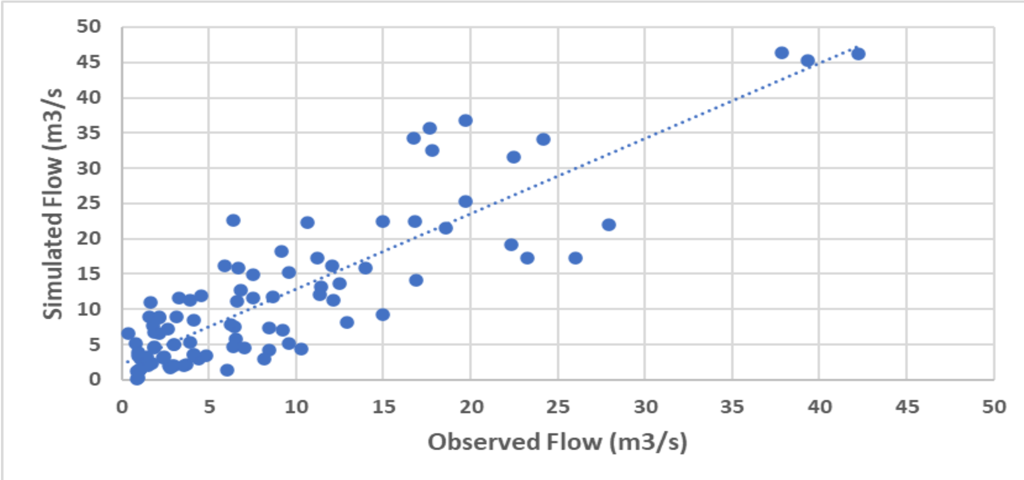

Figure 15 Fit line of average daily observed and simulated flow for validation period

As shown in Table 21 and 22 and figure13 and 15, all the statistical model performance indicators quite agree with the acceptable ranges of the values recommended by SWAT developers such as Santhi *et al.* (2001), in which they recommend an acceptable value for model calibration and validation for hydrology to be an $R^2 > 0.6$, NSE > 0.5 and RSR < 0.7. Similarly, its performance is very good when compared with the statistical performance values recommended by Morais *et al.* (2007). Consequently, it can be inferred that the SWAT model accurately simulated the stream flow at Weyib watershed outlet.

Alemayehu (2014) reported the efficiency of the SWAT model in replicating the streamflow with an R^2, NSE and PBIAS values of 0.81, 0.75 and 23, respectively in the calibration period and with an R^2, NSE and PBIAS values of 0.65, 0.59 and 20, respectively in the validation period. In the study conducted by Samuel (2013), NSE value of 0.65, RSR of 0.4 and PBIAS of 15 was reported during calibration at monthly time step and NSE value of 0.5, RSR of 0.5 and PBIAS of 31was reported for validation period. Bieger *et al.* (2011) Reported an R^2 of 0.89 and NSE of 0.84 for calibrated monthly flows and for validation the following monthly flows statistics were reported an R^2 of 0.82 and NSE of 0.82. Whereas, Setegn (2008) stated an R^2 of 0.80 and NSE of 0.73 for calibration and an R2 of 0.80 and NSE of 0.71 for validation periods. Here it can be seen that there is some discrepancy in the reported statistical values among scholars, including this particular study too. This discrepancy might be due to mainly variation in spatial input data used (predominantly land use land cover data), variation in sensitive flow parameters of the study watershed, which significantly influence the calibration processes. Other reasons could be uncertainty during data handling and due to many more cases.

The model underestimated the stream flow during 1994, 1998, 2001, 2005, 2007, 2008 and 2010. While it overestimated for the rest of the time periods. Despite overestimations, both during the calibration and validation periods, the model outputs reflect a good relationship between the observed and the simulated stream flows. Overestimation could be due to Curve Number (CN2) method that is used to predict the surface runoff. The CN2 method assumes a unique relationship between cumulative rainfall and cumulative runoff for the same antecedent moisture condition. In the Ethiopian Highlands, however, Liu *et al.* (2008) showed that the ratio of discharge to effective precipitation (Q/(P-ET)) is increasing with cumulative precipitation and consequently the watersheds behave differently depending on how much moisture is stored in the watershed, suggesting that saturation excess processes play an important role in watershed response.

Moreover, differences in simulation and observed streamflow (both during the calibration and validation period) may be observed due to the limitation of the curve number method (Yuan, 2010). According to him, the curve number method does not take into account the impacts of duration and intensity of precipitation. Since only the daily total rainfall depth is used as an input, the uncertainties can be high. Another reason for the discrepancy between simulated and observed streamflow may be due to the fact that spatial variability of precipitation and limitations in the number of gauging stations in the watershed. The number of precipitations gauging stations within a given watershed significantly affect the model prediction. Similarly, Significant under or overestimations can occur when network of gauging station is not dense enough (David and Davidova, 2015).

Generally, the model calibration and validation outputs reflect the accuracy of the model in simulation of flow under time-periods outside of the calibration time period. Since the model performed well both during the calibration i.e., 1992.2004 and validation period i.e., 2004-2012 at Weyib watershed outlet, it can be inferred that the set of sensitive parameters listed in Table 12 during the sensitivity analysis and calibration process can be taken as representative flow parameters for Weyib watershed.

4.2.3 Model calibration and validation for sediment Yield

4.2.3.1 Model calibration for sediment Yield

Sediment yield in SWAT is estimated using the peak runoff rate calculated through the modified rational method. The modified rational formula peak runoff rate is a function of rainfall proportion, surface run off volume, sub basin area and time of concentration (Neistch *et al.,* 2005). The average yearly sediment load and the calibration statistics for observed and simulated sediment yields for the calibration period are presented in table 23 below.

Table 23 Yearly Observed and simulated sediment load during calibration period

Period	Average observed and simulated sediment load during calibration Period (1x10^{5}ton/yr)		Performance of the Model		
	Observed Sediment load	Simulated Sediment load	R2	NSE	RSR
1994-2004	29.07	29.58	0.79	0.78	0.43

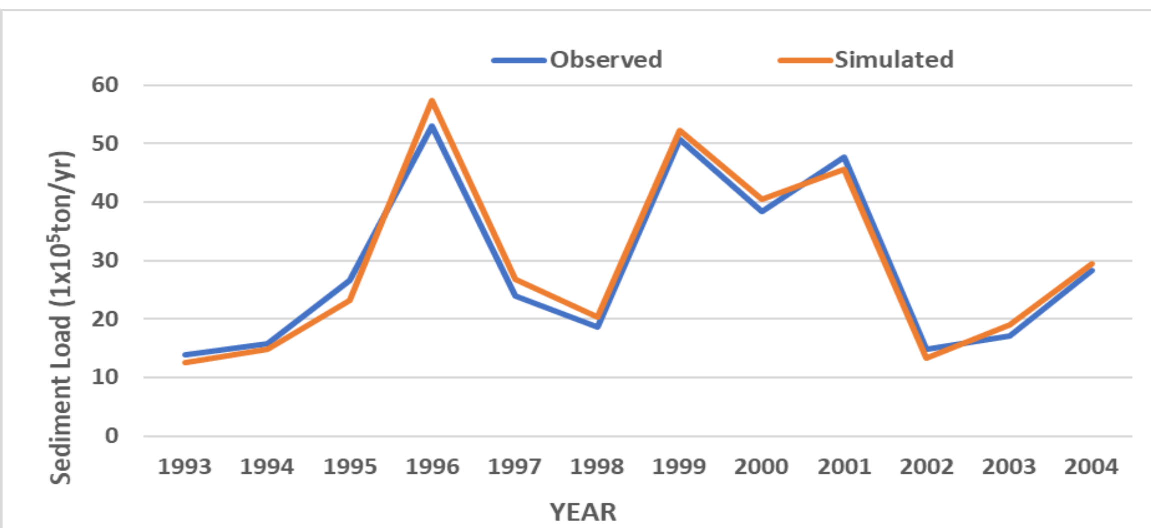

Figure 16 Yearly Observed and Simulated sediment load during calibration period

Table 23 and figures 16 and 17 present the values and plots of observed and simulated monthly sediment data at Weyib outlet for simple visual comparison. In order see the goodness of fit between them, the observed and simulated sediment yield were plotted against each other. The value of the coefficient of determination (R^2) and Nash-Sutcliffe coefficient of efficiency (NSE) for monthly sediment data for the calibration period was 0.79 and 0.68, respectively, which is very good (Arnold *et al.,* 1998 and Morais *et al.,* 2007). Similarly, its performance is very good when compared with the statistical performance values recommended by Santhi *et al.* (2001), which is $R^2 > 0.6$, NSE > 0.5 and RSR < 0.7.

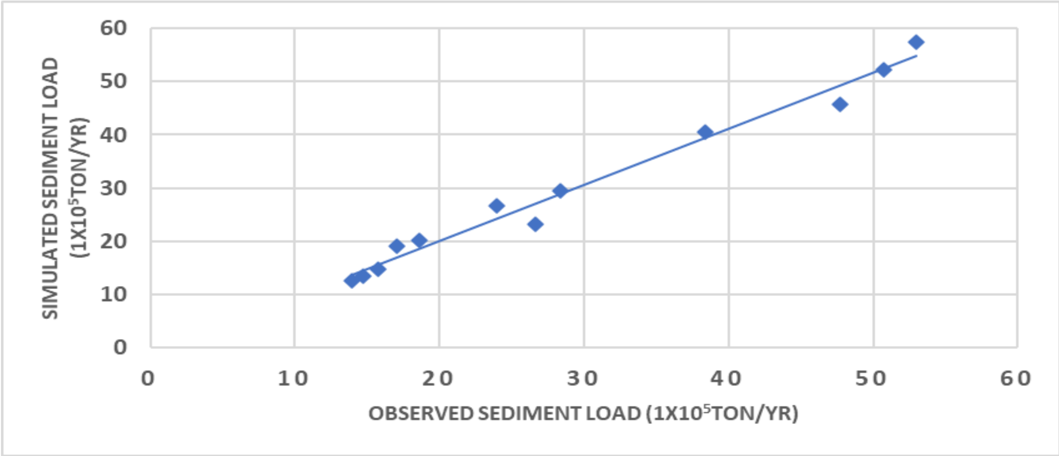

Figure 17 Fit line for observed and simulated sediment load during calibration

4.2.3.2 Model validation for sediment

The statistical model performance indicators for the validation period are presented in table 24. As shown in Table 24 and figure19, all the statistical model performance indicators quite agree with the acceptable ranges of the values recommended by SWAT developers such as Santhi *et al.* (2001), in which they recommend an acceptable value for model calibration and validation for sediment yield to be an $R^2 > 0.6$, NSE > 0.5 and RSR < 0.7. Similarly, its performance is very good when compared with the statistical performance values recommended by Morais *et al.* (2007).

Table 24 Average yearly Observed and simulated sediment yield for validation period

Year	Average observed and simulated sediment for Validation (1x10^{5}ton/yr)		Model efficiency		
	Observed	Simulated	R2	NS	RSR
2005-2012	50.30	50.42	0.84	0.76	0.45

The average yearly observed and simulated sediment loads properly agree with one another, reflecting the model precision in prediction of the sediment load. However, the model slightly over predicted the peak sediment yield during 2009 and under predicted the sediment yield during 2008.

Moreover, there was under prediction by the model for the sediment load for the time period 2006-2008 and 2011-2012 and over predicted from 2005-2006 and 2009-2010, figure 19 below.

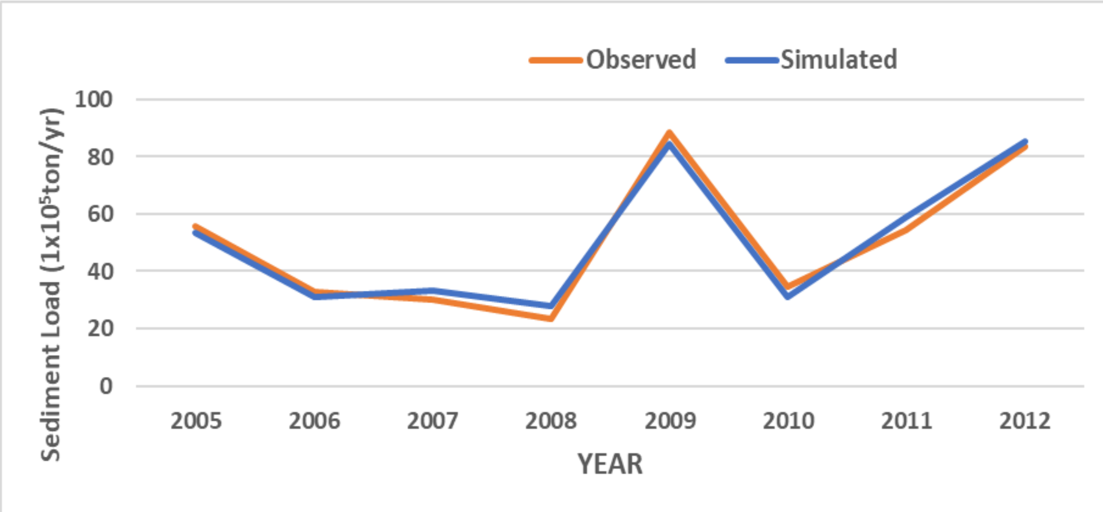

Figure 18 Yearly Observed and Simulated sediment for Validation period

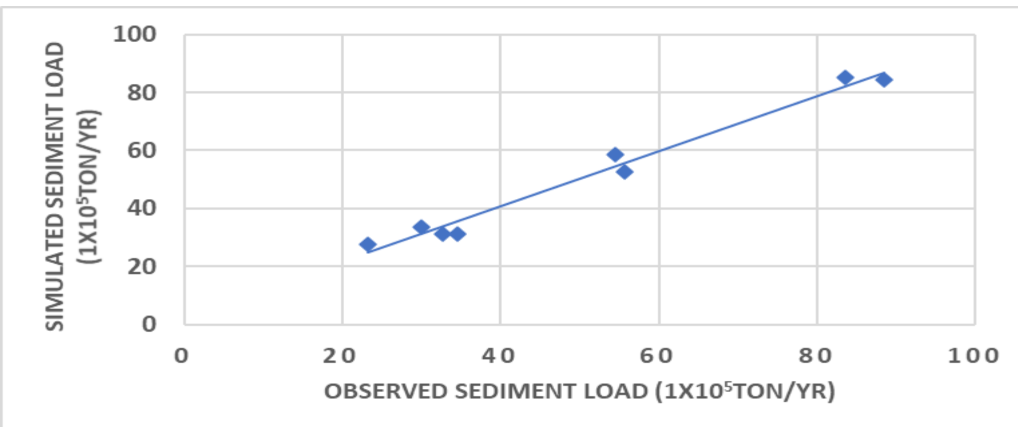

Figure 19 Fit line for observed and simulated sediment load during validation period

Consequently, it can be inferred that the SWAT model accurately simulated the sediment yield at Weyib outlet. The model performance for this study is comparable to the results reported by Steenhuis *et al.* (2009), in which an NSE value of 0.75 was reported for the calibration period and NSE of 0.69 for the validation period. Similarly, Betrie *et al.* (2011) reported the efficiency of the SWAT model in replicating the sediment yield with NES value of 0.92, RSR of 0.29 and PBIAS of −0.21% for the calibration and NES of 0.88, RSR of 0.34, and PBIAS of −11% for the validation periods.

Alemu *et al.* (2018) Reported an R^2 of 0.71, NSE of 0.74, RSR of 0.54 and PBIAS of -7.87 for calibrated daily sediment yield, and for validation the following daily sediment yield statistics were reported R^2 of 0.71, NSE of 0.75, RSR of 0.53 and PBIAS of -12.25 for Maki sub-basin. In the meantime, for Katar sub-basin an R^2 of 0.67, NSE of 0.72, RSR of 0.58 and PBIAS of -16.68 for the calibration period and R^2 of 0.75, NSE of 0.79, RSR of 0.50 and PBIAS of -16.25 for the validation period was reported by the same study (Alemu et al., 2018). On the other hand, Gebiaw *et al.* (2017), in their study in the upper Blue Nile River Basin, stated an R^2 of 0.65, NSE of 0.58, RSR of 0.65 and a PBIAS of 24.5 for calibration period while an R2 of 0.67, NSE of 0.58, RSR of 0.64 and a PBIAS of 8.8 for validation period were reported for monthly sediment yields.

Alike the model results for the stream flow, there is also a discrepancy in the recommended statistical values among scholars, including the performance indicators values found for this particular study. This discrepancy might be due to mainly variation in spatial input data used (predominantly land use land cover data), variation in sensitive flow parameters of the study watershed, which significantly influence the calibration processes. Other reasons could be uncertainty during data handling and due to many more cases (Kilemo, 2017).

The calibration and validation outputs of the model indicate that there is a good relationship between the observed and the simulated sediment yield. Thus, it can be judged that the SWAT model can be applied in the study watershed for estimation of flow and sediment yield. The calibration and validation statistical results indicated that the model simulation is almost comparable to the observed sediment yield.

The total sediment load (annual sediment yield estimated by the model from the study watershed for the whole period including the calibration and validation time period) was 2,997,460 tons/year. Whereas, the entire area of the study watershed was 24369.6 km^2. Hence, the annual specific sediment yield of the watershed is equal to 1.23 ton/ha/year.

Generally, the annual soil loss estimated by the model for the Weyib watershed during the simulation period 1992-2012 ranges from 12.49 to 88.36 ha^{-1} $year^{-1}$, with an average value of 37.33 tons ha^{-1} $year^{-1}$ is higher when compared to the average annual losses calculated on a global scale estimated in the range 30–40 tons ha^{-1} $year^{-1}$ (Schiettecatte *et al.,* 2008). The average soil erosion level in the watershed falls under moderate category when compared with the findings of

Betrie *et al.* (2011), in which soil erosion levels were classified into low (0–20 t ha^{-1} yr^{-1}), moderate (20–70 t ha^{-1} yr^{-1}), severe (70–150 t ha^{-1} yr^{-1}) and extreme (≥150 t ha^{-1} yr^{-1}) in sediment management modelling in the Blue Nile Basin. Nevertheless, when it is compared with the maximum tolerable soil loss rate it exceeded the maximum tolerable soil loss (11 t ha^{-1} yr^{-1}), which is the maximum allowable soil loss that will sustain optimum agricultural productivity, signifying the presence of a soil erosion problem (Wischmeier and Smith, 1978).

The average annual sediment load of the study watershed seems overestimated when compared with the findings of Hurni (1988) for the soil loss of the Ethiopian highlands, which is equal to 12 tons ha^{-1} $year^{-1}$. The simulation result of the model for the sediment load was also found to be higher when compared with the average annual soil loss determined by Shiferaw (2011), for the South Wollo highlands for the entire Borena Woreda, i.e., 27 tons ha^{-1} $year^{-1}$. Since the average soil loss rate estimated for Weyib watershed exceeded the maximum tolerable soil loss i.e., 11 t ha^{-1} yr^{-1} (Wischmeier and Smith, 1978) and 15–20 tons ha^{-1} $year^{-1}$ (Morgan, 2005), it can be inferred that there is significant soil erosion problem in the study watershed, implying a need for immediate actions.

4.3 Soil conservation practices in Weyib Watershed

Field visits to the watershed revealed that there is minimum soil conservation practiced in the area. Some of the soil conservation measures found in the watershed were Soil bund, Stone bunds, Hillside terraces, moisture retaining structures including different types of trenches, micro-basins and disposal structures. Other conservation measures include contour farming, plantation and enclosure of degraded areas. On the flat area of the watershed where flooding happens during the rainy season, drainage ditches are common. Farmers also use BBM (Broad Bed Maker) during high rainfall season to drain excess water from crop root zones. However, the adoption rate of these conservation measures is generally low for the entire watershed and therefore their impact on reducing soil erosion is still very low.

4.4 Model outputs of Water Balance Elements

The water which percolates without joining the water table and which then joins the streams as sub-surface flow is also considered as part of surface runoff (Taffa, 2002). From table 25 and figure 21 below one can see that about 39 percent of the annual precipitation is converted in to stream flow. While, 22 percent of the stream flow infiltrates to shallow aquifers which latter joins streams in the form of baseflow. Moreover, from the total flow/stream flow, about 78 percent is contributed by the surface runoff (Q). On the other hand, the **Base Flow Index** (which is the ratio of Baseflow to the Stream Flow/Total Flow) is 0.22.

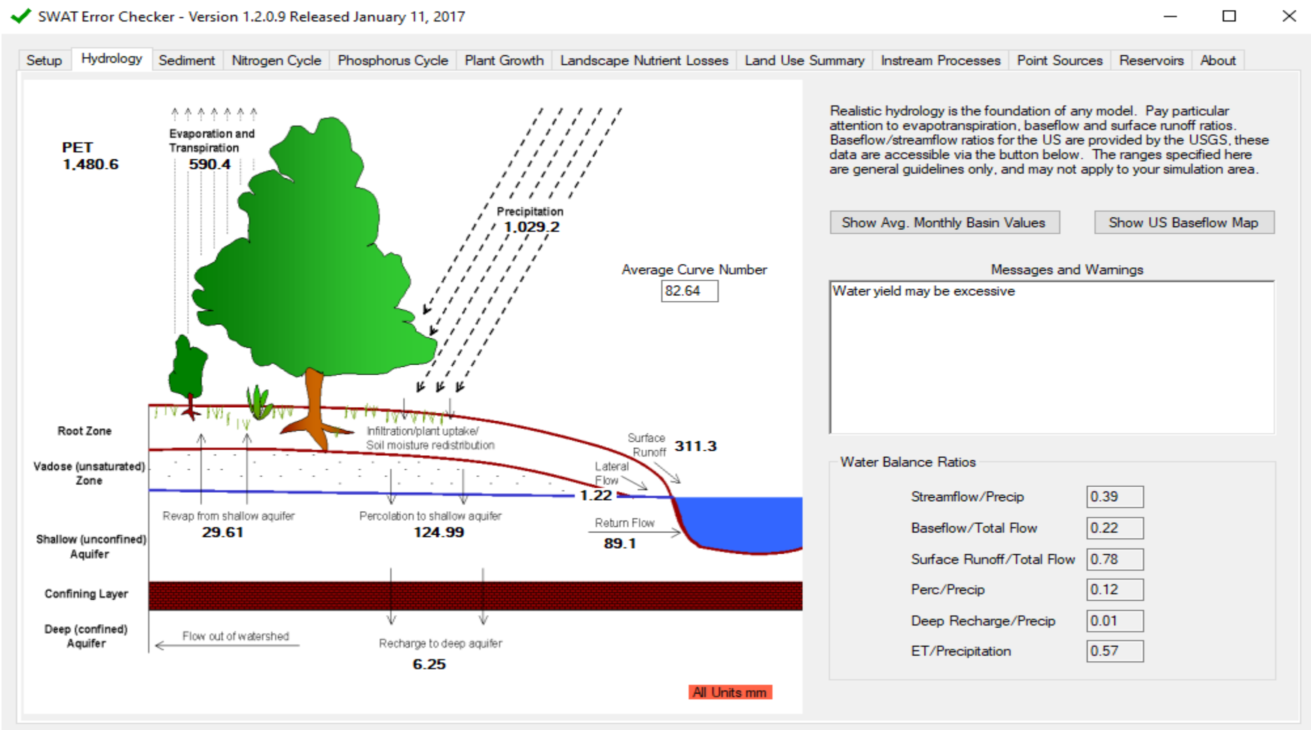

Figure 20 Model Outputs for Water Balance

Table 25 Model Outputs for various Water Balance Elements

No	Model Outputs for Water Balance		Water Balance Ratios	
	Elements	Values	Elements	Values
1	Precipitation (P)	1029.2	Str_flow/P	0.39
2	Surface Runoff (Q)	311.3	B_flow/Str_flow	0.22
3	Evapotranspiration (ET)	590.4	Q/Str_flow	0.78
4	Recharge to Shallow Aquifer (G_shal)	124.99	G_shal/P	0.12
5	recharge to Deep Aquifer (G_deep)	6.25	G_deep/P	0.01
6	Lateral Flow (L-flow)	1.22	ET/P	0.57
7	Return Flow (R_flow)	89.1		
8	Revap from Shallow Aquifer (EVAP_shal)	29.61		
9	Transmission Loss (T-Loss)	0		
#	Stream flow (Str_flow)	401.62		
#	Baseflow (B_flow)	89.1		

Furthermore, according to the model output, the average curve number value, CN, which is the average value of annual floods, for Weyib watershed is 82.64, which shows that much of the precipitation is converted in to runoff rather than infiltrating down the soil profile to shallow or deep aquifers. Thus, from the above model output analysis, it can be inferred that the study watershed may be characterized by an excessive water yield.

4.5 Temporal variation in sediment yield

The soil loss/sediment yield from a given watershed is affected by those factors like the size of the watershed, land use, soil type, slope and climate (Taffa, 2002). The SWAT model was employed to compute the temporal variation of sediment yield in the study watershed. The model output indicated a direct relationship between the rainfall, discharge and sediment yield. The higher the amount of rainfall the more would be the runoff and sediment yield. Table 26 depicts the temporal (yearly) variation of sediment yield for the study watershed

Table 26 Temporal Variation in Sediment Yield

Year	Pcp (mm)	Flow (m3/s)	Sediment Yield (t/ha/yr)	Year	Pcp (mm)	Flow (m3/s)	Sediment Yield (t/ha/yr)
1992	852.3	25.36	12.49	2003	844.7	21.33	17.09
1993	624.8	12.89	13.93	2004	921.9	37.99	28.38
1994	682.9	15.23	15.72	2005	1424.6	74.65	55.6
1995	999.8	37.38	26.61	2006	1043.4	51.11	32.63
1996	1091.9	67.89	52.96	2007	1013.1	48.21	30.03
1997	916	34.48	23.94	2008	959.4	40.04	23.21
1998	729.6	23.04	18.64	2009	1708.8	76.82	88.36
1999	1087.8	71.57	50.73	2010	1023.7	50.23	34.55
2000	1063.9	65.78	38.38	2011	1249.7	65.38	54.5
2001	1081.7	61.09	47.69	2012	1457.8	76.57	83.5
2002	721.2	14.61	14.74	-	-	-	-

There is a temporal variation in sediment yield, the highest sediment load was recorded for the duration 1996, 1999, 2005, 2009, 2011 and 2012 with a value 52.96, 50.73, 55.6, 88.36, 54.5 and 83.5 tons pe hectare per year, respectively. This is attributed to the higher runoff discharge/ flow during this period. The volume of suspended sediment load increases as the volume of the transporting material i.e., runoff increases. A higher flow implies a higher suspended sediment. Since there was a higher flow during this period, the sediment load was higher for this time period. The higher flow in turn is attributed to higher rainfall occurred during this time period. Thus, it can be concluded that sediment yield is dependent on seasons, i.e., sediment yield varies with seasons. From the above table it can be seen that, there is a direct relationship between the three elements rainfall, runoff and the sediment yield. The temporal variation of sediment load in the study watershed is shown in the following graph, figure 21.

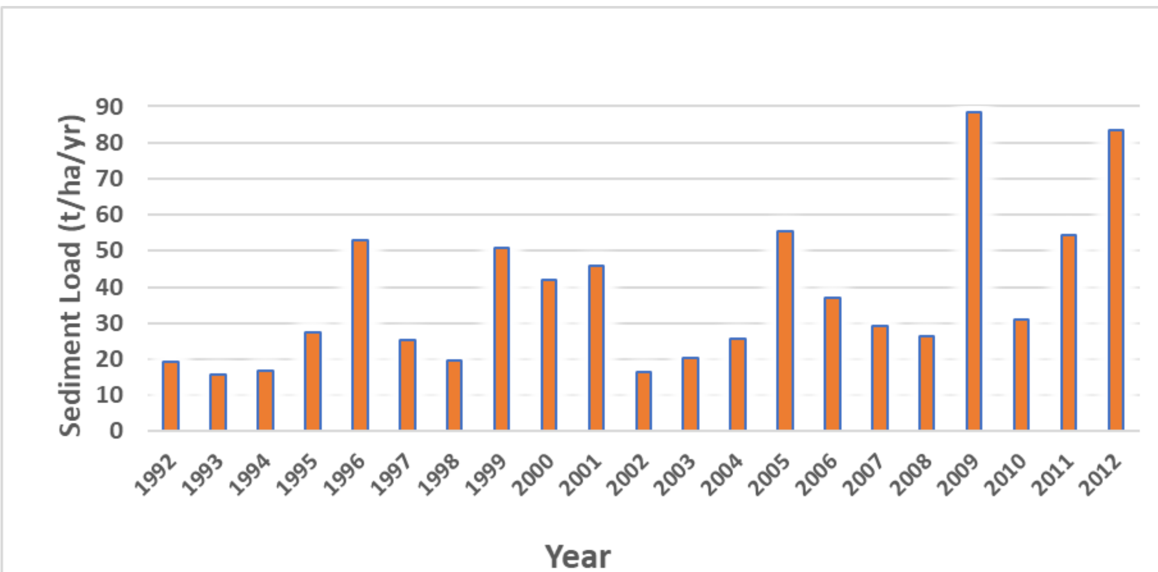

Figure 21 Temporal variation of sediment load

The annual soil loss estimated for the Weyib watershed ranging from 15.63 to 88.36 ha^{-1} $year^{-1}$, with an average value of 37.33 tons ha^{-1} $year^{-1}$ (see table 20 and figure 22 above), is higher when compared to the average annual losses calculated on a global scale estimated in the range 30–40 tons ha^{-1} $year^{-1}$ (Schiettecatte *et al.*, 2008). The average soil erosion level in the watershed falls under moderate category when compared with the findings of Betrie *et al.* (2011), in which soil erosion levels were classified into low (0–20 t ha^{-1} yr^{-1}), moderate (20–70 t ha^{-1} yr^{-1}), severe (70–

150 t ha^{-1} yr^{-1}) and extreme (≥150 t ha^{-1} yr^{-1}) in sediment management modelling in the Blue Nile Basin.

Even though the estimated soil loss in the Weyib watershed is moderate in comparison to estimates elsewhere in Ethiopia, it exceeded the maximum tolerable soil loss (11 t/ha/yr), which is the maximum allowable soil loss that will sustain optimum agricultural productivity, denoting the presence of a soil erosion problem (Wischmeier and Smith, 1978). Similarly, it also exceeds the threshold level recommended by Morgan (2005), in which he estimated the maximum threshold level to be 15–20 tons ha^{-1} year^{-1}, with a generally acceptable mean tolerable soil loss of 11 tons ha^{-1} year^{-1}. Whereas, the recommended value for sensitive areas were less than 2 t ha^{-1} year^{-1}.

4.5.1 The relation between rainfall and runoff

After simulation of surface runoff, a trend analysis was made. This is illustrated in figure below. Despite the fact that many factors are responsible for runoff, rainfall is the main driving factor for the runoff to occur. Based on the trend analysis, the amount of runoff volume was increased because of the increment in the rainfall amount. This can be argued by the statistical result of the correlation coefficient between the rainfall amount and the runoff volume. The correlation coefficient was r = 0.88. It showed that the rainfall amount and the runoff volume were positively and strongly correlated. Their relation is illustrated in the following figure. The relation between rainfall and runoff was modeled by the following function figure 22, consequently, this equation can be employed to estimate the amount of runoff that can be produced from the given rainfall on yearly basis.

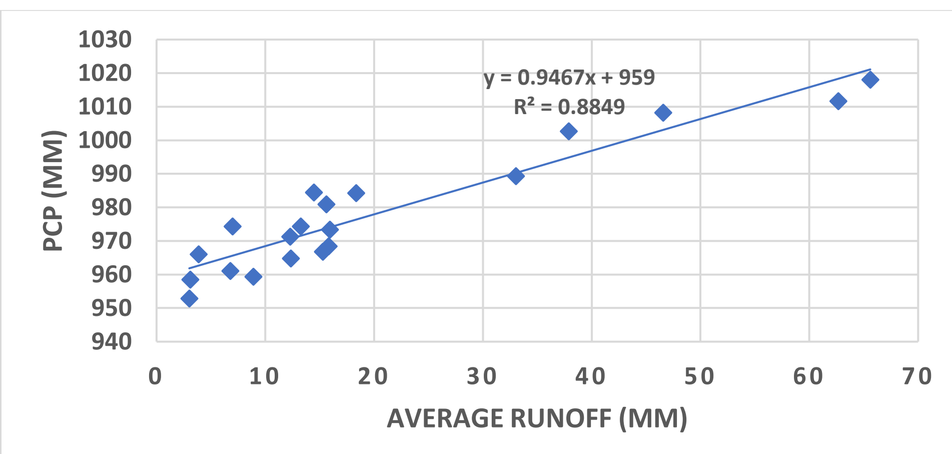

Figure 22 the relationship between Runoff and Rainfall

4.5.2 The relation between Runoff and Sediment Yield

The sediment yield was simulated from 1992-2012 and then summarized on yearly basis. A trend analysis was made to see the correlation between runoff and sediment yield. There was a positive and strong correlation between the two variables; annual surface runoff volume and the sediment yield. The correlation coefficient between the runoff volume and soil loss/sediment yield was 0.9. The relationship between the two variables is illustrated in the following figure 23. The equation of the function can be used to compute the annual sediment yield from a given annual surface runoff.

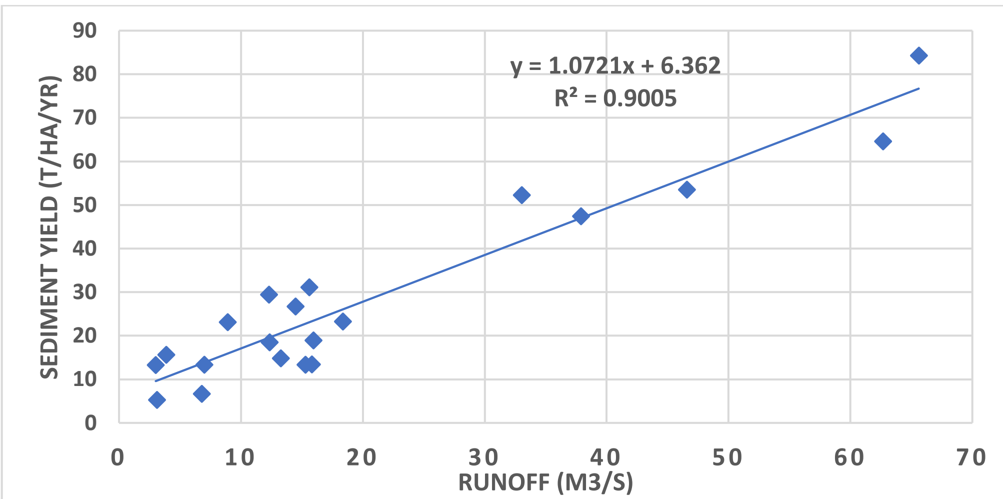

Figure 23 the relationship between Runoff and Sediment Yield

Soil loss is positively correlated to runoff volume (Feleke, 1987). Sonneveld *et al.* (1999) find that annual soil loss is an almost linear function of total annual runoff. Mulugeta (1988) finds a good correlation between runoff volume and soil loss for individual storms on a runoff plot without conservation measures and concludes that soil erosion on steeper slopes can effectively be controlled if the runoff volume is reduced by means of soil conservation measures.

4.5.3 The relationship between rainfall and Sediment Yield

After analyzing the relationship between the runoff with rainfall and sediment yield, lastly, the relationship between the rainfall and sediment yield was analyzed. The amount of rainfall and sediment yield was related by the correlation coefficient of 0.84. This value again indicated that rainfall was positively correlated with soil erosion/sediment yield, the degree of correlation was as strong as the correlation coefficient between runoff and sediment yield. Consequently, it can be concluded that, both rainfall and runoff significantly influence the soil loss in the study watershed. The relationship between the rainfall and soil loss is illustrated in figure 24 below.

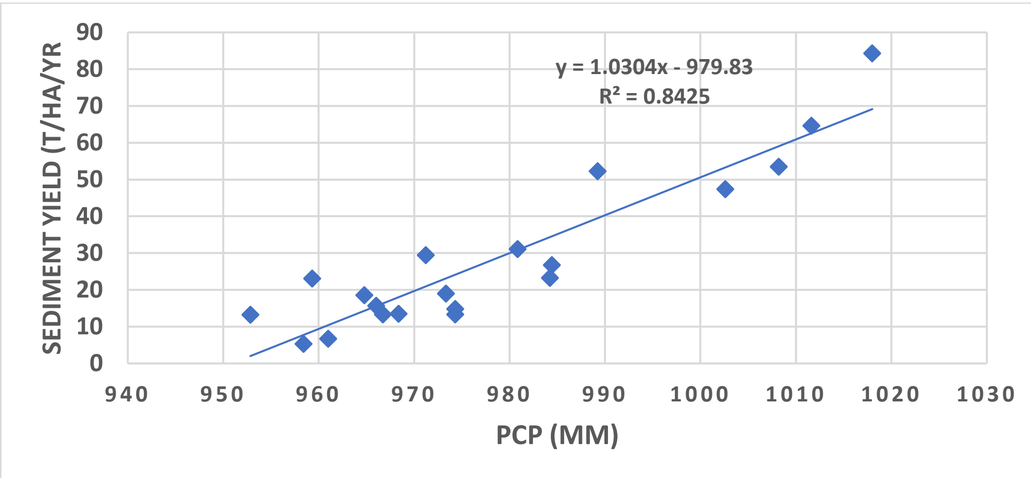

Figure 24 the relationship between Rainfall and Sediment Yield

Soil loss is closely related to rainfall partly through the detaching power of raindrops striking the soil surface and partly through the contribution of rain to runoff (Morgan, 1994). The average annual rainfall of the watershed is approximately 1015 mm (Sisay *et al.*, 2019). Studies conducted to estimate soil loss rates at plot and catchment scales in Ethiopia indicated that soil degradation process varies strongly spatially, with a mean soil loss 29.9 t ha^{-1} yr^{-1} and variation in mean annual rainfall was found to explain 35% of the soil loss variability (Haregeweyn *et al.*, 2015). Studies in the northern Ethiopian highlands and the Central Rift Valley of Ethiopia reported larger erosive power of rainfall (Nyssen *et al.*, 2005). Similarly, a strong and positive correlation was found between the rainfall and the sediment yield in the study watershed. There is seasonal variation in the sediment yield due to wide spread of cultivated area and uneven distribution of rainfall in the study watershed. Sediment yield was found to be higher for higher rainfall seasons. The highest sediment load was recorded for the duration 1998-2001 (table 26 above)

4.6 Spatial Variability of Sediment Yield

The simulation results indicated that, there is also spatial variability in the sediment load in the study watershed. From this spatial variability in the sediment load, it was possible to identify erosion prone areas. This ultimately, helps to identify and plan appropriate intervention measures to reduce erosion. Among the many tasks that a SWAT model can accomplish is the spatial analysis of erosion prone areas. This capacity of the model simplifies the identification of those areas that produces or yield high amount of sediment at sub-watershed or HRU level. Watershed

management programs can be planned from Spatial assessment of soil erosion variability. The spatial distribution of sediment in the watershed is provided in table 27 and figure 25.

Table 27 Spatial Variability of Sediment by sub-watershed

Sub-watershed	Precip (mm/yr)	Surface Runoff, Q (mm/yr)	Sediment load ton/ha/year	Sub-watershed	Precip (mm/yr)	Surface Runoff, Q (mm/yr)	Sediment load ton/ha/year
1	991.36	181.23	8.64	17	1011.63	228.91	13.08
2	1018.63	282.1	9.62	18	959.33	228.89	14.84
3	974.24	97.14	15.99	19	1000.74	152.66	16.22
4	993	30.87	13.3	20	954.98	123.25	6.81
5	984.44	11.78	18.24	21	1004.47	123.22	4.42
6	974.29	16.31	19.19	22	944.12	132.64	8.42
7	985.84	65.65	27.6	23	974.62	147.4	6.33
8	972.03	65.69	40.38	24	1011.81	196.12	5.53
9	997.32	113.44	18.09	25	965.28	228.86	5.6
10	984.74	95.58	32.38	26	894.94	158.4	10.84
11	1008.21	193.33	7.19	27	988.8	172.48	4.39
12	1004.01	65.6	21.15	28	799.97	123.19	3.71
13	980.83	181.98	14.67	29	892.63	175.22	3.83
14	973.93	211.87	13.08	30	984.19	178.91	6.46
15	945.77	137.2	14.84	31	1014.84	191.9	5.32
16	1002.61	65.56	16.22				

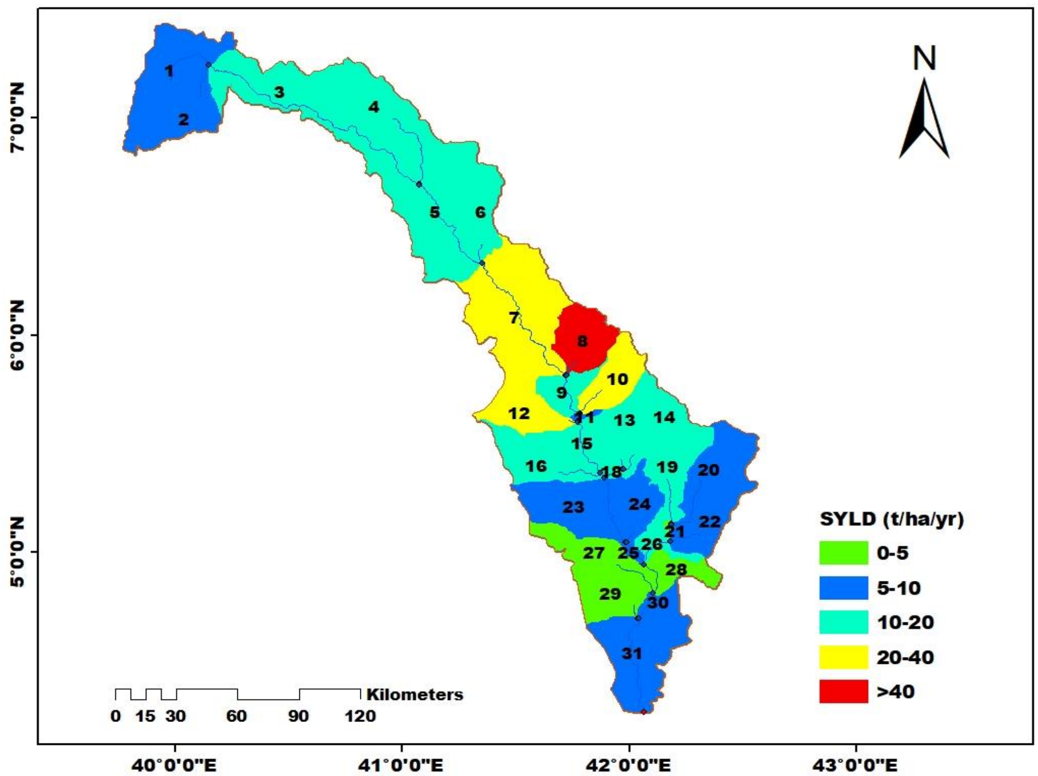

Figure 25 Spatial variability of erosion

From table-27 and figure-26 above, Sub-watershed 7, 8, 10 and 12 have the maximum annual sediment load. These sub watersheds have an annual sediment load above 20 tons/ha/yr, and hence labeled as most sensitive to erosion. Sub-watersheds 21, 27, 28 and 29 have a relative minimum annual sediment yield, that is an annual sediment yield of less than 5 tons/ha/yr. By relative comparison, sub-watersheds 7, 8 and 10 are the most erodible area, sub-watershed 8 being the highest erodible area. From the HRU analysis report it was found that Leptosols and Arenososls are the only soil types distributed in the entire area of sub-watershed 8, which contributed the highest sediment in the entire area of Weyib watershed. Moreover, this sub-watershed is dominated by agricultural land use type, covering 97.91% of the sub-watershed. Besides, unlike the rest of the sub-watersheds, this sub-watershed has the highest proportion of land slope classes ranging between 20-40% and slope of more than 40%. Consequently, this sub-watershed contributed the highest sediment yield in the Weyib watershed and hence labeled as erosion prone area. The average annual sediment load for the study watershed varies from 3.71 ton/ha/yr to 40.38 tons/ha/yr.

From the simulation results, the proportional areas of different sediment yield rate are shown in the table 28 below.

Table 28 Sediment yield and their proportional area coverage

No	Sed. Yld (t/ha/yr)	Area (km^2)	Area (%)
1	0-5	1547.48	6.35
2	5-10	7668.24	31.46
3	10-20	10388.60	42.63
4	20-40	3979.24	16.33
5	>40	786.04	3.23
	Total	24369.6	

Generally, about 93% of the study area produces more than 5 tons/ha/yr. 31.5% of the study watershed produces 5-10 tons/ha/yr, 42.6% of the area produces 10-20 tons/ha/yr and 16% percent of the study watershed yields 20-40 tons/ha/yr. On the other hand, 3% of the study area has a sediment yield of more than 40 tons/ha/yr. On short slopes there is less opportunity for rill erosion to occur and hence the soil loss from this plot will be minimum (Foster *et al.*, 2002).

4.6.1 The correlation between topography and sediment yield

The sediment yield from the study watershed is higher on sloppy areas. About 47% of the total sediment yield was generated from the land slope of >20%. The next higher sediment yield was contributed from a land slope between 10 and 15 (10-15%), which accounted 17% of the total sediment yield. On the other hand, the sediment yield from a land with a slope class of 15-20% was relatively lower than that of the sediment yield from a land slope ranging from 5-10%. This is so because, the land area with a slope class of 15-20% covers only 0.36% of the study watershed, unlike that of 5-10% slope class, which covers 32% of the study watershed. But, with respect to their area coverage the land slope ranging between 15-20% generated the highest sediment load followed by areas with a land slope of >20% and 10-15%. Table 29 below shows the correlation between the sediment yield and topography.

Table 29 The proportion of sediment yield at different land slope classes

No	SLOPE (%)	AREA (km2)	AREA (%)	SYLD (t/ha/yr)	SYLD (%)
1	0-5	3631.36	14.9	6.87	7.34
2	5-10	7814.75	32.07	13.25	14.17
3	10-15	3853.79	15.81	16.05	17.16
4	15-20	86.71	0.36	12.78	13.67
5	>20	8982.98	36.86	44.58	47.66
Total		24369.6			

Generally, it can be said that, there is a direct relationship between the slope and the sediment yield. Thus, proper soil and water conservation and land management intervention measures need to be taken in the study watershed, specifically on sloppy areas. Beside to this, agricultural practices on sloppy areas has to be exercised with careful land management options.

The soil erosion from the landscapes with a slope of more than 20% must have been aggravated by the presence of high rainfall intensity and the fact that during the rainy seasons, forests' canopy starts to open up, creating a concentrated runoff flowing down the hilly landscape. Similar findings were reported for the Medego watershed of Northern Tigray, where the highest soil loss is recorded in steeper slopes (>30°) and low in flat areas (Brhane and Mekonen, 2009). The soil erosion in open and steep slope areas of the watershed was very high. However, flat areas of the watershed reflected modest erosion. Although most of the cultivated landscapes of the watershed are in very flat to gentle slope areas, farming activities are also very common in hilly landscapes of the watershed. Consequently, this part of the watershed is seriously affected by sheet and rill erosion.

4.6.2 The correlation between land use and sediment yield

The following table shows the average annual sediment yield proportions of different land use. From the table it can be seen that agricultural land use type was the main contributor of sediment, accounting for 30.85 % of the total sediment generated in the watershed. On the other hand, forest areas contributed only 4.81% of the total sediment generated. Range grasses, range bushes and pasture land use types were considered to be the next most significant contributor to sediment, accounting 15.91%, 15.45% and 14.69% respectively of the total sediment yield. The sediment generated from each land use type and their proportional area coverage are provided in table 30 below.

Table 30 Simulated Average Annual Sediment Yield from different land use Types

Land Use	AREA	AREA (%)	SYLD (t/ha/yr)	SYLD (%)
AGRC	19342.16	79.37	30.85	32.98
FRST	531.26	2.18	4.81	5.14
PAST	3777.29	15.50	14.69	15.71
RNGB	206.33	0.85	15.45	16.51
RNGE	275.38	1.13	15.91	17.01
URML	2.44	0.01	11.83	12.64
Total	24369.60			

Model simulation results indicated that, erosion hotspot areas are linked to land use types and slope/topography. To overcome this problem, several area specific intervention and management approaches could be considered. Agricultural land occupies 79.4% of the of the study watershed consequently supplied 30.85% of the sediment yield, suggesting that targeted soil erosion control measures on agricultural land are important, especially on the upstream part of the farmland, which is exercised and distributed on steep slopes. Moreover, poor and traditional farming practices on steep slopes and conversion of forest lands to farmland could likely produce more soil erosion and may cause a subsequent increase in sediment yield. Overall, agricultural land use type was the main contributor of sediment yield, followed by Range grasses, range bushes and pasture land use types. while forest appeared to contribute a relatively low amount of sediment to the watershed

The soil loss is highly reliant on land use and land cover of the watershed. The soil loss from Weyib watershed seems underestimated when compared with the findings of Hurni (1983), where he found the soil loss for the Ethiopian highlands to be 12 tons ha^{-1} $year^{-1}$ and that of cultivated fields (cropland) in the highlands to be 42 tons ha^{-1} $year^{-1}$; however, it is overestimated when compared with the estimations of Shiferaw (2011), the study in which the average annual soil loss of the South Wollo highlands for the entire Borena Woreda was found to be 27 tons ha^{-1} $year^{-1}$.

As agriculture is the dominant land use and land cover type of the Weyib watershed, accounting for 79%, the soil loss value was found to comply with the study results reported by (Hurni, 1988). Although Weyib watershed is part of the Bale ecoregion of Ethiopia, there is a large-scale conversion of forest land into cropland between the years 1973 and 2015, which intensified soil erosion and eventually resulted in gully erosion (Hurni *et al.*, 2016). Brhane and Mekonen (2009) found the highest soil loss in croplands and steeper slopes with poor vegetation cover in Medego watershed in Northern Tigray, Ethiopia. Multiple studies have demonstrated that conversion of forest land into other land use, mainly to cropland, intensifies soil loss (Hurni *et al.*, 2016).

A higher risk of erosion occurs in the interface between agricultural and vegetated landscapes, where forest cover is currently being converted to cropland and settlement. Thus, erosion is lower in areas under natural vegetation cover, such as forest (Bewket and Teferi, 2009). Consequently, the existing scenario has to be reversed by working on each factor i.e., improving the land cover dynamics in the area and then soil erodibility thereby altering the soil characteristics and its infiltration rate capacity.

4.6.3 The correlation between Soil types and Sediment yield

The table below shows the average annual sediment yield proportions of different soil types. From the table it can be seen that, Cambisol was the main contributor of sediment, accounting for 23.43 % of the total sediment generated in the watershed. Leptosols, arenosols, regosols, Luvisols and Fluvisols were considered to be the next most significant contributor to sediment, accounting 18.52%, 16.59%, 10.50%, 10.26% and 9.82%. respectively of the total sediment yield generated in the study watershed. On the other hand, the sediment yield from Solontez and Vertisol soil types was only 1.35% each, of the total sediment generated. Nonetheless, with respect to their area coverage, Regosol followed by Solonchak, Fluvisol, Arenosol and Solontez was the main contributor of the sediment generated.

Table 31 Simulated Average Annual Sediment Yield from different Soil Types

SOIL TYPE	AREA	AREA (%)	SYLD (t/ha/yr)	SYLD (%)	SYLD/AREA (%)
Cambisol	7541.1	30.94	21.92	23.43	29.07
Leptosol	3685.3	15.12	17.32	18.52	47.01
Arenosol	2064.1	8.47	15.52	16.59	75.18
Regosol	742.31	3.05	9.82	10.50	132.23
Luvisol	4656.9	19.11	9.6	10.26	20.60
Fluvisol	948.38	3.89	8.66	9.26	91.27
Solonchak	450.11	1.85	5.31	5.68	117.90
Calcisol	2987.4	12.26	2.87	3.07	9.62
Vertisol	1274.7	5.23	1.26	1.35	9.82
Solontez	19.29	0.08	1.26	1.35	65.63

Soil erosion is highly influenced by the cohesive character of a soil type and its resistance to dislodging and transport due to raindrop impact and overland flow shear forces (Gelagay and Minale, 2016). Most of the soil types in the study watershed which demonstrated a higher sediment yield have such characteristics, for instance, Cambisol. Consequently, Cambisols, Leptosols and Arenosols exhibited the highest sediment load in the study watershed.

4.7 Sub-watersheds Prioritization for intervention measures

Controlling, managing and utilizing runoff for useful purposes and reducing the effect of erosion is the objective of a comprehensive watershed management. Hence, it is vitally important to assess the level of erosion in a given area and to prioritize sub-watersheds for treatment. In this study, the prioritization of erosion hotspot areas of the watershed was done using the average annual soil loss rate. Then, rank was given for each sub-watershed taking the amount of the average sediment yield as a criterion for ranking, whereby hotspot areas with maximum sediment yield are given the first rank. Similarly, other areas were ranked in decreasing order of their sediment yield, where the last rank was assigned to those the sub watershed with the least sediment yield. Ultimately, prioritization map was then prepared based on this erosion severity index. The sediment yield from each sub-watershed (in tons per hectare per year) with their corresponding ranks and area coverage are given in table 32 below. Sub-watersheds were ranked to identify and prioritize them for appropriate intervention measures.

Table 32 Ranks of Sub-watersheds in terms of their average annual Soil Loss rate

Sub-watersheds	Area(ha)	SYLD (t/ha/yr)	Rank	Sub-watersheds	Area(ha)	SYLD (t/ha/yr)	Rank
1	147100	8.64	16	17	1020	6.81	20
2	64580	9.62	15	18	7964	4.42	26
3	201092	15.99	9	19	86564	8.42	17
4	149168	13.3	12	20	91076	6.33	22
5	199732	18.24	6	21	2784	5.53	24
6	55352	19.19	5	22	69748	5.6	23
7	259064	27.6	3	23	128608	10.84	14
8	78604	40.38	1	24	52384	4.39	27

Sub-watersheds	Area(ha)	SYLD (t/ha/yr)	Rank	Sub-watersheds	Area(ha)	SYLD (t/ha/yr)	Rank
9	43976	18.09	7	25	7824	3.71	30
10	71424	32.38	2	26	28624	3.83	28
11	4184	7.19	18	27	69772	6.46	21
12	67436	21.15	4	28	42732	3.79	29
13	53184	14.67	11	29	78352	7.05	19
14	63532	13.08	13	30	15220	3.45	31
15	68824	14.84	10	31	151644	5.32	25
16	75392	16.22	8				

The estimated soil loss values with an average soil loss rate of 37.33 t ha^{-1} yr^{-1} and its spatial distribution in the study watershed is generally reasonable, compared to similar studies reported by FAO (1986) in the central and northern highlands (35 t ha^{-1} $year^{-1}$) and SCRP (1996) in the South Wollo Zone (35 t ha^{-1} $year^{-1}$). It falls under very high severity class when compared with the study findings of Temesgen et al. (2017) for Gelad watershed (which is 30-50 t ha^{-1} yr^{-1}). However, the average annual soil rate is lower when compared with other similar studies carried out in different parts of the highlands of the country. For example, the mean soil loss rate was estimated to be 93 t ha^{-1} $year^{-1}$ in the Chemoga watershed (Bewket and Teferi, 2009); 0.2 to 321 t ha^{-1} $year^{-1}$ in the eastern escarpment of Wollo (Amare, 2007); 84 t ha^{-1} $year^{-1}$ in Northwestern Ethiopia (Yihenew and Yihenew, 2013); 243 t ha^{-1} $year^{-1}$ in northwestern highlands of Ethiopia (Gete, 2000) and 47.4 t ha^{-1} $year^{-1}$ in the Koga watershed (Gelagay and Minale, 2016).

Based on the sediment yield and their ranks, sub-watersheds were classified into three categories. Those sub-watersheds with a sediment yield of greater than 11 t/ha/yr were classified under high priority categories, sub-watersheds with a sediment yield between 5 and 11 t/ha/yr were classified under the moderate priority categories; whereas, sub-watersheds with a sediment yield less than 5 t/ha/yr were assigned to low priority categories. This classification of sub-watersheds was done based on the recommended value of the tolerable soil loss limit for tropical areas, which is equal to 11 t/ha/yr (Rose, 1994). Similar annual soil loss rates based sub-watershed classification was done by Tibebe and Bewket (2011) for Keleta watershed, in which sub-watershed with annual soil loss rate of <4 t $ha^{-1}yr^{-1}$ were categorized under low, 4-8 t $ha^{-1}yr^{-1}$ under moderate, 8-11 t $ha^{-1}yr^{-1}$ under high and sub-watersheds with >11 t $ha^{-1}yr^{-1}$ were put under very high severity classes.

The judgment of what level is tolerable depends on the local situation and in particular the type and depth of soil, the rate of soil formation, land use/cover status, topography and amount, intensity and duration of rainfall (Foster *et al.*, 2002). Moreover, the acceptable soil loss that can maintain an economic and a high level of production ranges from 5 to 11 t ha^{-1} $year^{-1}$ (Wischmeier and Smith 1978 and FAO, 1986 and Renard *et al.*, 1996). Thus, the watershed categorization was done taking this threshold values.

Furthermore, implementing soil conservation measures in the entire watershed at a time is impractical due to resource constraints. Thus, it is imperative to prioritize intervention areas based on the magnitude and risks of soil erosion. Hence, based on the estimated rates of erosion, Weyib watershed was classified and ranked into three priority classes.

4.7.1 High Priority Sub-watersheds

Those sub-watersheds which were categorized under this class are characterized by high soil loss rate. Thirteen sub-watersheds (sub-watersheds 8, 10, 7, 12, 6, 5, 9, 16, 3, 15, 13, 4 and 14) produced a sediment yield from 13-40.38 t ha^{-1} $year^{-1}$ which is greater than the threshold value 10 t ha^{-1} $year^{-1}$ and hence labeled as high priority/hotspot areas.

The sediment yield from these sub-watersheds exceeds the soil loss tolerance limit recommended for tropical areas (Rose, 1994) and for Northern Ethiopian highland (Hurni,1986). Moreover, it was also higher when compared with the threshold values suggested for the sustainable agricultural land uses by Morgan (1995), which is equal to 10 tons/ha.

The total area of the sub-watersheds under this category is 13867.17km^2, which is 57% of the entire watershed. These sub-watersheds are found in the steep slope and middle part of the watershed. The area is dominated by Cambisols, which have medium texture, weakly weathering nature and without full development of horizons, the feature that makes them susceptible to erosion. This in combination with backward traditional agricultural practices and poor conservation measures, is the amin reason for the soil erosion taking place in these sub-watersheds.

Consequently, appropriate intervention measures need to be implemented in these sub-watersheds. Areas with a slope gradient of more than 25% and that are not recommended for agricultural activities should be closed or need to be used with proper biological and physical conservation measures that can facilitate infiltration.

4.7.2 Moderate priority sub-watersheds

sub-watersheds under these categories are characterized by moderate soil loss rate. Twelve sub-basins (sub-watersheds 23, 2,1, 19, 11, 29, 17, 27, 20, 22, 21 and 31) fall under this category, with a sediment yield ranging between 5 and 11 t/ha/yr. These sub-watersheds are found in areas with moderate to gentle slopes gradients. The total area of the sub-watersheds under this category is 8954.32km^2, comprising about 37% of the entire watershed. The Cambisol, luvisol and fluvisol soil types dominate this area. Cambisols are characterized by their medium texture nature, having weakly weathering nature with no full development of horizons, fluvisols are recent alluvial deposits with little horizon developments and luvisols are medium textured soils with much of the clay contents transported by soil forming processes. These soil types are susceptible to erosion.

These factors accompanied by improper agricultural practices with poor conservation, are responsible for the soil erosion occurring in these sub-watersheds. Hence, the type of soil found and the agricultural activity practiced in these areas are the principal factor for the soil loss in these sub-watersheds. Consequently, appropriate soil and water conservation measures which can be recommended for such slope gradient, land use type and soil types should be implemented. The recommended measures include soil bunds, fanya juu, stone bunds, broad bed maker (BBM), tied ridge, etc. accompanied by biological measures like, strip cropping, alley cropping, conservation tillage.

4.7.3 Low Priority Sub-Watersheds

These sub-watersheds are characterized by low soil loss rate. Based on the threshold values, six sub-watersheds (sub-watersheds 18, 24, 26, 28, 25 and 30) fall under this category, with a soil loss rate below 5 t/ha/yr. The total area of the sub-watersheds under this category is 1548.11km^2, comprising about 6% of the entire watershed. These sub-watersheds are found on flat to gentle and steep slopes areas and are located in the downstream part of the watershed. Leptosol, arenosol and regosol soil types dominate this sub-watershed. Although some of the sub-watersheds are found in steep slopes, their soil loss rate was relatively very small. The main reason for this could be the land use type and land cover type found in these sub-watersheds. These sub-watersheds are covered by bushes and forest, which have a positive impact on the reduction of the runoff and hence the sediment yield. The summary of the soil loss rate of sub-watersheds and their corresponding priority classes are provided in table 33.

Table 33 Priority classes of Sub-Watersheds

No	Soil Loss Rate (t/ha/yr)	Priority Class	No of sub-watersheds	Sub-watersheds	Total area coverage (km2)	Area (%)
1	>11	High	13	3, 4, 5, 6, 7, 8, 9, 10, 12, 13, 14, 15 and 16	13867.17	56.90
2	5-11	Moderate	12	1, 2, 11, 17, 19, 20, 21, 22, 23, 27, 29 and 31	8954.32	36.74
3	<5	Low	6	18, 24, 26, 28, 25 and 30	1548.11	6.35
#	Total				24369.6	

The priority map for the soil conservation planning is shown in figure 26. As it is illustrated in figure, areas shaded with red colors are high priority areas, those watersheds shaded with yellow color depict moderate priority sub-watersheds and those with blue color indicate low priority sub-watersheds.

The watershed's total average soil loss rates are higher compared to the soil formation rate for Ethiopia's different land units, ranging from 2 to 22 t ha^{-1} year^{-1} (Hurni 1983). When compared to the limits of soil loss tolerance suggested by Rose (1994) (i.e., 10 t ha^{-1} year^{-1} for tropical region) and Hurni (1986) 2–18 t ha^{-1} year^{-1} for the various agro-ecological belts of Ethiopia and 10 t ha^{-1} year^{-1} to the northern highlands of Ethiopia, the simulation result of this study is still higher. The annual soil loss threshold for sustainable agricultural land use is 10 t ha^{-1} yr^{-1}, as recommended by Morgan (1995). Any soil loss rate exceeding 10 t ha^{-1} year^{-1} will not be reversed in a time period of 50 to 100 years (Kouli *et al.,* (2008). Taking this threshold into account, the total area with a probability of soil erosion greater than the tolerance of soil loss was 13867.17 km^2 (Table 33 and Figure 26), comprising 56.9 percent of the entire watershed area.

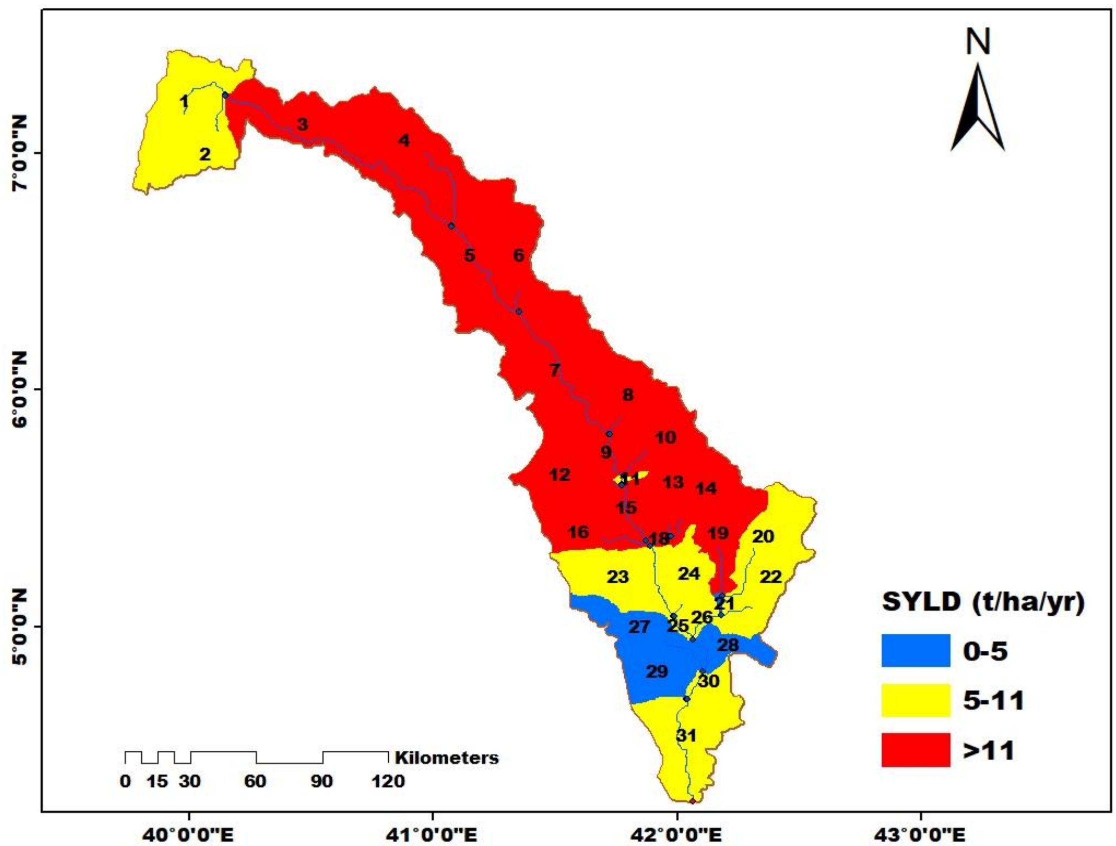

Figure 26 Priority Map for Erosion Intervention

4.8 Scenarios development for intervention

Various scenarios were developed to estimate the effect of intervention measures on the sediment yield. In this study two factors were considered for scenario development. The first factor considered for scenario development was Land Use Land Cover. Here five scenarios were set to see the effect of land use change on soil erosion. The second criteria considered as the driving forces for soil erosion and hence for scenario development were factors related to topography (land-slope). Likewise, five scenarios were developed to evaluate the effect of topography modification on the soil erosion.

4.8.1 Scenarios developed based on Land Use Land Cover types

The calibrated SWAT model was applied in order to evaluate the effect of intervention measures on the flow and sediment yield. The study watershed has the following dominant land use and land cover types.

Land use covers at two different conditions, base-scenario and scenario-(1-5) were used as input variables in the SWAT model in order to compare output as a result of the changes made in land use land covers. Each scenario (1-5) was simulated separately and then compared with the base scenario. The simulated results of the sediment yield in Weyib watershed under different land use and land cover scenarios using the SWAT model are shown in table 34 below. The table summarizes the results of simulations.

Table 34 Sediment Yield reduction due to Land use change Scenarios

Scenario	Description	Average Sediment Yield ($1x10^4$ t/yr.)	Reduction in Sediment Yield ($1x10^4$ t/yr.)	Reduction in sediment yield (%)
Baseline-Scenario	Original condition (without any intervention)	406.38	0	0
Scenario-1	Changing AGRC to FRST by 10%	353.13	-43.22	10.63
Scenario-2	Changing AGRC to FRST by 20%	320.71	-64.56	18.28
Scenario-3	Changing AGRC to FRST by 30%	271.65	-103.01	32.12
Scenario-4	Changing AGRC to FRST by 40%	252.76	-106.89	38.35
Scenario-5	Changing AGRC to FRST by 50%	233.53	-114.56	45.32

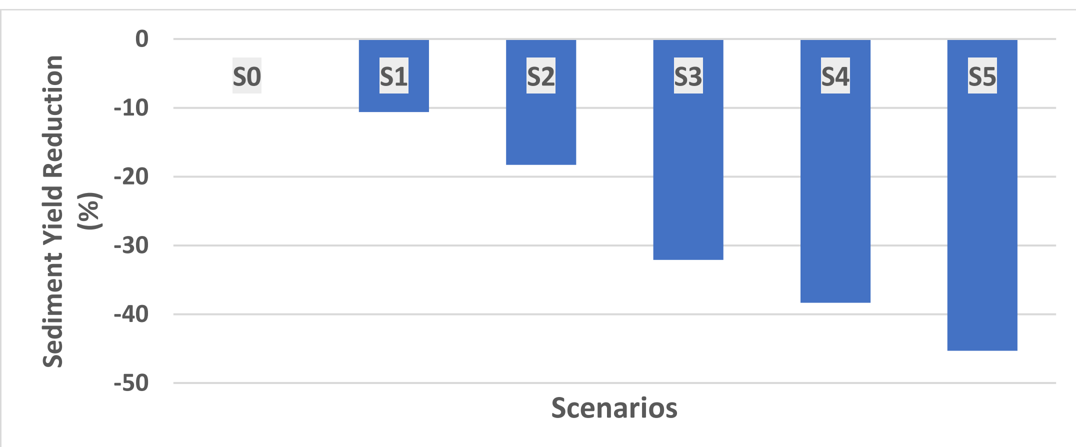

Figure 27 Scenarios versus changes in Sediment Yield

Table 34 and figure 27 given above show changes in sediment yield due to the scenarios. The sediment yield decreases as the percentage of the AGRC land converted in to FRST increases. For instance; a 50% change from AGRC Agricultural land use type to forest mixed (FRST) resulted in 45% reduction in the sediment yield. However, the livelihood of the watershed residents is highly adhered to agriculture (particularly on crop production). Consequently, implementing scenario five (converting 50% of agricultural land to forest land) is not an easy management task. There has to be a tradeoff between the benefits of the agricultural activities and the intervention measures.

However, farmers who practice agricultural activities on marginal land and consequently their production decreased due to nutrient depletion, can engage in other activities e.g., plantation for their income generation, allowing their farm lands to fallow for some seasons. For instance, now a day's farmers leaving in different parts of the country have involved in plantation industries. Eucalyptus species can be a good source/option for this activity, as it is less labor intensive for management and takes shorter duration for harvesting permitting farmers gain immediate benefits. traditional agroforestry, reforestation/afforestation of degraded lands is often seen as the reasonable rehabilitation technique in the tropics and in Africa including Ethiopia (Lemenih, 2004). On the other hand, Payment for Ecosystem Services (PES) can be evaluated for the watershed to find ways of giving incentives to the farmers who do conservation if they will have to give up part of their land for plantation of carbon sequestering forest species, that they would otherwise use for crop production (Mwangi, 2011).

Thus, degraded farm lands can be converted to plantation forests by diverting farmers livelihoods to other activities. Therefore, land use management and watershed management plans need to give much emphasis to these issues.

The reduction in sediment yield due to the scenarios is attributed to the fact that; forests break up the raindrop into a number of tiny droplets (masses) that can hardly disintegrate the soil particles and cause splash erosion. The barrier does not only change the big mass into smaller, but also intercepts the velocity of the raindrop before reaching the ground thereby nullifying its erosive force. Thus, the forest cover, being a barrier to both mass and velocity of the raindrop kills the kinetic energy of the raindrop and its erosivity. Forests, uniformly covering the ground, spreads out the surface flow thinly so that it does not concentrate in one spot to form bigger volume of water that eventually creates erosive runoff. They also increase resistance of the soil to erosion. This is achieved by the improvement of soil aggregates through soil organic matter management. With the improvement of soil organic matter content, the percentage of water stable soil aggregates substantially increases, thereby increasing its resistance to detachment by the direct impact of rain drops. Consequently, as more of a given watershed is converted in to forest land use type, there will be a tremendous reduction in the sediment yield.

4.8.2 Scenarios Developed Based on land management/support practices

In this study, running SWAT model with different watershed management/support practice scenarios presented results that are considerably different from the model results under existing condition (base-scenario). The simulation results of the filter-strips scenario indicated a total sediment yield of 262.87x10^4t/yr, which is equivalent to 35% reduction from the base-scenario (see table 36 below). Model simulation results for contour bund scenarios reflected a total sediment yield of 128.79 x10^4t/yr, which is equivalent to 68% reduction from the base scenario. The simulation results of other scenarios (i.e., Stone bunds, Fanya juu and Bench terraces scenarios) exhibited a total sediment yield of 92.69 x10^4t/yr, 92.20 x10^4 t/yr and 90.74 x10^4 t/yr, respectively. The reduction in sediment yield for these three scenarios (Scenario 2, 4 and 5) is equivalent to 77% reduction from the base scenario. On the other hand, a combination of filter strips, stone buds, contour farming, fanya juu terraces and bench terraces exhibited 78% reduction from the base scenario. The reduction in sediment yield under different Scenarios is given in table 35 below.

Table 35 Summary of Reduction in Sediment Yield due to Scenarios

Scenarios	Description	Sum of SYLD (1x10^4 t/yr)	Reduction in Sediment Yield	
			Difference (1x10^4 t/yr)	%
Scenario-0	Existing condition	406.38	0	0
Scenario-1	Filter-Strips	262.87	-143.51	35.32
Scenario-2	Stone bunds	92.69	-313.69	77.19
Scenario-3	Contour-Farming	128.79	-277.59	68.31
Scenario-4	Fanya-juu Terraces	92.20	-314.18	77.31
Scenario-5	Bench-Terraces	90.74	-315.64	77.67
Scenario-6	Combined (S1+S2+S3+S4+S5)	89.28	-317.1	78.03

The sediment yield reduction benefits of combined filter-strips, contour farming, stone bunds, fanya juu and bench terracing indicate that, sediment reduction followed the order: filter-strips< Contour farming< tone-bunds < Fanya Juu terracin< bench terracing. The same result was reported by Kilemo (2017), in which the efficiency of bench terracing was higher than that of fanya juu terracing, which in turn is also higher than the efficiency of contour farming. Simulation results show that the model successfully demonstrated what would be the effect of each SWC scenario relative to the baseline.

A combination of filter strips, stone buds, contour farming, fanya juu terraces and bench terraces would reduce sediment yield by 78%. Although, compared to other scenarios, filter-strips and contour farming appears to have less impact in sediment reduction owing to the topography of the study watershed, which restricts contour farming scenario only to areas with slopes ≤ 20 %, other studies have demonstrated that it can effectively reduce sediment yield at watershed scale (e.g., Gassman *et al.*, 2006 and Arabi *et al.*, 2007). Mwangi (2011) also found that contour farming would reduce sediment loading by 49%. Areas not covered by the particular scenario remain unchanged. The reduction in sediment yield under each scenario for each sub-watershed is presented in table 36 below.

Table 36 Sediment Yield reduction due to Scenarios by sub-watersheds

sub-watersheds	**Sum of Sediment-Yield (t/ha/yr) by sub-watersheds**						
	Scenario-0	Scenario-1	Scenario-2	Scenario-3	Scenario-4	Scenario-5	Scenario-6
	Existing condition	Filter-Strips	Stone-Bunds	Contour-Farm	Fanya Juu Terraces	Bench-Terrace	S1+S2+S3+S4+S5
1	8.64	5.75	2.84	3.72	2.84	2.84	2.79
2	9.62	7.94	6.17	7.32	6.09	6.09	5.99
3	15.99	10.62	4.32	6.61	4.20	4.20	4.13
4	13.3	8.42	3.57	4.83	3.57	3.51	3.45
5	18.24	11.55	4.28	6.25	4.28	4.28	4.21
6	19.19	12.15	4.78	6.45	4.78	4.78	4.70
7	27.6	15.46	4.15	6.42	4.15	4.15	4.08
8	40.38	25.55	6.72	10.65	6.72	6.72	6.61
9	18.09	11.45	4.60	5.09	4.60	4.60	4.53
10	32.38	20.50	6.46	8.68	6.46	6.46	6.36
11	7.19	4.55	2.07	2.40	2.07	2.07	2.04
12	21.15	13.39	3.52	5.67	3.52	3.52	3.46
13	14.67	9.28	3.05	4.35	3.05	3.05	3.00
14	13.08	8.28	2.21	4.05	2.21	2.21	2.17
15	14.84	9.40	3.24	4.30	3.24	3.24	3.19
16	16.22	10.27	2.85	4.44	2.85	2.85	2.80
17	13.08	8.78	3.92	4.03	3.92	3.92	3.86
18	14.84	9.90	3.97	4.46	3.97	3.97	3.91
19	16.22	10.77	3.16	4.70	3.16	2.73	2.69
20	6.81	4.81	1.16	2.19	1.16	0.73	0.72

Sub-watersheds	Sum of Sediment-Yield (t/ha/yr) by sub-watersheds						
	Scenario-0	Scenario-1	Scenario-2	Scenario-3	Scenario-4	Scenario-5	Scenario-6
	Existing condition	Filter-Strips	Stone-Bunds	Contour-Farm	Fanya Juu Terraces	Bench-Terrace	S1+S2+S3+S4+S5
21	4.42	3.30	0.85	1.61	0.56	0.43	0.42
22	8.42	5.83	1.85	2.59	1.85	1.43	1.41
23	6.33	4.51	1.48	2.13	1.48	1.48	1.46
24	5.53	4.00	1.38	1.95	1.38	1.38	1.36
25	5.6	4.05	1.57	2.00	1.57	1.57	1.54
26	10.84	7.36	2.74	3.26	2.74	2.74	2.70
27	4.39	2.78	1.13	1.64	1.13	1.13	1.11
28	3.71	2.35	0.77	1.42	0.77	0.77	0.76
29	3.83	2.42	1.01	1.51	1.01	1.01	0.99
30	6.46	4.09	1.80	2.17	1.80	1.80	1.77
31	5.32	3.37	1.09	1.90	1.09	1.09	1.07
G-total	406.38	262.87	92.69	128.79	92.20	90.74	**89.28**

The effect of watershed management practices (scenarios developed) revealed great spatial variability on sediment yield at sub-watersheds level. The simulation results depicted that, the reduction in sediment yield under filter strips scenario ranged from 17.44% to 43.97%, the range in percentage reduction under stone bunds scenario was from 35.86% to 84.96%, the percentage reduction in sediment yield under Contour farm scenario ranges from 23.94% to 76.75%, the range in percentage reduction under Fanya juu terrace scenario was from 36.69% to 87.33% whereas, the range in sediment yield reduction under Bench terrace scenarios was from 36.69% to 90.16%. on the other hand, the combined scenario reflected a sediment yield reduction ranging from 37.71% to 90.43%.

The sediment accumulating on bunds gradually changes the original slope of the plot, making it more suitable for cultivation. Gebremichael *et al*, 2005 found that the mean slope gradient of study plots changed from 14.1% to 11.2% and decreased annually at an average rate of 0.33% per year due to bunds. Since the reduction in slope gradient is more pronounced on steeper slopes, the importance of the bunds for reclaiming land is greater on more steeply sloping land.

Parallel terraces, by reducing the slope length by 75%, gave the highest reduction in sediment yield for the upper Awash, which is from 21.53 t/ha/yr. to 6.09 t/ha/yr (Dilnesaw, 2006). Terraces primarily control water runoff and hence erosion. Runoff sediment yield modeling and development of management intervention scenario from Guder watershed, shows that applying filter strips and terraces reduced the sediment yield from catchment by 48% and 53% respectively (Nadew *et al.*, 2018).

Implementing contour farming together with grass filter strips would be more beneficial than implementing either of the conservation practice separately (Mwangi, 2017). Contour farming is an insitu soil conservation method and would ensure minimum soil displacement and minimum loss of soil fertility. On the other hand, the filter strips will trap sediments that have been eroded and carried by the runoff before they get to the streams thus ensuring good water quality. Soil conservation efforts on watershed management has shown some success in reducing run off, soil erosion and associated downstream siltation, increased crop production and productivity (Haregeweyn *et al.*, 2015).

Table 37 Percentage reduction in Sediment Yield from the base scenario by sub-watershed

Sub-watershed	Filter-Strips	Stone-Bunds	Contour-Farm	Fanya Juu Terraces	Bench-Terrace	Combined Scenario
1	-33.48	-67.13	-56.93	-67.13	-67.13	-67.66
2	-17.44	-35.86	-23.94	-36.69	-36.69	-37.71
3	-33.60	-72.98	-58.66	-73.73	-73.73	-74.16
4	-36.69	-73.16	-63.72	-73.16	-73.61	-74.03
5	-36.69	-76.54	-65.74	-76.54	-76.54	-76.91
6	-36.70	-75.09	-66.38	-75.09	-75.09	-75.49
7	-43.97	-84.96	-76.75	-84.96	-84.96	-85.21
8	-36.72	-83.36	-73.63	-83.36	-83.36	-83.63
9	-36.69	-74.57	-71.85	-74.57	-74.57	-74.98
10	-36.70	-80.05	-73.18	-80.05	-80.05	-80.37
11	-36.70	-71.26	-66.56	-71.26	-71.26	-71.67
12	-36.71	-83.37	-73.18	-83.37	-83.37	-83.62
13	-36.71	-79.24	-70.32	-79.24	-79.24	-79.54
14	-36.69	-83.07	-69.04	-83.07	-83.07	-83.38
15	-36.68	-78.19	-71.05	-78.19	-78.19	-78.52
16	-36.70	-82.46	-72.63	-82.46	-82.46	-82.71
17	-32.87	-70.05	-69.19	-70.05	-70.05	-70.51
18	-33.32	-73.26	-69.95	-73.26	-73.26	-73.68
19	-33.62	-80.52	-71.01	-80.52	-83.15	-83.44
20	-29.33	-82.98	-67.89	-82.98	-89.24	-89.45
21	-25.38	-80.83	-63.65	-87.33	-90.16	-90.43

Sub-watershed	Filter-Strips	Stone-Bunds	Contour-Farm	Fanya Juu Terraces	Bench-Terrace	Combined Scenario
22	-30.76	-78.00	-69.25	-78.00	-83.06	-83.29
23	-28.78	-76.62	-66.32	-76.62	-76.62	-77.00
24	-27.65	-74.97	-64.79	-74.97	-74.97	-75.45
25	-27.75	-71.93	-64.28	-71.93	-71.93	-72.42
26	-32.09	-74.76	-69.93	-74.76	-74.76	-75.13
27	-36.70	-74.25	-62.53	-74.25	-74.25	-74.67
28	-36.70	-79.24	-61.78	-79.24	-79.24	-79.58
29	-36.70	-73.60	-60.69	-73.60	-73.60	-74.05
30	-36.71	-72.14	-66.33	-72.14	-72.14	-72.60
31	-36.70	-79.59	-64.32	-79.59	-79.59	-79.89

Sub-watersheds 6, 7, 8, 10, 11, 12, 13, 16, 27, 28, 29, 30 and 31 exhibited relatively the highest reductions for sediment yield under the filter strip scenario, with a percentage reduction of 36.7%, 43.97%, 36.7%, 36.7%, 36.69%, 36.7%, 36.7%, 36.7%, 36.69%, 36.71%, 36.71%, 36.69%, and 36.7%, respectively from the base scenario; sub-watersheds 7, 8, 10, 12, 14, 16, 19 and 20 were those sub-watersheds which exhibited relatively the highest reductions for sediment yield under the stone bund scenario with a percentage reduction of 89.96%, 83.35%, 80.04%, 83.36%, 83.1%, 82.46%, 80.52%, 83% and 80.83% respectively from the base scenario; sub-watersheds 7, 8, 9, 10, 12, 13, 15, 16 and 19 were those sub-watersheds which exhibited the highest reduction in sediment yield for contour farm scenario, with a percentage reduction of 76.75%, 73.62%, 71.85%, 73.18%, 73.18%, 70.31%, 71.05%, 72.62% and 71.01% respectively from the base scenario; sub-watersheds 7, 8, 10, 12, 14, 16, 19, 20 and 21 were those sub-watersheds which exhibited relatively the highest reductions for sediment yield under the fanya juu terrace scenario with a percentage reduction of 84.96%, 83.35%, 80.04%, 80.36%, 82.5%, 80.52%, 83% and 87.33%, respectively from the base scenario and sub-watersheds 7, 8, 10, 12, 14, 16, 19, 20, 21 and 22 were those sub-watersheds which exhibited relatively the highest reductions for sediment yield under the bench terrace and for the combined scenarios with a percentage reduction of 84.96%, 83.36%, 83.1%, 82.5%, 83.14%, 89.23%, 90.16% and 83.05% respectively for the bench terrace and 84.96%, 83.63%, 80.37%, 83.62%, 83.38%, 82.71% 83.44%, 89.45% and 90.43%, respectively from the base scenario.

From the above discussion and table 37 and 38, sub-watersheds 7, 8, 10, 12 and 16 were those sub-watersheds which responded highly for all intervention scenarios. On the other hand, while sub-watersheds 2, 20, 21, 23, 24 and 25 exhibited the least sediment reduction under filter strip scenario, sub-watersheds 1, 2, 3, 4, 21, 25, 27, 28, 29 and 30 reflected the least sediment yield under contour-bund scenario. Moreover, sub-watersheds 1, 2, 11, 17, 25 and 30 reflected the least sediment reduction under stone-bund, fanya juu and bench-terrace scenarios. Here it can be seen that sub-watersheds 2 and 25 reflected the least sediment reduction under all the five scenarios.

The model results reflected that the impact of filter strips became higher as the percentage of the area for slope class was kept ≤20%. This is ascribed to the fact that, as a given field gets more steeper, the concentration of overland flow becomes higher. Simulation results indicated that, 35-77% sediment yield reduction can be achieved by implementing various soil conservation intervention measures (scenarios).

The effectiveness of the combined scenarios in sediment yield reduction is higher than that of individual scenarios. This is attributed to the cumulative impact of individual scenarios in their recommended slope thresholds. The soil and water conservation structures are located strategically to match with the topographical setting of the watershed and thus achieving the highest surface run-off reduction which in return also leads to highest reduction in sediment yield. Sediment yield is reduced at specific sites where the scenario is being implemented only (Kilemo, 2017). Areas not covered by the particular scenario will be addressed by other scenarios making the resultant effect more significant. Thus, at watershed scale, the reduction in sediment will be higher. Moreover, the relative percentage change in sediment yield at watershed scale increases with the percentage increase in agricultural area under scenarios. Since the agriculture land-use is the major contributor of sediments in Weyib watershed, the impact of reducing sediment yield within the agriculture land-use will be reflected at watershed level. Thus, implementing a combined scenario would cover 100% of the agricultural area and hence brings the highest reduction in sediment yield.

On the other hand, S2, S4 and S5 show that the sediment reduction at HRU scale equals to the reduction at watershed scale (combined Scenario). This is attributed to the fact that these scenarios cover almost the entire agriculture area (because they address almost all the slope classes). Therefore, all the HRUs within agriculture land-use are impacted by the intervention measures (scenarios) and thus decreasing the watershed wide average sediment yield.

The model results for intervention scenarios also revealed a reduction of surface runoff, which is attributed to increased infiltration rate caused by conservation structures; specially, stone bunds, fanya juu and bench terraces. Since these structures impound water into small depression, water will be permitted to percolate down the soil profile efficiently. These structures reduce peak flow rate because of the reduction in slope length (Taffa, 2002).

The sediment yield reduction by filter strips scenario, 35%, looks over estimated when compared to the model results for filter strip reported by Verstraeten *et al.* (2006), which is 20%. This is attributed to the fact that, about 63% of the study area has a slope less than 20%. Since the effectiveness of filter strips increases as the slope of a field is kept less than 20%, the simulation result for this scenario found to be higher than the simulation result reported by Verstraeten *et al.* (2006). However, studies conducted in Iowa for bromegrass strip of 3m width indicated a 70 percent reduction in the sediment load and a strip of 9.1m removed 85 percent (Gardiner and Miller, 2004). The same study reported that, strips wider than 9.1m were found to be unnecessary.

Stone bunds scenario appeared to have higher impact in sediment reduction, 77.2 percent. This result is a bit overestimated when compared to the effects of stone bund reported by Gebremichael *et al.* (2005), which is 68 percent. Their research was conducted in the northern part of Ethiopia. However, In the Ethiopian and Eritrean highlands, Herweg and Ludi (1999) found a 72-100 percent reduction in sediment yield by applying stone-bonds on the plot scale. Thus, the model result for stone bund scenario of this study satisfactorily agrees with their findings.

Simulation results for Contour farming (contour bunds) scenario revealed 68 percent sediment yield reduction. Their effectiveness is ascribed to the fact that contour bunds reduce the volume and velocity of the surface runoff. As a result, soil erosion decreases and eroded soil particles are detained in the bund. As compared to the findings stated by Gassman *et al*. (2006) and Arabi *et al.* (2008), which is 49 percent, the model outcome for this study was found to be a bit overestimated. On the other hand, when compared to up and down cultivation, contour farming can reduce soil erosion by 50% (Mati, 2007). The variation among results may be attributed to the varying bio-physical factors such as soils in the study watersheds.

Model results for Fanya juu and Bench terraces scenarios revealed that both scenarios significantly reduced sediment yield by about 77%. Although, due to several reasons/factors, the degree of reduction varies between watersheds, terraces are extremely effective in reducing sediment yield at the watershed scale (Chekol *et al.*, 2007). Both scenarios are effective erosion mitigation measures; however, the efficacy of bench terraces in reducing sediment yield (77.6 percent) was marginally greater compared to that of fanya juu terraces (77.3 percent). This is due to the disparity in their ability to withstand multi-magnitude peak runoff rates. There are solid embankments on the bench terraces, which gives them extra strength to withstand peak storms. Moreover, the variations are more pronounced in HRUs with slope >40%. This is attributed to the spatial heterogeneity of topographical and geomorphological features (Kilemo, 2017) in the watershed especially the slope percentage, slope shape, slope length and steepness. These are among of the factors determining the magnitude of sediment yield simulated by sediment models.

Although stone bunds, fanya juu and bench terraces have significant effect through increased infiltration, they differ in effectiveness. Generally, the effectiveness of terraces is enhanced by the maintenance operations. According to Arnáez *et al.* (2015), if terraces are not regularly maintained, they become less effective. Fanya juu terraces are effective in retarding surface runoff in areas with slope up to 49% beyond which the terraces will collapse during peak runoff events (Hurni, 1986). This is because the embankment of fanya juu terraces develops from the soils being thrown and piled up during construction of a trench. Such piled soils should be stabilized by planting some grass plant species and require regular maintenance. Thus, the strength of embankment of fanya juu terraces will depend on maintenance operations and the quality of soil and plant materials used (Kilemo, 2017).

Generally, for the effectiveness of soil and water conservation measures, watershed residents would have to compromise some of the crop land for conservation if filter strips are to be implemented. This may not be easy due to the land they would forgo for the purpose of the conservation and due to the small sizes of land that most of the farmers in the watershed have. Thus, farmers need to be educated on the benefits of conservation. On the other hand, Payment for Ecosystem Services (PES) should be evaluated for the watershed to find ways of giving incentives to the farmers who do conservation if they will have to give up part of their land that they would otherwise use for crop production, for instance for filter-strips (Mwangi, 2011). Moreover, the vegetation types in the biological erosion control measures can be selected to have multiple use. According to Borin *et al.* (2010), the vegetative erosion control measures can also be selected to comprise trees and grass that could offer other benefits like timber production, carbon dioxide sequestration, aesthetics, increasing the biodiversity of flora and fauna and providing habitat for wildlife. Furthermore, the grass species selected in the vegetative erosion control measures can also be good sources of fodder for livestock. Therefore, the Weyib watershed residents can get a direct economic benefit from the multipurpose trees and the fodder and thus would be encouraged to adopt conservation activities.

5 CONCLUSION AND RECOMMENDATION

5.1 Conclusions

In this study, SWAT2012 was employed to predict the runoff and sediment from Weyib watershed. The general objective of this thesis was to estimate the runoff and sediment yield from Weyib watershed using SWAT model and to identify hotspot erosion areas and to recommend suitable erosion control measures. Arc GIS interface was used to prepare and process the geospatial data needed to run the model. The SUFI2 algorithm in the SWAT-CUP program was used for model calibration and validation. After preprocessing all the temporal and spatial input data required by the model, SWAT was run for simulation.

The SWAT model reasonably simulated the flow and the sediment yields for the Weyib watershed. In order to evaluate model efficiency in terms of its simulation, statistical model performance indicators (R2 and NSE) were used; the model satisfactorily simulated both surface runoff and sediment yield with NSE of 0.67 and an R^2 of 0.74 for daily flow and NSE of 0.79 and an R^2 of 0.78 for sediment yield, during the calibration period and NSE of 0.79 and an R^2 of 0.82 for daily flow and NSE of 0.76 and an R^2 of 0.84 for sediment yield during the validation period, respectively.

The SCS runoff curve number (CN2) followed by Base-flow alpha factor (ALPHA_BF), Soil evaporation compensation factor (ESCO), Available water capacity of the soil layer (SOL_AWC) and Deep aquifer percolation fraction (Rchrg_DP) were the highest in their sensitivity to flow. SLSOIL, SOL_Z, CANMX, REVAPMN, GW_REVAP, SOL_K and GWQMN were found to be the most effective hydrologic parameters for the simulation of streamflow in the study watershed. While, CN2, SOL_AWC, SPEX, HRU_SLP, USLE_K, USLE_P, CH_COV2 and CH_BED_BD were those sediment parameters that were found to highly influence the sediment prediction of the model

The analysis of temporal and spatial sediment yield variation indicated that, the sediment yield from the study watershed varied from time to time or season to season. Sub-watersheds 6, 7, 8, 10 and 12 generated the highest sediment in the watershed, this is so because during this period there was high amount of rainfall and runoff. There was a strong and positive correlation between the rainfall, runoff and the sediment yield, with a correlation coefficient greater than 0.75. Hence, both rainfall and the resulting surface runoff were the main erosive agents.

Soil erosion was higher on those sub-watersheds that are characterized by agricultural land use system, dominated by Cambisol (which are medium textured soil that weakly weather), Leptosols and Arenosols (which are sensitive to erosion) and with slope gradient greater than 25%. On the other hand, since sub-watersheds 11, 24, 27, 29 and 31 are dominated by RNGB and FRST land use types and found in flat to gentle slopes, they generated, relatively, the least sediment with an annual sediment yield of less than 6 tons/ha/yr.

Simulation results for the scenarios reflected that, 35-78% sediment yield reduction can be achieved by implementing filter strips, stone bunds, contour farming, fanya juu and bench terraces. Scenario simulation outputs indicated that sub-watersheds 7, 8, 10, 12 and 16 were those sub-watersheds which responded highly for all intervention scenarios whereas, sub-watersheds 2 and 25 reflected the least sediment reduction under all the five scenarios.

10-45% sediment yield reduction can be achieved by conversion of intensively cultivated and degraded farm lands to plantation forests. Rather than farming unproductive degraded land, farmers can engage in other activities like plantation industries for their income generation, letting the degraded fam land lie fallow and rehabilitate either through natural regeneration or through plantation, the output thereof can be sold to generate income (e.g., timber). Eucalyptus species can be a good source/option for this activity, as it is less labor intensive for management and because of its shorter duration requirement for harvesting.

Generally, high soil erosion rate is attributed to higher slope length and gradient of the watershed. Areas with high erosion rates require immediate action of soil conservation practices. The land management strategies to be implemented should therefore comply with the characteristics of the topography and the land use and cover of the watershed. For sustainably management of erosion-prone areas in slopy mountains area, terracing, agroforestry, cut-and-carry system can be integrated.

5.2 Recommendations

- Hydrologic models are highly reliant on the input datasets. The recording and handling of time series data should, therefore, be given due attention. By deploying more staff/data recorders and by establishing more gauging stations, data needs to be collected on a regular basis. Otherwise, the calibration, validation and prediction efficiency of the model would be difficult.
- Studies need to rely on recent and accurate daily flow and sediment input data, as these are critical for simulation of current phenomena.
- The daily flow and the annual sediment yield in the Weyib watershed were satisfactorily simulated by the SWAT model. Thus, further simulations can be made in the study watershed by using this calibrated model. Moreover, this calibrated model can be used as a potential tool for flow and sediment yield simulation on ungagged and hydro-meteorologically similar watershed.
- The model simulation results from the various scenarios/intervention measure in this study can be used as an option for future planning and development activities undertaken in the watershed.
- A systematic plan and intervention is required to decrease the soil erosion rate in the watershed.
- The erosion map developed to display erosion hotspot areas and the intervention scenarios developed to determine their implementation effect on soil erosion/sediment yield can be a potential guiding tool for future planning and implementation of effective soil and water conservation activities.
- In order to get the required benefit, soil and water conservation structures has to be fixed and maintained periodically, especially after heavy storms.

6 REFERENCES

Abbaspour, K., Rouholahnejad, E., Srinivasan, R., Bacu, V. and Lehmann, A. (2014). Water resource of the Black Sea Basin at high spatial and temporal resolution. *Water Resource Res*, 50(7): 5866-5885.

Abdulkerim, S. and Arup, S. (2016). Impact of Climate Change on Water Availability in the Weyib River Basin, South-eastern Ethiopia. *International Journal of Innovative Research in Science, Engineering and Technology*, 5(6): 9704-9712.

Alemayehu, S. (2014). Climate Change Impact on the Hydrology of Weyib River Watershed, Bale Mountainous Area, Ethiopia: Landscape Dynamics, Soils and Hydrological Processes in Varied Climates. *Springer International Publishing*, 7(27): 587-613.

Alemu, O., Bayou, Ch. and Assefa, M. (2018). Soil Erosion Modelling and Risk Assessment in Data Scarce Rift Valley Lake Regions, Ethiopia. *Water*, 10 (1684): 5-12.

Aili, T., Soncini, A., Bianchi, A., Diolaiuti, G., Bocchiola, D. (2018). A method to study hydrology of high-altitude catchments: the case study of the Mallero river, Italian Alps. *Theoretical and Applied Climatology*, 135:135-156.

Amare, B. (2007). *Landscape transformation and opportunities for sustainable land management along the eastern escarpment of Wollo (EEW), Ethiopia.* PhD. Bern: University of Bern.

Arabi, M., Frankenberger, J., Engel, B. and Arnold, G. (2007). Representation of agricultural conservation practices with SWAT. *Hydrological Processes*, 22: 3042–3055.

Arnáez, J., Renault, L., Lasanta, T., Flano, R. and Castroviejo, J. (2015). Effects of farming terraces on hydrological and geomorphological processes. *Catena*, 128: 122-134.

Arnold, G. and Allen, M. (1993). A comprehensive surface-ground water flow model. *Journal of hydrology*, 142: 47-69.

Arnold, G. and Allen, M. (1996). Estimating hydrologic budgets for three Illinois watersheds. *Journal of Hydrology*, 176: 57-77.

Arnold, G., Srinivasan, R., Muttiah, R. and Williams, J. (1998). Large-area hydrologic modeling and assessment: Part I. Model development. *Journal of American Water Resource Association*, 34(1): 73-89.

Arnold, G., Moriasi, N., Gassman, W., Abbaspour, C. and White, J. (2012). SWAT: Model use, calibration, and validation. *Biological Systems Engineering: Papers and Publications*, 55(4): 1491-1508.

Bewket, W. and Sterk, G. (2003). Assessment of soil erosion in cultivated fields using a survey methodology for rills in the Chemoga watershed, Ethiopia. *Agriculture, Ecosystems and Environment,* 97: 81–93.

Bewket, W. and Teferi, E. (2009). Assessment of soil erosion hazard and prioritization for treatment at the watershed level: case study in the Chemoga watershed, Blue Nile Basin, Ethiopia. *Land Degradation and Development,* 20: 609–622.

Bracmort, K., Arabi, M., Frankenberger, J., Engel, B. and Arnold, G. (2006). Modeling long-term water quality impact of structural BMPs. *Transactions of the Asabe,* 49, pp.367–374.

Bayramin, I., Dengiz, O., Baskan, O. and Parlak, M. (2002). Soil erosion risk assessment with ICONA model: Beypazari Area, Turk. *Journal of Agriculture and Forestry,* 27: 105-116.

Betrie, G., Mohamed, Y., Van Griensven, A. and Srinivasan, R. (2011). Sediment management modelling in the Blue Nile Basin using SWAT model. *Hydrology and Earth System Science,* 15: 809-816.

Bieger, K., Hörmann, G. and Fohrer, N. (2015). Detailed spatial analysis of SWAT-simulated surface runoff and sediment yield in a mountainous watershed in China. *Hydrological Sciences Journal,* 60(5): 784-800.

Breivik, E., Baumgarten, A., Calzolari, C., Miller, B., Pereira, P., Kabala, C. and Jordan, A. (2015). Soil Mapping, Classification, and Modelling: history and future directions. *Geoderma,* 264: 253-255.

Bobe, B. (2004). *Evaluation of soil erosion in the Hararge Region of Ethiopia using soil loss models, rain fall simulation and field trials*. PhD. University of Pretoria, South Africa.

Borin, M., Vianello, M., Morari, F. and Zanin, G. (2005). Effectiveness of buffer strips in removing pollutants in runoff from a cultivated field in North-East Italy. *Agriculture, Ecosystems and Environment,*105: 101-114.

Brhane, G. and Mekonen, K. (2009). Estimating Soil Loss Using Universal Soil Loss Equation (USLE) for Soil Conservation planning at Medego Watershed, Northern Ethiopia. *Journal of American Science,* 5: 58–69.

Brooks, N., Folliott, P., Gregersen, H. and De-Bano, L. (1997). *Hydrology and the Management of Watersheds.* 2nd ed. Iowa: State University Press.

Chahinian, N., Tournoud, G., Perrin, L. and Picot, B. (2011). Flow and nutrient transport in intermittent rivers: a modelling case-study on the Vène River using SWAT 2005. *Hydrological Sciences Journal,* 56(2): 268–287.

Chekol, D., Tischbein, B., Eggers, H. and Vlek, P. (2007). Application of SWAT for assessment of spatial distribution of water resources and analyzing the impact of different land management practices on soil erosion in the Upper Awash River Basin watershed. *FWU Water Resources Publications,* 6: 75-86.

Church, M. (2006). Bed material transport and the morphology of Alluvial River Channels. *Annual Review of Earth and Planetary Science*, 34, pp.325-354.

Cunderlik M. (2003). Hydrologic model selection fort the CFCAS project: Assessment of Water Resources Risk and Vulnerability to Changing Climatic Conditions, *Project Report I*, 40: 123-127.

David, V. and Davidova, T. (2015). Precipitation Assessment from the Viewpoint Data Availability for Purposes of Flood Modelling. In: *Proceedings of the 14th International Conference on Environmental Science and Technology*. Rhodes, Greece.

Dennis, F. and Rorke, F. (1999). The relationship of soil loss by inter-rill erosion to slope gradient. *Catena*, 38: 211-222.

Dilnesaw, A. (2006). *Modeling of Hydrology and Soil Erosion of upper Awash River Basin*. PhD. University of Bonn.

FAO, (1986). *Ethiopian Highlands Reclamation Study*. Final Report volume-1. Rome: The Food and Agriculture Organization of the United Nations.

Feleke, A. (1987). Effect of vegetative cover, tillage and planting system on run-off, soil erosion and other soil physical properties. *Agricultural Mechanization in Asia, Africa and Latin America*, 18 (2): 23-28

Foster, D., Rowntree, M., Boardman, J. and Mighall, M. (2012). Changing sediment yield and sediment dynamics in the Karoo Uplands, South Africa; Post-European impacts. *Land Degradation & Development*, 23: 508-522.

Foster, R., Yoder, C., Weesies, A., McCool, K., McGregor, C. and Bringer, L. (2002). *Predicting soil erosion by water*: a guide to conservation planning with the Revised Universal Soil Loss Equation (RUSLE). USDA-Agricultural Research Services, Washington, DC.

Gardner, T. and Miller, W. (2004*). Soils in Our Environment*. 10th ed. New Jersey: Pearson Education, Inc.

Gassman, P., Osei, E., Saleh, A. and Rodecap, J. (2006). Alternative practices for sediment and nutrient loss control on livestock farms in northeast Iowa. *Agriculture, Ecosystems and Environment,* 117: 135–144.

Gebeyehu, A. (1989). *Regional Flood Frequency Analysis.* PHD. Stockholm.

Gebiaw, A., Ian, R., Engidasew, T. and Jaehak, J. (2017). Streamflow and Sediment Yield Prediction for watershed prioritization in the upper Blue Nile River Basin, Ethiopia. *Water,* 9: 782; doi:10.3390/w9100782.

Gebremichael, D., Nyssen, J., Poesen, J., Deckers, J., Haile, M., Govers, G. and Moeyersons, J. (2005). Effectiveness of stone bunds in controlling soil erosion on cropland in the Tigray highlands, Northern Ethiopia. *Soil Use and Management*, 21: 287–297.

Gelagay, S, and Minale, S. (2016). Soil loss estimation using GIS and remote sensing techniques: a case of Koga watershed, Northwestern Ethiopia. *International Soil and Water Conservation Research,* 4: 126–136.

Genale Dawa Master Plan main report (GDMP), (2007). GDRB *Integrated Resources Development Master Plan Study*. Lehimer International and Yeshi-ber Consultant, Volume-II.

Getachew, A. and Wagayehu, B. (2007). Determinants of Land Degradation in the lake Tana Basin and its Implications for Sustainable Land Management: The Case of Angereb and Gish-Abbay Watersheds. Ethiopian. *Journal of Agricultural Economics*, 6: 70-101.

Gete, Z. (2000). Landscape Dynamics and Soil Erosion Process Modeling in the Northwestern Ethiopian Highlands. African Studies Series A16. *Geographica Bernensia*. University of Berne Switzerland.

Green, H. and Ampt, A. (1911). The flow of air and water through soils. *Journal of Agricultural Science*, 4: 1–24.

Hellden, U. (1987). *An Assessment of Woody Biomass, Community Forests, Land Use and Soil Erosion in Ethiopia*. Lund: Lund University Press.

Herweg, K. and Ludi, E. (1999). The performance of selected soil and water conservation measures-case studies from Ethiopia and Eritrea. *Catena*, 36: 99–114.

Hudson, N. (1996). *Soil conservation*. Second ed. London: B.T. Bats-ford Ltd.

Hurni, H. (1985). Erosion Productivity Conservation Systems in Ethiopia. In: *4th International Conference on Soil Conservation*. Maracay, Venezuela: 654-674.

Hurni, H. (1988). Degradation and conservation of the resources in the Ethiopian highlands. *Mountain Research and Development. Mountain Research and Development*, 8: 123–130

Hurni, H.1993. Land degradation, famine, and land resource scenarios in Ethiopia. In: *World Soil Erosion and Conservation.* D. Pimentel (ed.), Cambridge University Press: 89-97.

Hurni, H., Tato, K. and Zeleke, G. (2005). The implications of changes in population, land use, and land management for surface runoff in the Upper Nile Basin Area of Ethiopia. *Mountain Research and Development. Mountain Research and Development*, 25(2): 147–154.

Hurni, H., Solomon, A, Amare, B., Berhanu, D., Ludi, E., Portner, B., Birru,Y. and Gete, Z. (2010). Land degradation and sustainable land management in the highlands of Ethiopia. Global change and sustainable development: A synthesis of regional experiences from research partnerships, *Geographica Bernensia*, 5: 187-201.

Hurni, K., Gete, Z., Minale, K., Berhan, T., Tibebu, K., Ermias, T., Aderajew, M., Deme, T., Mohamed, A., Yohannes, D., Zeleke, K., Elias, H., Ahmed, A., Asnake, M., Berhanu, D., Deichert, G. and Hurni, H. (2015). *Economics of Land Degradation (ELD) Ethiopia Case Study*. Soil Degradation and Sustainable Land Management in the Rain fed Agricultural Areas of Ethiopia: An Assessment of the Economic Implications. Report for the Economics of Land Degradation Initiative: 94.

Hurni, H., Berhe, A., Chadhokar, P., Daniel, D., Gete, Z., Grunder, M. and Kassaye, G. (2016). *Soil and Water Conservation in Ethiopia*: Guidelines for Development Agents. 2nd ed. Bern, Switzerland: Centre for Development and Environment (CDE), University of Bern, with Bern Open Publishing (BOP): 134.

Jain, K. and. Kothyari, C. (2009). Estimation of soil erosion and sediment yield using GIS. *Hydrological Sciences Journal,* 45(5): 771-786.

Julien, P. (2010). *Erosion and Sedimentation.* 2nd ed. Geological Magazine, 148: 371.

Kannan, N., White, M., Worrall, F. and Whelan, J. (2007). Sensitivity analysis and identification of best Evapotranspiration and runoff options for hydrological modeling in SWAT 2000. *Journal of hydrology,* 332: 456-466.

Khassaf, I. and Hassan, S. (2014.). Suspended sediment rating curve for Tigris river upstream al-amarah barrage. *International Journal of Advanced Research,*2(5): 624-629.

Kilemo, D. (2017). *Impact of Land Management Practices on Water Balance and Sediment Transport in the Morogoro Catchment, Uluguru Mountains (Tanzania).* MSc. Technische Universität Dresden

Kinnell, P. (2000). AGNPS–UM: applying the USLE–M within the agricultural nonpoint source pollution model. *Environmental Modelling and Software,* 15: 331-341.

Kouli, M., Soupios, P. and Vallianatos, F. (2008). Soil Erosion Prediction using the Revised Universal Soil Equation (RUSLE) in a GIS framework, Chaina, Northwestern Crete, Greece. *Environmental Geology*, 57 (3): 483-497.

Liersch, S. (2003). *The Program pcpSTAT*: user's manual, Berlin.

Lim, J., Sagong, M., Engel, A., Tang, Z., Choi, J., and Kim, K. (2005). GIS-based sediment assessment tool. *Catena*, 64: 61-80.

Lemenih, M. (2004). *Effect of Land Use Change on Soil Quality and Native Flora Degradation and Restoration in the Highlands of Ethiopia*. PhD. Swedish University of Agricultural Sciences, Uppsala.

Liu, Q., Li, C. and Li, J. (2001). Influences of slope gradient on soil erosion. *Applied Mathematics and Mechanics,* 22: 510-519.

Luzio, M., Srinivasan, R., Arnold, G. and Neitsch, L. (2002). *ArcView Interface for SWAT2000 (AVSWAT2000)*, User's Guide, Grassland Soil and Water Research Laboratory, Blackland Research Center, Texas Agricultural Experiment Station, Texas Water Resources Institute, College Station, Texas. TWRI Report, TR-193: 345.

Mati, M. (2007). *100 ways to manage water for smallholder agriculture in East and Southern Africa.* A compendium of technologies and practices. SWMnet working paper 13. IMAWESA.

Mcmahon, T., Fenton, J., Stewardson, M., Costelloe, J. and Finlayson, B. (2002). Esimating Discahrge at Ungauged Site. *Australian Journal of Water Resource,* 5: 113-117.

Merritt, S., Letcher, A. and Jackman, J. (2003). A review of erosion and sediment transport models. *Environmental Modelling and Software,* 18: 761- 799.

Mirzaei, S., Raoof, M., Ghasemi, A., Esmali, A., Etaati, H., Moradnezhadi, M. and Mirzaei, Y. (2014). Determination of Some Simple Methods for Outlier Detection in Maximum Daily Rainfall (Case Study: Baliglichay Watershed Basin – Ardebil Province – Iran). *Bulletin of Environment, Pharmacology and Life Sciences,* 3 (3): 110-117

Morgan, C. (1995). Soil erosion and conservation. 2nd ed. Essex: Longman Group UK Limited.

Morgan, C., Quinton, N., Smith, E., Govers, G., Poesen, A., Auerswald, K., Cnisci, G. and Torri, D. (1998). The European Soil Erosion Model (Eurosem): A Dynamic Approach for Predicting Sediment Transport from Fields and Small Catchments. *Earth Surf. Process. land forms,* 23: 527–544.

Moriasi, N., Arnold, G., Van Liew, W., Bingner, L., Harmel, D. and Veith, L. (2007). Model Evaluation Guidelines for Systematic Quantification of Accuracy in Watershed Simulations. *Transactions of the Asabe,* 50(3): 885– 900.

Mulugeta, T. (1988). Soil conservation experiments on cultivated land in the Maybar Area, Wello Region, Ethiopia. In: *Soil Conservation Research Project, Research Report 16*. Berne: University of Berne:127

Mwangi, H. (2011). *Evaluation of the impacts of soil and water conservation practices on ecosystem services in Sasumua watershed, Kenya, using SWAT model.* MSc. Jomo Kenyatta University of Agriculture and Technology.

Mwendera, E. and Mohamed, S. (1997). Hydrologic response to cattle grazing in the Ethiopian highlands. *Agriculture, Ecosystems and Environment*, 64: 33-41.

Nadew, B., Chaniyalew, E. and Tsegaye, T. (2018). Runoff Sediment Yield Modeling and Development of Management Intervention Scenarios, Case Study of Guder Watershed, Blue Nile Basin, Ethiopia. *Hydrology: Current Research*, 9: 306.

Nash, J. and Sutcliffe, J. (1970). River flow forecasting through conceptual models part 1–a discussion of principles. *Journal of Hydrology*, 10: 282-290.

Neitsch, L., Arnold, G., Kinrvand, R. and Williams, R. (2002). *Soil and Water Assessment Tool, Theoretical Documentation:* Version 2002. Temple, TX. USDA Agricultural Research Service anti Texas A& M Black land Research Center.

Neitsch, L., Arnold, G., Kinrvand, R. and Williams, R. (2005). *Soil and Water Assessment Tool, Theoretical Documentation*: Version 2005. Temple, TX. USDA Agricultural Research Service anti Texas A& M Black land Research Center.

Neitsch, L., Arnold, G., Kiniry, R. and Williams, R. (2011). *Soil and Water Assessment Tool Theoretical Documentation*: Version 2009. Texas Water Resource Institute Technical Report No. 406. 720 East black land Road, Temple Texas.

Nemec, J. (1973). *Engineering Hydrology*. T.M.H. edition. Tata McGraw-Hill publishing Company, New Delhi.

Nyssen, J., Clymans, W., Poesen, J., Vandecasteele, I., De Baets, S., Haregeweyn, N., Naudts, J., Hadera, A., Moeyersons, J., Mitiku, H. and Deckers, J. (2009a). How Soil Conservation Affects the Catchment Sediment Budget – a Comprehensive Study in the North Ethiopian Highlands. *Earth Surf. Process. Landforms,* 34: 1216–1233.

Nyssen, J., Poesen, J., Mitiku, H., Moeyersons, J., Deckers, J. and Hurni, H. (2009b). Effects of land use and land cover on sheet and rill erosion rates in the Tigray highlands, Ethiopia. *The Geomorph. N. F*, 53 (2): 171-197.

Parajuli, B., Mankin, R. and Barnes, L. (2008). Applicability of targeting vegetative filter strips to abate fecal bacteria and sediment yield using SWAT. *Agricultural water management*, 95: 1189- 1200.

Pendleton, C. (2007). The migration, Environment and Conflict Nexus in Ethiopia: A case study of Amhara migrant-settlers in East Wollega Zone. *Eastern Africa Social Science Research Review, 23: 131-132.*

Peter, P. (1992). *GIS and Remote Sensing for Soil Erosion Studies in Semi-Arid Environments.* PhD. University of Lund.

Pimental, D. (2006). Soil erosion: a Food and Environmental threat. *Environmental, Development and Sustainability*, 8: 119-137.

Pimentel, D., Harvey, C., Resosudarm, P., Sinclair, K., Kurz, D., McNair, M. and Crist, S. (2006). Environment, Development and Sustainability. *Agriculture and Life Sciences*, 8: 119-137.

Renard, G., Foster, R., Wessie, A. and Porter, P. (1994). Revised universal soil loss equation. *Journal of Soil and Water Conservation*, 46: 30-33.

Renard, G., Foster, R., Weesies, A., McCool, K., and Yoder, C. (1996*). Predicting soil erosion by water*: a guide to conservation planning with the Revised Universal Soil Loss Equation (RUSLE), Handbook No. 703. United States Department of Agriculture: 384.

Refsgaard, C. (1997). Parameterization, calibration, and validation of distributed hydrological models. *Journal of Hydrology*, 198(1): 69-97.

Richard, G., Luis, S., Dirk, R. and Martin, S. (2006). *Crop Evapotranspiration*. guidelines for computing crop water requirements. FAO Irrigation and Drainage Paper No. 56.

Ringo, E. (1999). *Assessment of erosion in the Turasha catchment in the lake Naivasha area, Kenya.* MSc thesis. Enschede University.

Robinson, A., Ghaffarzardah, M. and Cruse, M. (1996). vegetative filter strip effect on sediment concentration in cropland runoff. *Journal of soil and water conservation*, 50 (3): 220-223.

Rose, W. (1994). soil erosion processes and a basis for soil conservation practices. Soil erosion research methods. *Columbus:* 179–181.

Samuel, T. (2013). *Evaluation of the SWAT Model in Simulating Catchment Hydrology: Case Study of the Modder River Basin.* MSc. Thesis. Central University of Technology, Free State, South Africa.

Sang, K. (2005). *Modelling the impact of changes in land use, climate and reservoir storage on flooding in the Nyando basin*. MSc thesis. Jomo Kenyatta University of Agriculture and Technology.

Santhi, C., Arnold, G., Williams, R., Dugas, A., Srinivasan, R. and Hauck, M. (2001). Validation of the SWAT model on a large river basin with point and nonpoint sources. *Journal of American Water Resource. Association*, 37(5): 1169-1188.

Schiettecatte, W., Gabriels, D., Cornelis, W. and Hofman, G. (2008). Enrichment of Organic Carbon in Sediment Transport by Interrill and Rill Erosion Processes. *Soil Science. Society of American Journal*, 72: 50-55.

Schuol, J. and Abbaspour, K. (2006). Calibration and uncertainty issues of a hydrological model (SWAT) applied to West Africa. *Advances in Geosciences,* 9: 137–143.

Searcy, K. and Hardison, H. (1960). *General Surface-Water Techniques.* Manual of Hydrology: Part 1. United States Government Printing Office, Washington.

Setegn, S. (2008). *Hydrological and Sediment Yield Modelling in Lake Tana Basin, Blue Nile Ethiopia.* PhD. Royal Institute of Technology (KTH), Sweden.

Shi, H., Cai, F., Ding, W., Wang, W. and Chow, L. (2003). Soil conservation planning at the small watershed level using RUSLE with GIS: a case study in the Three Gorge Area of China. *Catena,* 55: 33-48.

Shiferaw, A. (2011). Estimating soil loss rates for soil conservation planning in the Borena Woreda of South Wollo Highlands, Ethiopia. *Journal of Sust. Dev. Afr.*, 13: 87–106.

Singh, H., Pandey, R., Singh, S. and Shukla, N. (2014). Assessment of Heavy Meta Contamination in Sediment of the River Ghaghara, a major tributary of the river Ganga in Northern India. *Appl Water Science*, 7: 4133-4149.

Sissay, D., Basam, K. and Fisaha, U. (2019). Biophysical Characteristics of Weyb Watershed, Bale Mountainous Area of the Southeastern Ethiopia. *International Journal of Innovative Technology and Exploring Engineering (IJITEE)*, 8(9): 515-519.

Sloan, P., Moore, I., Coltharp. G. and Eigle, J. (1983). *Modeling Surface and Sub-surface Stormflow on steeply-slopping forested watershed*. KWRRI Research Report: 61.

Sloan, P. and Moore, I. (1984). Modeling Sub-surface stormflow on steeply-slopping forested watershed. *Water Resources Research,*20(12): 1815-1822.

Soil Conservation Research Project (SCRP). (1996). *Soil erosion hazard assessment for land evaluation*. Research report. SCRP, Addis Ababa.

Soil Conservation Service (SCS). (1972). *National Engineering Handbook*. Section 4. U.S. Department of Agriculture. Washington, D.C.

Sonneveld, B., Keyzer, M. and Albersen, P. (1999). A non-parametric analysis of qualitative and quantitative data for erosion modelling: a case study for Ethiopia. In: *the conference of ISCO*, Lafayette, US: 24-28.

Steenhuis, T., Collick, A., Easton, Z., Leggesse, E., Bayabil, H., White, E., Awulachew, S., Adgo, E. and Ahmed, A. (2009). Predicting discharge and sediment for the Abay (Blue Nile) with a simple model. *Hydrological Process.* 23: 3728–3737.

Subramanya, K. (2008). *Engineering Hydrology*. Tata McGraw-Hill publishing Company, New Delhi.

Taffa, T. (2002). *Soil and Water Conservation for Sustainable Agriculture*. Addis Ababa. Mega publishing Enterprise.

Taye, G., Poesen, J., Van Wesemael, B. (2013). Effects of land use, slope gradient and soil and water conservation techniques, on runoff and soil loss in a semi-arid environment. *Journal of Physical Geography,* 34(3): 236–259.

Tibebe, D. and Bewket, W. (2011). Surface Runoff and Soil Erosion Estimation using the Swat Model in the Keleta Watershed, Ethiopia. *Land Degradation and Development*, 22: 551-564.

Van Griensven, A. and Bauwens. W. (2005). Application and evaluation of ESWAT on the Dender basin and Wister Lake basin. *Hydrological Proceedings,* 19(3): 827-838.

Vanoni, A. (2006). *Sedimentation Engineering*. American Society of Civil Engineers,Virginia.

Verstraeten, G., Poesen, J., Demaree, G. and Salles, C. (2006). Long-term (105 years) Variabiity in Rain erosivity as derived from 10-minute rainfall depth data for Ukkel (Brussels, Belgium): Implication for Assessing Soil erosion Rates. *Journal of Geographical Research,* 111, D22109, doi: 10. 1029/2006JD007169.

Wagayehu, B. and Drake, L. (2003). Soil and water conservation decision behavior of subsistence farmers in the Eastern Highlands of Ethiopia: a case study of the Hunde-Lafto area. *Ecological Economics,* 46: 437-451.

Walling, E. and Webb, W. (1987). Material transport by the world's rivers: evolving perspectives. *Hydrology in Perspective proceeding*, 164: 313–329.

Water Works Design and Supervision Enterprise. (2011). *Wabe shebelle-18 multi-purpose irrigation project draft feasibility hydrology report*. Addis Ababa.

Williams, R. (1969). Flood routing with variable travel time or variable storage coefficients. *Trans. ASABE,* 12: 100–103.

Williams, R. (1975). Sediment-yield prediction with universal equation using runoff energy factor. In: *Present and prospective technology for predicting sediment yield and sources. Proceedings of the Sediment Yield Workshop*, USDA Sedimentation Lab., Oxford, MS, ARS-S-40, Nov. 28-30, 1972: 244-252.

Williams, R. and Berndt, D. (1977). Sediment yield prediction based on watershed hydrology. *Trans. ASABE,* 20(6): 1100-1104.

Wischmeier, H. and Smith, D. (1978). *Predicting rainfall erosion losses*: A guide to conservation planning. U.S. Department of Agriculture. Agriculture Handbook No. 537. Washington, D.C. U.S. Government Printing Office.

Wolde, T. and Thomas, B. (1989). The effect of narrow grass strips in reducing soil loss and runoff on a Kabete Nitisol, Kenya. In: *Soil and water conservation in Kenya*. Proceedings of the third National workshop. Kabete, Nairobi, Department of Agricultural Engineering, University of Nairobi.

Yihenew, G. and Yihenew, B. (2013). Costs of nutrient losses in priceless soils eroded from the highlands of Northwestern Ethiopia. *Journal of Agricultural Science,* 5(7): 1916-9752.

Yuan, Y., Bingner, L. and Locke, A. (2009). A review of effectiveness of vegetative buffers on sediment trapping in agricultural areas. *Ecohydrology,* 2: 321-336.

7 APPENDIX

Table 38 slope classes of Weyib watershed

No	Slope (%)	Area [ha]	% Area of coverage
1	0-5	3631.36	14.90
2	5-10	7814.75	32.07
3	10-15	3853.79	15.81
4	15-20	86.71	0.36
5	>20	8982.98	36.86
Total		24369..6	100

Table 39 Input Parameters used for Flow and Sediment Calibration and Validation

Parameter Name	**Description**
r__CN2.mgt	Curve number for moisture condition II
r__SOL_BD.sol	Soil bulk density
r__SOL_AWC.sol	Soil available water storage capacity
r__SOL_K.sol	Soil hydraulic conductivity
r__SOL_ALB.sol	Moist soil albedo
v__ALPHA_BF.gw	Baseflow alpha factor
v__GW_DELAY.gw	Groundwater delay time
v__REVAPMN.gw	Threshold water in shallow aquifer
v__GW_REVAP.gw	Revap coefficient
v__RCHRG_DP.gw	Deep aquifer percolation fraction
v__EPCO.hru	Plant uptake compensation factor
v__ESCO.hru	Soil evaporation compensation factor
v__SLSUBBSN.hru	Average slope length
v__OV_N.hru	Manning's n value for overland flow
v__CH_N2.rte	Manning's n value for the main channel
v__CH_K2.rte	Main channel conductivity
v__SURLAG.bsn	Surface runoff lag coefficient
v__SPCON.bsn	Channel sediment routing parameter
v__SPEXP.bsn	Exponent parameter for calculating sediment re-entrained in channel
v__CH_EROD.rte	Channel erodibility factor
v__CH_COV.rte	Channel cover factor
r__USLE-K.sol	USLE soil erodibility factor

Table 40: SWAT parameters used for conservation structures representation

Scenario	Description	SWAT Parameters			
		Parameters Name (input file)	Slope (%)	Calibrated Value	Modified Value
Scenari-0	Baseline	-	-	Default value	Default value
Scenario-1	Filter-strips	FILTERW (.hru)	0-20% slope	0	1m
Scenario-2	Stone-bund	SLSUBBSN (.hru)	0-10% slope	61m	10m
			10-20% slope	24m	10m
			>20% slope	9.1m	7.3m
		CN2 (.mgt)	0-20% slope	84m	77m
		USLE_P (.mgt)		0.95	0.32
Scenario-3	Contour Farming	CN2 (.mgt)	0-20% slope	84m	77m
		USLE_P (.mgt)		0.95	0.6
Scenario-4	Fanya juu terrace	CN2 (.mgt)	20-40%slope	84m	77m
		SLSUBBSN (.hru)		9.1m	7.3m
		USLE_P (.mgt)		0.95	0.25
Scenario-5	Bench Terrace	CN2 (.mgt)	>40% slope	84m	71m
		SLSUBBSN (.hru)		9.1m	7.3m
		USLE_P (.mgt)		0.95	0.2
Scenario-6	S1+S2+S3+S4+S5	FILTERW (.hru)	All	0	1m
		SLSUBBSN (.hru)	All	61m	7.3m
		CN2 (.mgt)	All	84m	71m
		USLE_P (.mgt)	All	0.95	0.2

Table 41 SWAT model performance evaluation for Flow (Moriasi *et al.*, 2007)

Flow			
Parameter	**Calibration**	**Validation**	**Satisfactory if**
RSR	0.54	0.46	≤ 0.70
R2	0.74	0.82	>0.60
ENS	0.67	0.79	>0.5
PBIAS	-21.2%	-19.5%	±25%

Table 42 SWAT model performance evaluation for sediment (Moriasi *et al.*, 2007)

Sediment Yield			
Parameter	**Calibration**	**Validation**	**Satisfactory if**
RSR	0.43	0.45	≤ 0.70
R2	0.79	0.84	>0.60
ENS	0.78	0.76	>0.5
PBIAS	9.5%	-14.3%	± 55%

Table 43 Statistical Analysis of Daily Precipitation Data for Robe22 station (1988-2012)

Month	PCP_MM	PCPSTD	PCPSKW	PR_W1	PR_W2	PCPD	RAINHHM
Jan.	27.16	4.7832	7.8122	0.038	0.5538	2.6	13.58
Feb.	28.96	5.3888	9.2349	0.0393	0.6056	2.84	14.48
Mar.	81.54	7.5696	4.471	0.1407	0.5625	7.68	40.77
Apr.	198.38	13.6243	4.7855	0.3528	0.6781	16.28	99.19
May.	154.27	11.8538	7.571	0.3294	0.5706	13.88	77.135
Jun.	41.82	4.2524	4.7266	0.1561	0.4611	7.2	20.91
Jul.	38.43	3.4249	4.2873	0.1189	0.5674	7.12	19.215
Aug.	55.72	6.687	14.0364	0.1526	0.5826	8.72	27.86
Sep.	119.87	8.6372	5.061	0.3211	0.6403	14.68	59.935
Oct.	157.12	8.8063	2.6632	0.2883	0.7421	17.68	78.56
Nov.	79.15	7.4117	4.3596	0.1394	0.5896	8.48	39.575
Dec.	37.42	5.6125	7.3771	0.0564	0.5545	4.04	18.71

Table 44 Average Daily Dew Point Temperature Data for Robe22 station (1988-2012)

Month	**Tmp_Max**	**Tmp_Min**	**Hmd**	**Dewpt**
Jan	22.76	6.18	56.97	7.51
Feb	23.72	7.08	53.08	7.24
Mar	23.38	8.33	60.15	9.24
Apr	22.03	9.68	70.73	11.36
May	22.31	9.58	69.02	11.17
Jun	22.88	9.21	67.75	11.17
Jul	21.95	9.25	74.03	11.97
Aug	21.29	9.19	76.71	12.09
Sep	20.9	9.07	75.54	11.55
Oct	19.78	8.64	74.9	10.52
Nov	20.58	6.71	68.44	9.03
Dec	21.54	6.03	61.96	7.9

Table 45 Weather Generator Input Parameters for ROBE22 Station

PARAMETER	MONTH											
	Jan	Feb	Mar	Apr	May	Jun	Jul	Aug	Sep	Oct	Nov	Dec
TMPMX	22.76	23.72	23.38	22.03	22.31	22.88	21.95	21.29	20.9	19.78	20.58	21.54
TMPMN	6.18	7.08	8.33	9.68	9.58	9.21	9.25	9.19	9.07	8.64	6.71	6.03
TMPSTDMX	1.44	1.58	1.84	1.68	1.37	1.26	1.56	1.34	1.33	1.35	1.54	1.36
TMPSTDMN	2.12	1.96	1.91	1.39	1.49	1.45	1.26	1.28	1.58	1.93	2.18	2.32
PCPMM	18.07	25.19	59.62	120.13	75.48	54.32	105.41	143.97	117.05	81.63	35.07	18.93
PCPSTD	2.72	3.84	5.03	7.09	4.62	3.68	7.47	9.11	5.42	4.92	3.73	2.73
PCPSKW	7.14	7.65	4.27	2.85	3.29	3.32	4.47	5.37	2.5	3.28	4.97	7.51
PR_W1	0.06	0.08	0.19	0.42	0.37	0.34	0.46	0.52	0.53	0.25	0.11	0.07
PR_W2	0.48	0.51	0.59	0.64	0.61	0.54	0.59	0.72	0.75	0.73	0.57	0.48
PCPD	3.52	4.12	10.08	16.68	15.68	13.16	16.68	20.96	21.2	16.52	6.48	4.08
RAINHHMX	9.04	12.6	29.81	60.07	37.74	27.16	52.71	71.99	58.53	40.82	17.54	9.47
SOLARAV	20.28	22.02	21.18	19.95	21.48	21.51	19.19	19.58	18.28	17.28	18.76	19.14
DEWPT	7.51	7.24	9.24	11.36	11.17	11.17	11.97	12.09	11.55	10.52	9.03	7.9
WNDAV	1.62	1.79	1.87	1.61	1.63	1.79	1.69	1.77	1.56	1.23	1.16	1.21

Table 46 Weather Generator Input Parameters for GINIR1Station

PARAMETER	MONTH											
	Jan	Feb	Mar	Apr	May	Jun	Jul	Aug	Sep	Oct	Nov	Dec
TMPMX	24.16	25.66	25.43	23.91	23.52	23.48	23.29	23.84	24.45	22.63	23.03	23.92
TMPMN	10.53	11.98	13.57	13.56	13.6	12.64	12.34	12.24	12.73	12.43	11.57	11.11
TMPSTDMX	2.25	1.95	2.22	2.31	1.52	1.73	1.95	1.95	1.86	1.99	1.66	1.68
TMPSTDMN	3.71	3.56	2.65	2.57	2.32	2.44	2.07	2.28	2.29	2.74	2.68	3.06
PCPMM	27.16	28.96	81.54	198.38	154.27	41.82	38.43	55.72	119.87	157.12	79.15	37.42
PCPSTD	4.78	5.39	7.57	13.62	11.85	4.25	3.42	6.69	8.64	8.81	7.41	5.61
PCPSKW	7.81	9.23	4.47	4.79	7.57	4.73	4.29	14.04	5.06	2.66	4.36	7.38
PR_W1	0.04	0.04	0.14	0.35	0.33	0.16	0.12	0.15	0.32	0.29	0.14	0.06
PR_W2	0.55	0.61	0.56	0.68	0.57	0.46	0.57	0.58	0.64	0.74	0.59	0.55
PCPD	2.6	2.84	7.68	16.28	13.88	7.2	7.12	8.72	14.68	17.68	8.48	4.04
RAINHHMX	13.58	14.48	40.77	99.19	77.14	20.91	19.22	27.86	59.94	78.56	39.58	18.71
SOLARAV	20.41	22.06	21.07	19.88	21.37	21.61	19.6	19.85	18.4	17.11	18.57	19.25
DEWPT	10.48	11.69	13.24	14.97	14.93	14.86	14.81	14.59	14.25	13.51	12.64	11.63
WNDAV	1.59	1.75	1.73	1.78	1.67	2.12	2.3	2.3	1.98	1.58	1.5	1.49

Table 47 Sediment Load data computed using Regional equation

Year	Month	Col.1	Col.2	Col.3=1*2	Col.4	Col.5	Col.6=3*5	Col.7=6/4
		Days of month	Monthly mean flow (m3/s)	Monthly Flow (m3/s)	Area (million M2)	Time (sec)	Volume (m3)	Ro (mm)
1992	1	31	0.86	26.76	24369.6	86400	2312409.60	0.09
1992	2	28	2.32	64.82	24369.6	86400	5600865.10	0.23
1992	3	31	0.75	23.15	24369.6	86400	2000419.20	0.08
1992	4	30	1.25	37.56	24369.6	86400	3245097.60	0.13
1992	5	31	4.92	152.43	24369.6	86400	13170124.80	0.54
1992	6	30	3.01	90.16	24369.6	86400	7789737.60	0.32
1992	7	31	7.20	223.19	24369.6	86400	19283270.40	0.79
1992	8	31	57.35	1777.77	24369.6	86400	153599414.40	6.30
1992	9	30	20.39	611.58	24369.6	86400	52840339.20	2.17
1992	10	31	46.85	1452.43	24369.6	86400	125489606.40	5.15
1992	11	30	23.29	698.76	24369.6	86400	60373209.60	2.48
1992	12	31	13.07	405.10	24369.6	86400	35000380.80	1.44
1993	1	31	8.99	278.78	24369.6	86400	24086160.00	0.99
1993	2	28	18.56	519.79	24369.6	86400	44909683.20	1.84
1993	3	31	3.25	100.87	24369.6	86400	8715254.40	0.36
1993	4	30	6.08	182.25	24369.6	86400	15746572.80	0.65
1993	5	31	18.87	584.83	24369.6	86400	50528966.40	2.07
1993	6	30	10.73	321.91	24369.6	86400	27812764.80	1.14
1993	7	31	12.61	390.95	24369.6	86400	33778425.60	1.39
1993	8	31	19.04	590.09	24369.6	86400	50983430.40	2.09
1993	9	30	13.94	418.23	24369.6	86400	36134899.20	1.48
1993	10	31	19.29	597.88	24369.6	86400	51656486.40	2.12
1993	11	30	15.34	460.24	24369.6	86400	39764563.20	1.63
1993	12	31	1.82	56.31	24369.6	86400	4864924.80	0.20
1994	1	31	1.09	33.89	24369.6	86400	2928268.80	0.12
1994	2	28	0.81	22.80	24369.6	86400	1969574.40	0.08
1994	3	31	0.83	25.68	24369.6	86400	2218320.00	0.09
1994	4	30	2.63	79.01	24369.6	86400	6826118.40	0.28
1994	5	31	3.76	116.51	24369.6	86400	10066809.60	0.41
1994	6	30	2.60	78.13	24369.6	86400	6750518.40	0.28
1994	7	31	16.90	523.87	24369.6	86400	45262540.80	1.86
1994	8	31	59.05	1830.64	24369.6	86400	158167641.60	6.49
1994	9	30	20.15	604.59	24369.6	86400	52236748.80	2.14
1994	10	31	19.77	612.85	24369.6	86400	52950326.40	2.17
1994	11	30	25.03	750.82	24369.6	86400	64870588.80	2.66

Year	Month	Col.1	Col.2	Col.3=1*2	Col.4	Col.5	Col.6=3*5	Col.7=6/4
		Days of month	Monthly mean flow (m3/s)	Monthly Flow (m3/s)	Area (million M2)	Time (sec)	Volume (m3)	Ro (mm)
1994	12	31	5.26	162.93	24369.6	86400	14077324.80	0.58
1995	1	31	1.51	46.84	24369.6	86400	4046889.60	0.17
1995	2	28	1.41	39.46	24369.6	86400	3409171.20	0.14
1995	3	31	1.89	58.49	24369.6	86400	5053363.20	0.21
1995	4	30	18.11	543.42	24369.6	86400	46951228.80	1.93
1995	5	31	8.62	267.12	24369.6	86400	23079513.60	0.95
1995	6	30	36.18	1085.38	24369.6	86400	93776400.00	3.85
1995	7	31	3.48	107.87	24369.6	86400	9320140.80	0.38
1995	8	31	35.09	1087.90	24369.6	86400	93994128.00	3.86
1995	9	30	44.84	1345.12	24369.6	86400	116218022.40	4.77
1995	10	31	57.77	1790.78	24369.6	86400	154723392.00	6.35
1995	11	30	6.30	188.89	24369.6	86400	16319664.00	0.67
1995	12	31	4.37	135.39	24369.6	86400	11698041.60	0.48
1996	1	31	49.32	1528.78	24369.6	86400	132086246.40	5.42
1996	2	28	20.36	570.20	24369.6	86400	49265589.85	2.02
1996	3	31	1.74	54.07	24369.6	86400	4671475.20	0.19
1996	4	30	5.15	154.60	24369.6	86400	13357267.20	0.55
1996	5	31	20.56	637.35	24369.6	86400	55067299.20	2.26
1996	6	30	20.68	620.45	24369.6	86400	53606966.40	2.20
1996	7	31	28.16	873.10	24369.6	86400	75435494.40	3.10
1996	8	31	34.37	1065.44	24369.6	86400	92054102.40	3.78
1996	9	30	19.05	571.49	24369.6	86400	49376649.60	2.03
1996	10	31	10.87	336.98	24369.6	86400	29115072.00	1.19
1996	11	30	2.36	70.76	24369.6	86400	6114009.60	0.25
1996	12	31	1.47	45.65	24369.6	86400	3944160.00	0.16
1997	1	31	1.14	35.25	24369.6	86400	3045340.80	0.12
1997	2	28	0.81	22.54	24369.6	86400	1947628.80	0.08
1997	3	31	1.01	31.18	24369.6	86400	2694038.40	0.11
1997	4	30	7.09	212.74	24369.6	86400	18380563.20	0.75
1997	5	31	6.10	189.07	24369.6	86400	16335993.60	0.67
1997	6	30	3.19	95.55	24369.6	86400	8255606.40	0.34
1997	7	31	8.35	258.85	24369.6	86400	22364985.60	0.92

Table 48 Annual sediment load computed using Regional equation

Year	Col.8	Col.9=Regional Equation	Col.10=0.1*9	Col.11=9+10	Col.12=11*4
	Average Ro (mm/yr)	Sus Sed Inflow (t/km2/yr)	Bed load (t/km2/yr)	total load (t/km2/yr)	total load (t/yr)
1992	1.64	174.19	17.42	191.61	4669549.94
1993	1.33	157.78	15.78	173.56	4229588.54
1994	1.43	163.24	16.32	179.56	4375830.13
1995	1.98	189.96	19.00	208.95	5092102.71
1996	1.93	187.72	18.77	206.49	5032071.50
1997	1.56	170.06	17.01	187.06	4558613.45
1998	2.48	211.30	21.13	232.43	5664270.66
1999	5.02	293.58	29.36	322.94	7869875.90
2000	6.76	337.44	33.74	371.19	9045724.48
2001	7.07	344.59	34.46	379.04	9237151.52
2002	0.57	106.10	10.61	116.71	2844152.21
2003	1.72	177.84	17.78	195.63	4767307.48
2004	0.76	121.12	12.11	133.23	3246835.67
2005	1.32	157.48	15.75	173.23	4221496.19
2006	1.68	176.13	17.61	193.75	4721527.74
2007	1.71	177.21	17.72	194.93	4750298.01
2008	0.73	119.36	11.94	131.30	3199679.17
2009	0.32	81.62	8.16	89.78	2187891.44
2010	0.96	135.49	13.55	149.04	3632096.63
2011	0.42	91.73	9.17	100.91	2459033.10
2012	0.34	82.86	8.29	91.14	2221105.98

Table 49 Weyib Discharge data computed using Regional Equation

Date	Q-Sofumer (m3/s)	Area of sofumer (Km^2)	Area of weyib (Km^2)	Q -Weyib (m3/s)
1/1/1992	0.81	3792.7	24369.6	2.47
1/2/1992	0.81	3792.7	24369.6	2.47
1/3/1992	0.81	3792.7	24369.6	2.47
1/4/1992	0.80	3792.7	24369.6	2.44
1/5/1992	0.74	3792.7	24369.6	2.25
1/6/1992	0.73	3792.7	24369.6	2.22
1/7/1992	0.73	3792.7	24369.6	2.22
1/8/1992	0.73	3792.7	24369.6	2.22
1/9/1992	0.74	3792.7	24369.6	2.25
1/10/1992	0.80	3792.7	24369.6	2.44
1/11/1992	0.81	3792.7	24369.6	2.47
1/12/1992	0.82	3792.7	24369.6	2.51
1/13/1992	0.89	3792.7	24369.6	2.71
1/14/1992	0.91	3792.7	24369.6	2.77
1/15/1992	0.98	3792.7	24369.6	2.98
1/16/1992	0.99	3792.7	24369.6	3.02
1/17/1992	0.97	3792.7	24369.6	2.95
1/18/1992	0.83	3792.7	24369.6	2.54
1/19/1992	0.81	3792.7	24369.6	2.47
1/20/1992	0.81	3792.7	24369.6	2.47
1/21/1992	0.81	3792.7	24369.6	2.47
1/22/1992	0.81	3792.7	24369.6	2.47
1/23/1992	0.81	3792.7	24369.6	2.47
1/24/1992	0.81	3792.7	24369.6	2.47
1/25/1992	0.80	3792.7	24369.6	2.44
1/26/1992	0.75	3792.7	24369.6	2.28
1/27/1992	0.82	3792.7	24369.6	2.51
1/28/1992	0.97	3792.7	24369.6	2.95
1/29/1992	1.01	3792.7	24369.6	3.09
1/30/1992	1.19	3792.7	24369.6	3.62
1/31/1992	1.50	3792.7	24369.6	4.56
2/1/1992	2.52	3792.7	24369.6	7.69
2/2/1992	3.98	3792.7	24369.6	12.16
2/3/1992	4.12	3792.7	24369.6	12.58
2/4/1992	3.46	3792.7	24369.6	10.56
2/5/1992	2.77	3792.7	24369.6	8.47

Date	Q-Sofumer(m3/s)	Area of sofumer (Km^2)	Area of weyib (Km^2)	Q -Weyib (m3/s)
2/7/1992	2.15	3792.7	24369.6	6.55
2/8/1992	2.42	3792.7	24369.6	7.39
2/9/1992	5.05	3792.7	24369.6	15.43
2/10/1992	5.52	3792.7	24369.6	16.86
2/11/1992	4.30	3792.7	24369.6	13.14
2/12/1992	3.48	3792.7	24369.6	10.62
1/1/1992	0.81	3792.7	24369.6	2.47
1/2/1992	0.81	3792.7	24369.6	2.47
1/3/1992	0.81	3792.7	24369.6	2.47
1/4/1992	0.80	3792.7	24369.6	2.44
1/5/1992	0.74	3792.7	24369.6	2.25
1/6/1992	0.73	3792.7	24369.6	2.22
1/7/1992	0.73	3792.7	24369.6	2.22
1/8/1992	0.73	3792.7	24369.6	2.22
1/9/1992	0.74	3792.7	24369.6	2.25
1/10/1992	0.80	3792.7	24369.6	2.44
1/11/1992	0.81	3792.7	24369.6	2.47
1/12/1992	0.82	3792.7	24369.6	2.51
1/13/1992	0.89	3792.7	24369.6	2.71
1/14/1992	0.91	3792.7	24369.6	2.77
1/15/1992	0.98	3792.7	24369.6	2.98
1/16/1992	0.99	3792.7	24369.6	3.02
1/17/1992	0.97	3792.7	24369.6	2.95
1/18/1992	0.83	3792.7	24369.6	2.54
1/19/1992	0.81	3792.7	24369.6	2.47
1/20/1992	0.81	3792.7	24369.6	2.47
1/21/1992	0.81	3792.7	24369.6	2.47
1/22/1992	0.81	3792.7	24369.6	2.47
1/23/1992	0.81	3792.7	24369.6	2.47
1/24/1992	0.81	3792.7	24369.6	2.47
1/25/1992	0.80	3792.7	24369.6	2.44
1/26/1992	0.75	3792.7	24369.6	2.28
1/27/1992	0.82	3792.7	24369.6	2.51
1/28/1992	0.97	3792.7	24369.6	2.95
1/29/1992	1.01	3792.7	24369.6	3.09
1/30/1992	1.19	3792.7	24369.6	3.62

Table 50 USLE adaption for the Ethiopian highlands (adapted from Hurni, 1985)

RAINFALL ERROSIVITY (R)											
Annual rainfall (mm)		100	200	400	800	1200	1600	2000	2400		
Annual Factor R		48	104	217	441	666	890	1115	1340		
SOIL ERODIBILITY (K)											
Soil Color		Black	Brown	Red	Yellow						
Factor K		0.15	0.2	0.25	0.3						
SLOPE LENGTH (L)											
LENGTH (M)		5	10	20	40	80	160	240	320		
FACTOR L		0.5	0.7	1	1.4	1.9	2.7	3.2	3.8		
SLOPE GRADIENT S (%)											
Slope (%)		5	10	15	20	30	40	50	60		
Factor S		0.4	1	1.6	2.2	3	3.8	4.3	4.8		
LAND COVER (C)											
COVER	Dense Forest	Dense Grass	Degraded Grass	Badlands Hard	Badlands Soft	Fallow Hard	Fallow Ploughed	Sorghum, Maize	Cereals, Pulses	Ethiopian Teff	Continuous Fallow
FACTOR C	0.001	0.01	0.05	0.05	0.4	0.05	0.6	0.1	0.15	0.25	1
MANAGEMENT FACTOR (P)											
	Ploughing Up and Down	Ploughing on Contour	Strip Cropping	Intercropping	Dense Intercropping	Applying Mulch	Stone Cover 80%	Stone Cover 40%			
FACTOR P	1	0.9	0.8	0.8	0.7	0.6	0.5	0.8			

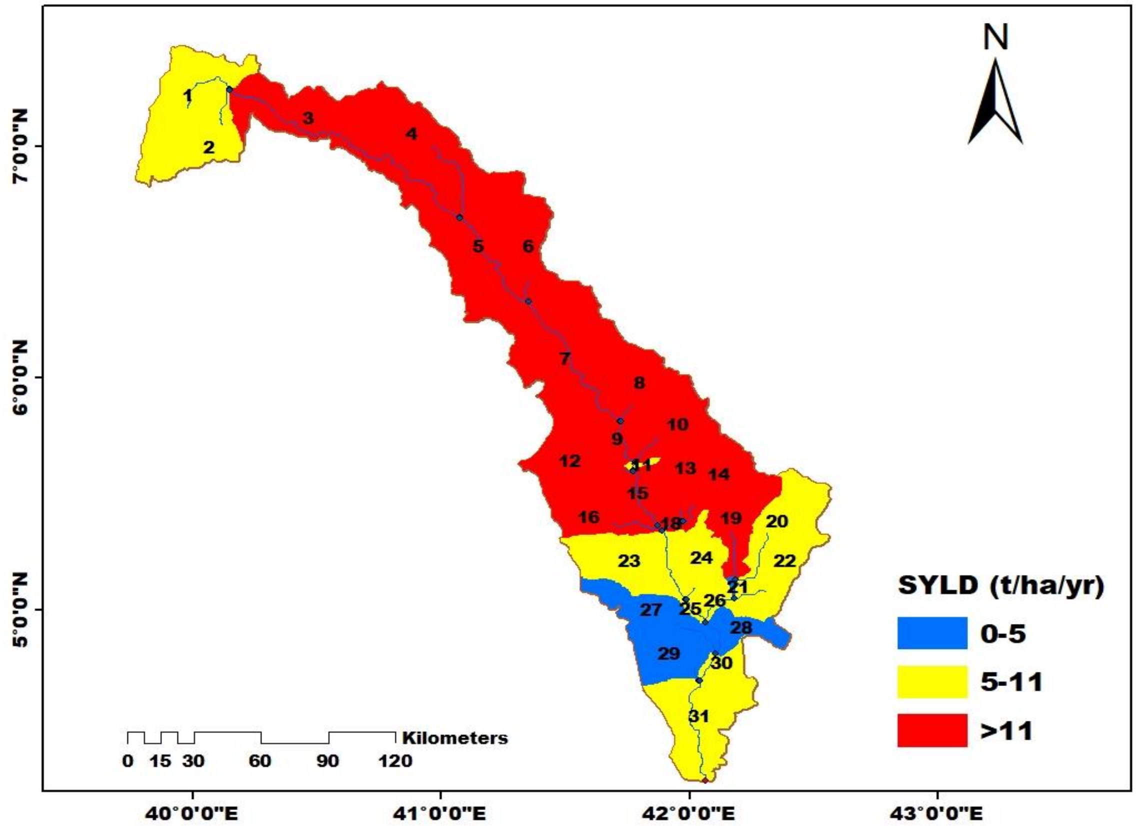

Figure 28 Erosion rate map of Weyib watershed

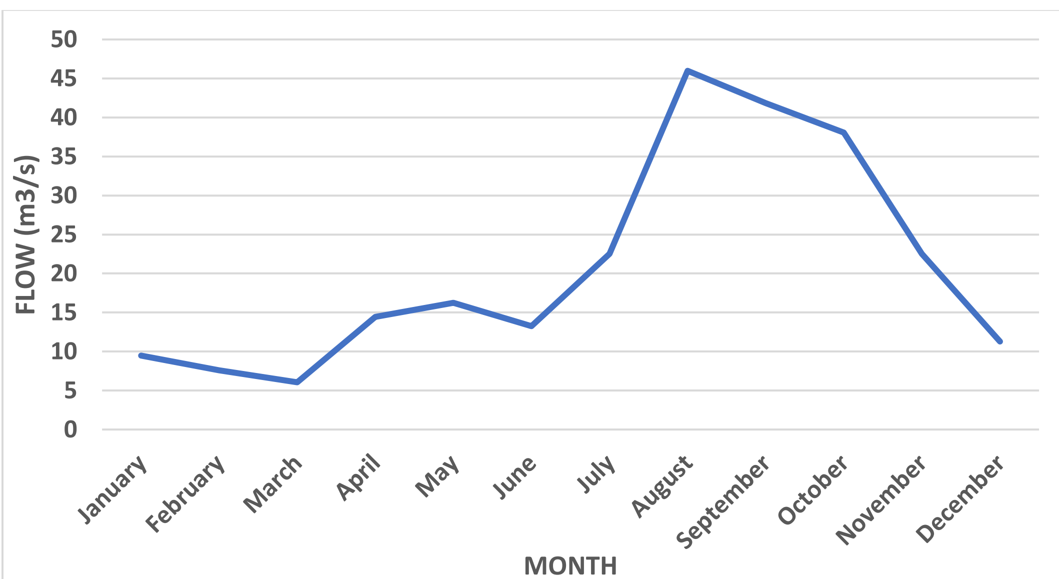

Figure 29 Average Monthly Flow for Weyib Watershed at its outlet

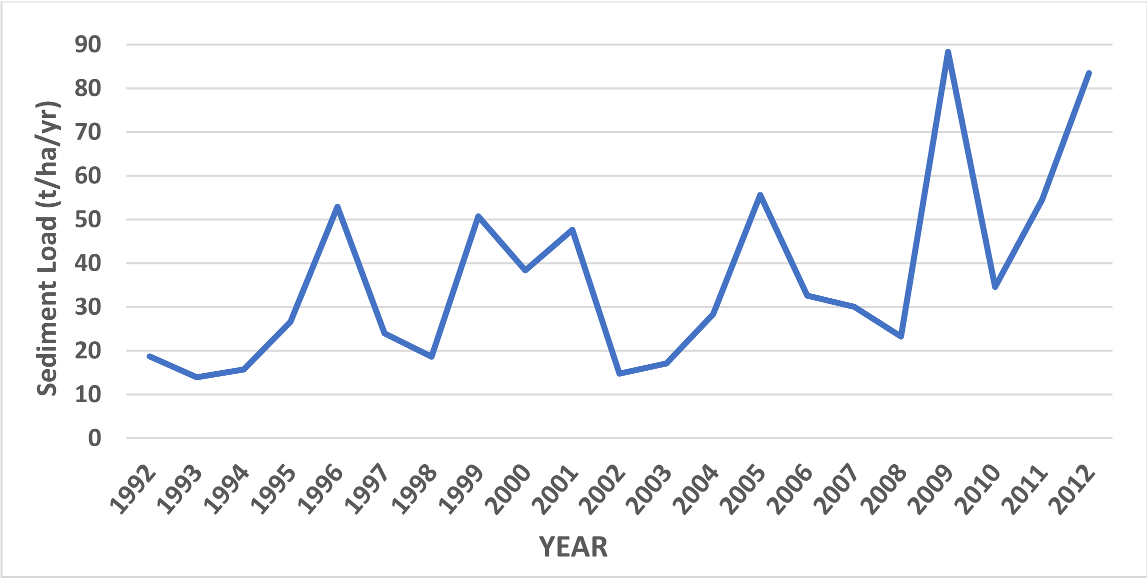

Figure 30 Yearly Sediment Load of Weyib Watershed at its outlet

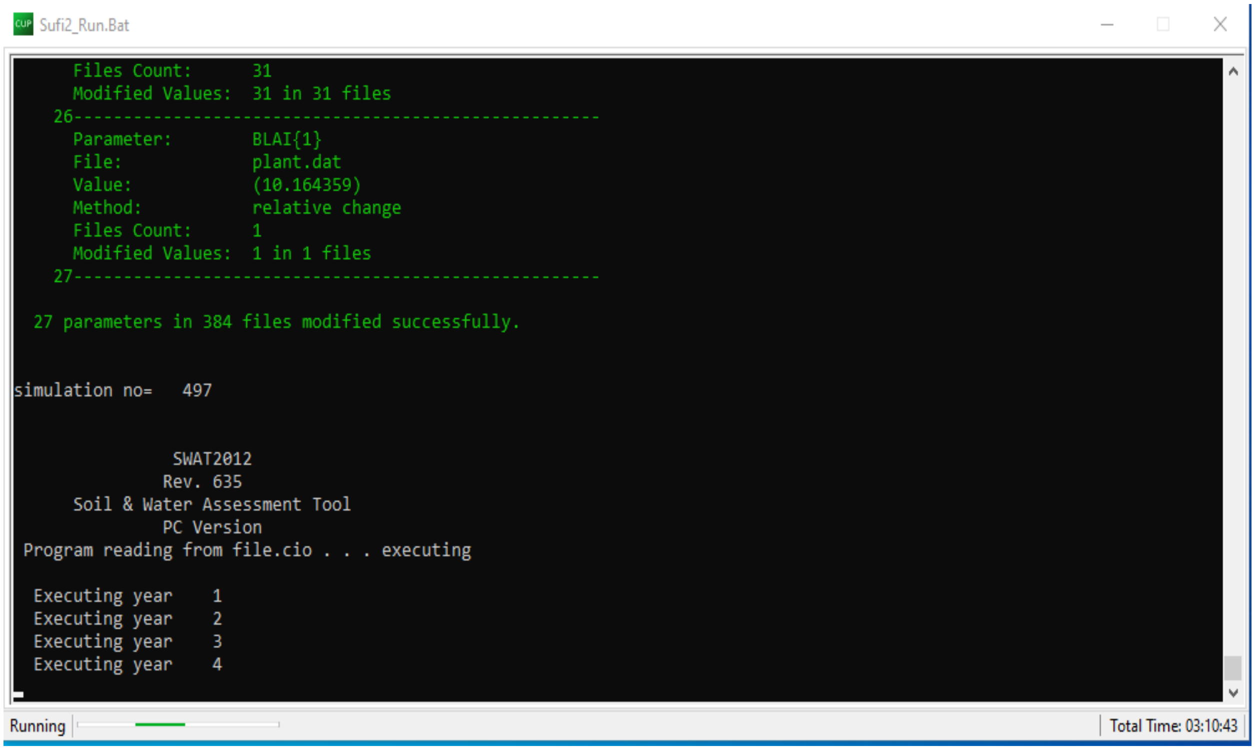

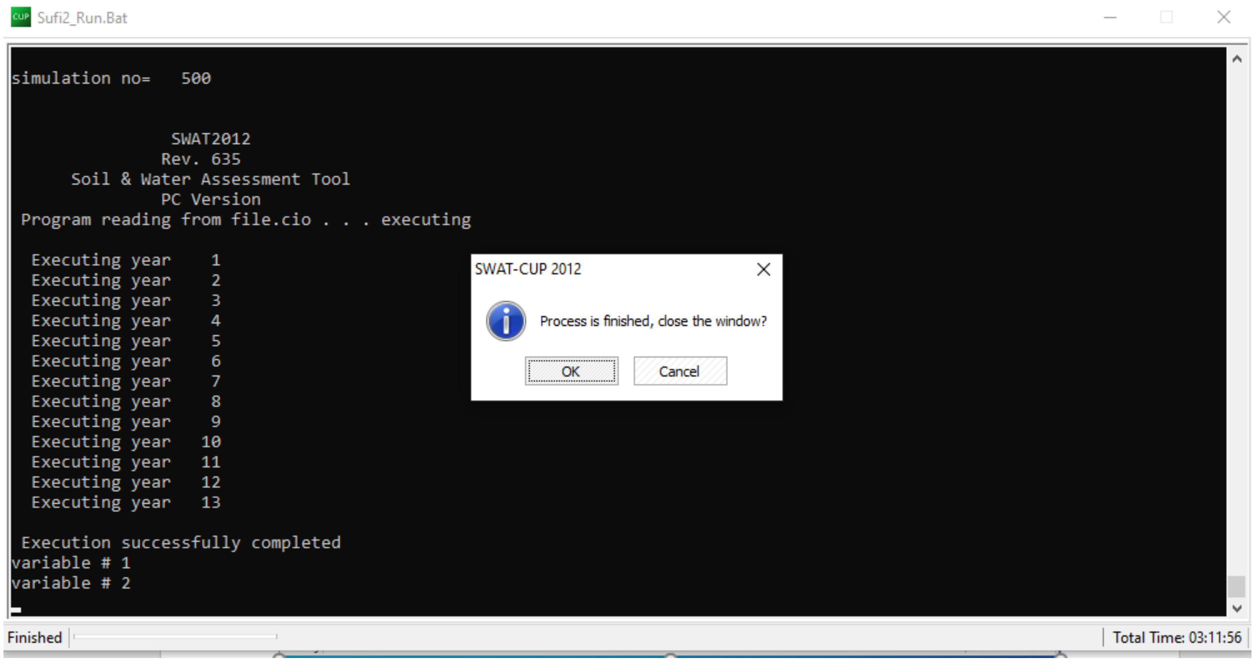

Figure 31 SWAT-CUP (SUFI2) program Running for Calibration and Validation

Table 51 Average Annual Basin Values of the model for various water balance Elements

AVERAGE ANNUAL BASIN VALUES	
Precipitation	1029.2mm
Snow fall	0.00mm
Snow Melt	0.00mm
Sublimation	0.00mm
Surface Runoff Q	311.30mm
Lateral Soil Q	1.22mm
Tile Q	0.00mm
Groundwater (Shal Aq) Q	89.10mm
Groundwater (Deep Aq) Q	6.23mm
Revap (Shal Aq=>Soil/plants)	29.61mm
Deep Aq Recharge	6.25mm
Total Aq Recharge	124.99mm
Toatal Water Yld	407.74mm
Percolation out of Soil	125.23mm
ET	590.4mm
PET	1480.6mm
Transmission Losses	0.00mm
Septic Inflow	0.00mm
Total Sediment Loading	1.23t/ha

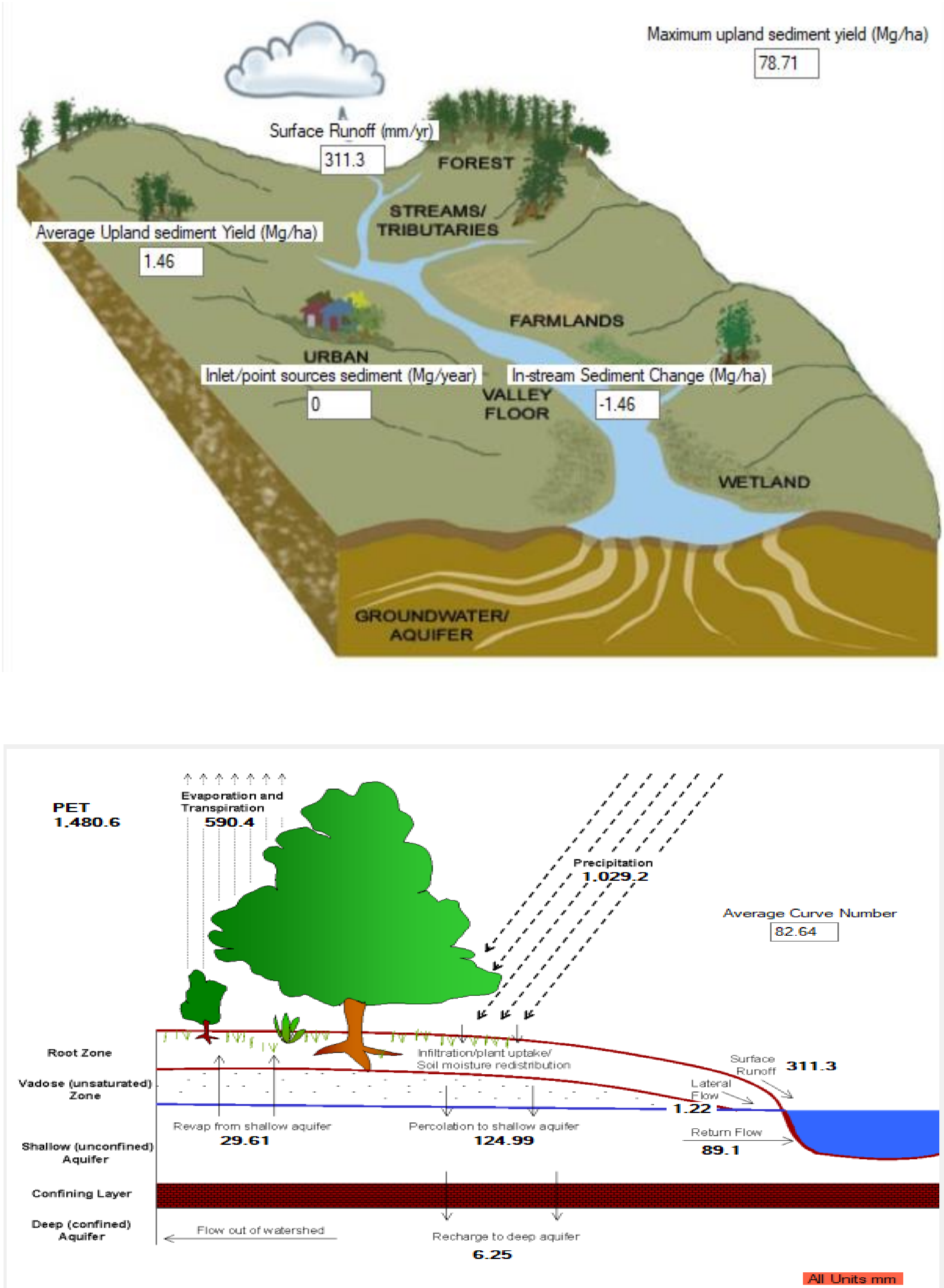

Figure 32 Model Outputs Values for Water Balance Elements